Visual Behaviour and Ocular Morphology of Larval and Adult Zebrafish with an Eye towards Art

---

Dissertation

zur

Erlangung der naturwissenschaftlichen Doktorwürde
(Dr. sc. nat.)

vorgelegt der

Mathematisch-naturwissenschaftlichen Fakultät

der

Universität Zürich

von

Corinne Hodel

von

Malters LU

Promotionskomitee

Prof. Dr. Stephan Neuhauss (Leitung der Dissertation)
Prof. Dr. Christian Grimm
Prof. Dr. Esther Stoeckli

Zürich, 2010

INDEX

I PREFACE

„Pass auf, jetzt kommt mein Frühlingsschrei!
Aaaaaaaaaaaaaaaaaaaaah...
So musste ich schreien, sonst wäre ich geplatzt.“

Ronja Räubertochter

II SUMMARY

Vision is the primary sense of humans. The structure and function of the retina, the light capturing and processing apparatus in our eyes, is remarkably conserved in vertebrates. I have used the zebrafish (*Danio rerio*) as a model to study vision and its defects.

The zebrafish mutant *partial optokinetic response b (pob)* is red-blind. Intriguingly, the defective gene is expressed not only in red cone photoreceptors, but in all cone types. In order to address this paradox, we identified a second *pob* paralogue *(pob1b)* in the zebrafish genome. We found that key residues in the amino acid sequence of the two paralogues are conserved, arguing for conservation in function between these two genes.

We found a similar duplication in the Usher syndrome 1B gene *myosinVIIa (myo7a)*. Mutations in this gene lead to deaf-blindness in humans. The original observation did neither report *myo7a* expression in the wild-type zebrafish retina, nor visual deficits in the corresponding mutant strain *mariner*. We identified a second paralogue of this gene *(myo7a2)* and raised specific antibodies against the zebrafish protein encoded by the first paralogue. In immunohistological stainings we localised Myo7a to the accessory outer segment, a teleost-specific structure not yet described in zebrafish. Therefore, we investigated the ultrastructure of the zebrafish cone accessory outer segment, which rises from the connecting cilium and runs along the cone outer segment only connected via a thin cytoplasma bridge.

In contrast to the *mariner* mutant, the *bumper* mutant has an apparent visual defect. Although the locus is now genetically mapped, the underlying gene defect still awaits identification. It has been found in a mutagenesis screen to be defective in terms of lens development. Performing a closer inspection we found that the lens epithelium initially hyperproliferates and then regresses and that the secondary lens fibre cells but not the primary ones are maldifferentiated. Although the *bumper* retina is morphologically not affected by the mutation, *bumper* mutants are functionally blind.

The visual performance of a vision mutant such as *bumper* can be tested by measuring the optokinetic response (OKR). The OKR is a stereotyped eye movement elicited by slow motion in the visual field which can be suitable studied in transparent zebrafish larvae as the movement of their pigmented eyes can easily be observed. We precisely described a method to computationally measure the OKR in zebrafish larvae which allows detection of even subtle visual defects.

The last part of my thesis is a rather unconventional project as it has been done with an artist. This trans-disciplinary collaboration culminated in *The Electric Retina* an interactive sculpture artistically interpreting zebrafish vision research. The art work projects movies from underwater landscapes seen from a visual impaired zebrafish. Simultaneously, pictures and figures of research related to the visual impairment are shown. This allows the general public to understand how the zebrafish can help to investigate the visual system.

III ZUSAMMENFASSUNG

Der Sehsinn ist mitunter der wichtigste Sinn für den Menschen. Beim visuellen Sinneseindruck ist die Retina von entscheidender Bedeutung, da dort der ins Auge einfallende Lichtreiz auftritt und bereits weitgehend verarbeitet wird. Struktur und Funktion der Retina sind innerhalb der Wirbeltiergruppen stark konserviert. Mithilfe des Zebrafisches (*Danio rerio*) habe ich das Wirbeltiersehsystem und seine Pathologien untersucht.

Die Zebrafischmutante *partial optokinetic response b (pob)* ist rotblind. Interessanterweise ist das defekte Gen aber nicht nur in den Rotzapfen exprimiert, sondern in allen Zapfentypen. Wir haben ein zweites *pob* Paralog *(pob1b)* im Zebrafischgenom identifiziert. Vergleiche der beiden Paraloge haben ergeben, dass Schlüsselelemente der Aminosäuresequenzen konserviert sind; diese Tatsache spricht für eine Konservierung der Genfunktion.

Eine ähnliche Duplikation haben wir im Gen *myosinVIIa (myo7a)* gefunden. Patienten mit einer *myo7a*-Genmutation leiden am sogenannten Usher-Syndrom 1B, welches durch fortschreitende Taub-Blindheit charakterisiert ist. Die ersten Zebrafischstudien zum Usher-Syndrom 1B haben weder *myo7a* in der Wildtyp-Retina, noch einen visuellen Defekt in der entsprechenden *mariner* Mutante gefunden. Wir haben ein zweites *myo7a*-Paralog identifiziert *(myo7a2)* und Antikörper gegen jenes Zebrafischprotein hergestellt, das vom ersten Paralog kodiert wird. Mittels immunhistochemischen Färbungen haben wir Myo7a im sogenannten ‚accessory outer segment' (AOS) der Zapfen gefunden. Da diese Teleosten-typische Struktur bislang im Zebrafisch nicht beschrieben wurde, haben wir deren Ultrastruktur untersucht. Das AOS geht aus dem Zilium, welches inneres und äusseres Segment miteinander verbindet, hervor und läuft dem äusseren Segment entlang mit dem es über eine dünne, zytoplasmatische Brücke verbunden ist.

Im Gegensatz zur *mariner* Mutante weist die *bumper* Mutante einen starken visuellen Defekt auf. Obwohl der betroffene Lokus nun genetisch kartiert ist, steht die Identifikation des zugrundeliegenden Gendefekts noch aus. *bumper* wurde in einem Mutagenesescreen als Linsenmutante identifiziert. Eine genauere Analyse hat nun ergeben, dass das Linsenepithel zuerst hyperproliferiert, dann aber wieder rückläufig ist. Zudem haben die sekundären Linsenfasern, nicht aber die primären, einen

Differenzierungsdefekt. Obwohl die *bumper* Retina morphologisch normal ist, sind *bumper* Mutanten funktionell blind.

Die Sehleistung einer Augenmutante, wie beispielsweise *bumper*, kann durch Messen der optokinetischen Antwort (OKR) bestimmt werden. Als OKR wird eine stereotype Augenbewegung bezeichnet, die durch langsame Bewegungsmuster im Gesichtsfeld ausgelöst wird. Die OKR von Zebrafischlarven lässt sich hervorragend erfassen, da sich ihre dunkel pigmentierten Augen deutlich vom transparenten Körper abheben. Wir haben eine Computer-basierte Methode beschrieben, die es erlaubt die OKR so präzise zu analysieren, dass selbst äusserst subtile Sehdefekte beschrieben werden können.

Ein Projekt meiner Doktorarbeit war in Zusammenarbeit mit einer Künstlerin. Das Produkt dieses transdisziplinären Projektes ist die interaktive Skulptur *The Electric Retina*, welche die Augenforschung am Zebrafisch künstlerisch interpretiert. Das Kunstwerk zeigt einerseits Abbildungen aus unserer Forschung und gleichzeitig verfremdete Bilder der Unterwasserwelt, welche die Sicht des kranken Zebrafisches darstellen. Dieses Konzept ermöglicht es dem Betrachter zu verstehen, wie der Zebrafisch helfen kann, das visuelle System zu erforschen.

1. GENERAL INTRODUCTION

1.1. Forward Genetics in Zebrafish: Potentials and Limitations

'We have chosen the tropical freshwater cyprinid zebrafish *Brachydanio rerio* for several desirable attributes' proclaimed George Streisinger and his colleagues 30 years ago (Streisinger et al., 1981). This work brought the zebrafish (today simply *Danio rerio*) from the rice fields in South East Asia into laboratories all around the world culminating in a special issue of *Development* (*Development* 123, 1996) fully dedicated to zebrafish already 15 years later demonstrating its significance as a vertebrate model organism in biomedical research. In particular developmental biologists and geneticists appreciate the high number of transparent offspring, the amazingly fast and extracorporal development and the short generation time (Streisinger et al., 1981).

The zebrafish genome which is fully sequenced and nearly assembled (http://www.sanger.ac.uk/Projects/D_rerio/) can be easily manipulated by mutagenesis (Mullins et al., 1994; Solnica-Krezel et al., 1994). Given the ease to keep a high number of fish lines, large scale mutagenesis is a powerful tool - unprecedented in other vertebrate model organisms - to generate large numbers of mutant strains. In order to create a mutant line, an adult male zebrafish is exposed to water containing *N*-ethyl-*N*-nitrosourea (ENU), a potent mutagen inducing germ cell mutations (Figure 1). Outcrossing an ENU-treated male with a wild-type female then gives rise to a F1 progeny carrying various recessive mutations. To isolate a certain mutagenized fish strain, a heterozygous F1 fish is again crossed with wild-type fish resulting in a F2 family which in turn is randomly incrossed. If both of the mated siblings carry the recessive mutation, statistically 25% of their offspring displays the mutant phenotype (Mullins et al., 1994).

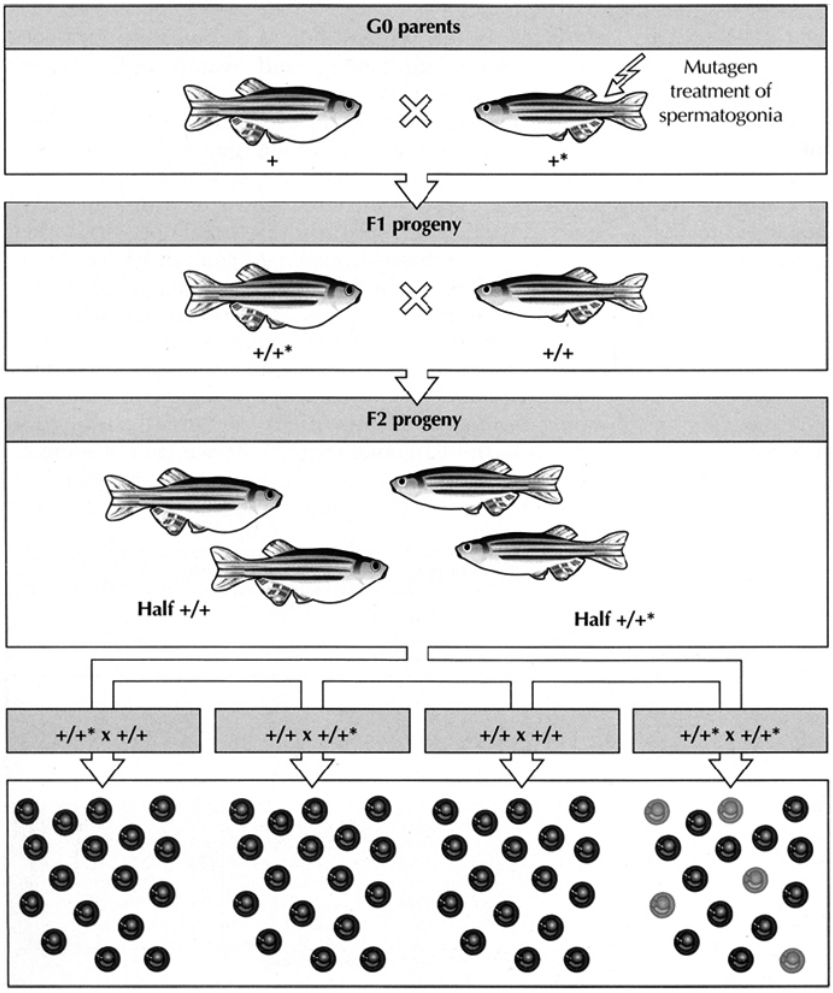

Figure 1 Crossing scheme to isolate a mutant strain in a forward genetics screen. The cross of a randomly mutagenized (+*) male to a wild-type female (+) results in the F1 progeny consisting of heterozygous carriers (+/+*). To isolate a certain mutant strain a particular F1 individual is crossed to a wild-type fish. Half of the resultant F2 progeny is heterozygous and carries the mutation. If two heterozygous carriers are incrossed 25% of the offspring is homozygous (+*/+*) for the mutation. (Modified from Mullins et al., 1994)

In a large-scale screen a particular phenotype must be identifiable efficiently. By means of an appropriate assay it is possible to identify subtle phenotypes not apparent by visual inspection. In zebrafish screens for vision mutants several behavioural assays have been successfully applied in order to reveal deficiencies in development of visual pathways in a fast and reliable way (Figure 2). Typically, a potential vision mutant is exposed to a visual stimulus such as moving stripes or a light flash eliciting a certain visually mediated behaviour. This behavioural response is investigated and compared to wild-type behaviour. An impaired visual performance may indicate a mutation affecting the visual system and can then be analyzed in more detail (Brockerhoff et al., 1995; Neuhauss et al., 1999).

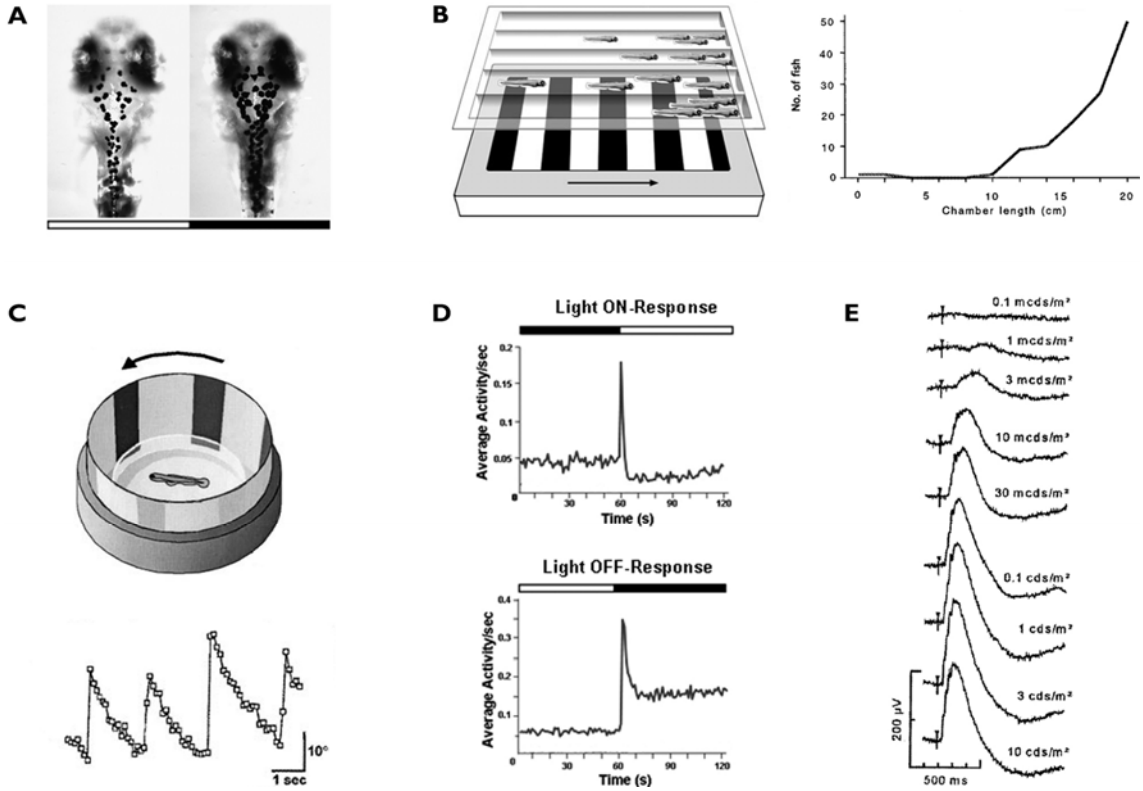

Figure 2 Functional assays for testing vision. **(A)** Visual background adaptation, VBA **(B)** Optomotor response, OMR **(C)** Optokinetic response, OKR **(D)** Visual-mediated response, VMR and **(E)** Electroretinogram, ERG. All pictures show wild-type situations. Modified from Neuhauss et al., 1999 (B, C and E), Neuhauss, 2003 (B) and Emran et al., 2008 (D).

Visual background adaptation (VBA, Figure 2A) is a physiological response of body pigmentation to ambient light. The extent of VBA can be used as a criterion in a vision screen. Adapted to a light background a wild-type zebrafish larva appears pale, adaptation to a dark background leads to a blackish outer appearance. The underlying mechanism takes place in melanophores, the melanin-containing pigment cells. Depending on the visual input of the retina, the pituitary gland is induced via the hypothalamus to secrete either melanin-concentrating hormone (MCH) in the case of light or melanocyte-stimulating hormone (MSH) in the absence of light. The light dependent hormone release induces dispersion or aggregation of pigment granuli within the melanophores leading to a pale or darkish outer appearance, respectively (Logan et al., 2006). The degree of VBA is a qualitative measure for visual ability as blind mutants do not adapt to light. In a screen for visually impaired mutants the failure of melanosome aggregation as a consequence of adaptation to a light background can be macroscopically observed. The zebrafish mutant *bumper* is such a functionally blind fish unable to adapt to a light background. This mutant

was isolated in a large scale mutagenesis screen focused on genes involved in zebrafish development (Haffter et al., 1996) and later characterized as a lens mutant (Haffter and Nusslein-Volhard, 1996; Heisenberg et al., 1996; Neuhauss et al., 1999; Schonthaler et al., 2010).

The optomotor response (OMR, Figure 2B) assay is a tool to test zebrafish larvae for blindness by exposing them to directionally moving stripes. As an innate reflex, wild-type larvae follow the motion in the surround by swimming in direction of the movement. In a large scale screen for vision mutants clutches of zebrafish larvae are placed on top of a moving grate in a transparent basin. Wild-type larvae follow the grating and eventually they pole on one end of the basin whereas vision mutants are distributed randomly. Provided a zebrafish mutant has no locomotion deficits missing OMR is a clear indication for visual impairment (Neuhauss et al., 1999; Orger and Baier, 2005).

The optokinetic response (OKR, Figure 2C) is another very robust innate visual-meditated behaviour elicited by slow movements in the surround. The OKR is characterized by stereotyped eye movements tracking moving objects in the visual field. Zebrafish larvae having strongly pigmented eyes standing out against the transparent body are suitable specimens to study the OKR in vertebrates (reviewed in Huang and Neuhauss, 2008). Mechanically immobilized and exposed to a striped rotating drum zebrafish larvae show a strong OKR observable with a dissecting microscope. In a large scale mutagenesis screen up to 20 larvae can be simultaneously tested within less than a minute (Neuhauss et al., 1999). For quantitative analysis the OKR elicited by a computer-generated sine-wave grating moving forth and back is automatically tracked and statistically evaluated (Hodel and Neuhauss, 2008; Rinner et al., 2005). By this means properties of the moving grate such as contrast, colour, temporal or spatial frequency can easily be changed during a session making the OKR a powerful assay in screening mutants even with subtle visual defects. Exemplarily, the *partial optokinetic b* (*pob*) mutant shows a normal OKR when exposed to black and white stripes but a reduced response to a red - black grating (Brockerhoff et al., 1997). Thus, it was possible to find a red blind zebrafish mutant by testing the OKR under this specific condition.

The visual mediated response (VMR, Figure 2D) is caused by a sudden and dramatic change in ambient light intensity and expressed in immediate increase of motor activity. This behaviour can easily be analysed in large scale zebrafish larvae older than 4dpf (Emran et al., 2008), nevertheless it has not been used to screen for vision mutants. Since this approach is independent of motion detection it could be applied to OMR- and OKR-blind mutants in order to specify the visual defect in more detail.

The electroretinogram (ERG, Figure 2E) is the change in the electrical sum potential of the eye as a response to a light flash recorded with an electrode placed on the cornea. It is characterized by a composite wave of three major components each corresponding to the activity of a certain retinal cell type. The small negative deflection representing the activity of photoreceptor cells is followed by two positive deflections. The earlier and larger deflection is due to the activity of ON bipolar cell whereas the smaller deflection emerges only after the light flash and is caused by OFF bipolar cell activity. Such an electrophysiological approach allows the location of a vision defect within the retina (reviewed in Dowling, 1987).

Since the forward genetic approach is based on random mutagenesis it is not possible to target a particular gene of interest. However, using appropriate screening criteria many mutants could already be isolated and identified as models for human diseases. Among them are mutants originally found in a screen for locomotor deficiency (Granato et al., 1996) and later described as defective in hair cell mechanosensation (Nicolson et al., 1998). Three of these mutants are now known as models for human Usher Syndrome (Ernest et al., 2000; Seiler et al., 2005; Sollner et al., 2004). The Usher syndrome (USH) is an autosomal recessive hereditary disease, which impairs both the retina and the organ of Corti causing retinitis pigmentosa and hearing defects (Usher, 1914). USH is the most common cause of human sensorineural vision and hearing loss. There are three clinical subtypes of USH (USH1, USH2 and USH3), distinguished by differences in onset and degree of retinal and auditory symptoms (Davenport and Omenn, 1977). The three USH zebrafish mutants identified so far (Table 1) are all defective in genes related to USH1, the most severe subtype which is characterized by innate deafness and early onset of retinitis pigmentosa leading to complete blindness.

Table 1: Usher Syndrome (USH) zebrafish mutants

Zebrafish Mutant	USH Subtype	Defective Gene	Reference
sputnik	USH1D	*cadherin23*	Sollner et al., 2004
mariner	USH1B	*myosin7a*	Ernest et al., 2000
orbiter	USH1F	*protocadherin15*	Seiler et al., 2005

Another drawback of forward genetics is the time consuming and difficult identification of the mutated gene. Reverse genetics offers a more straightforward alternative in terms of manipulation of a particular gene and the investigation of its effect. With the turn of the century the morpholino reverse genetic technique has been established in zebrafish. It allows a transient knockdown of any gene of choice (Nasevicius and Ekker, 2000). Morpholino antisense oligomers reversibly inactivate a defined gene by specific binding to mRNA and blockage of its translation or its splicing (Summerton, 1999; Summerton and Weller, 1997). As Morpholino oligonucleotides - injected into one-cell stage zebrafish embryos - are diluted by every cell division the effect is non-permanent. In the last few years heritable reverse genetic approaches have been adopted to zebrafish. TILLING (**t**argeting **i**nduced **l**ocal **l**esions **in g**enomes) is a reverse genetic technique based on target selected mutagenesis and first described in plants (McCallum et al., 2000). The procedure starts off as described above with the outcross of an ENU mutagenized male to a wild-type female. Instead of going on with the three generation cross resulting in an elaborate phenotypic analysis of the F3 progeny (see Figure 1), the genomic DNA of every F1 fish is investigated directly by PCR. Defined primers amplify a gene fragment of interest which in turn is denatured and rehybridized. If a F1 fish is heterozygous for this gene region half of the rehybridized double stands contain mismatches. As particular restriction enzymes selectively cut mismatched double strands the number of DNA fragments after such a restriction digest gives information about the genotype. After verification of the genotype by direct sequencing the identified F1 fish becomes the founder of a mutant strain (Wienholds et al., 2003). Alternatively, the mutation can be identified by direct sequencing of nested PCR products of F1 zebrafish (Wienholds et al., 2002). Another reverse genetic approach is based on zinc finger nucleases (ZFN). Designed ZFNs recognize a specific DNA site and cleave the double strand at this position. Depending on the endogenous repair machinery a deletion or insertion is induced in germ line genome (Porteus and Carroll, 2005). In zebrafish, mRNA encoding a particular ZFN is injected into one-cell stage embryos leading to a hereditary mutant allele of a gene of interest (Doyon et al., 2008; Meng et al., 2008).

1.2. Zebrafish Outer Retina and Optical Apparatus

The vertebrate outer retina harbours two main photoreceptor types: rods and cones differing both in shape (Figure 3A) and function. The elongate and slender rod photoreceptor cell is used for low-light vision as its visual pigment rhodopsin is very light sensitive. This benefit comes at the expenses of saturation in bright light, low temporal and spatial resolution and monochromatism. The rod's weaknesses are the cone's strengths: cone photoreceptors provide high temporal and spatial resolution and enable colour vision since there are different cone types with different maximal absorption frequencies. Cones are less light sensitive then rods thus their contribution to perception is shifted toward higher light intensities. Cones start to contribute to vision at starlight intensity and still function in bright light, when rods are already long saturated. Such a duplex retina comprising rod and cone receptors allows visual performance under a wide range of light intensities enabling adaptive behaviour in a variety of habitats at different times of the day (reviewed in Purves et al., 2001).

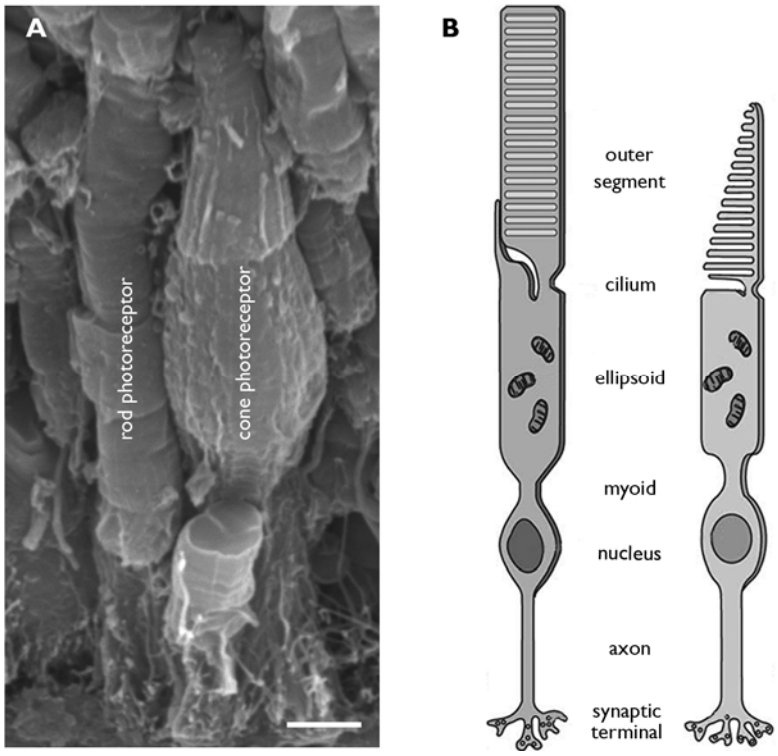

Figure 3 Rod and cone photoreceptor structure. **(A)** Scanning electron microscopic picture of adult zebrafish rod and cone; scale bar = 2,5µm **(B)** Schematic drawings of vertebrate rod (left) and cone (right) photoreceptors. B modified from Purves et al. 2001.

Although shape and function of vertebrate rod and cone photoreceptors are obviously different, the structural concept of the cell is the same (Figure 3B). Photoreceptors are highly polarised cells located in the outer retina which span from the retinal pigment epithelium to the outer synaptic layer. The photoreceptor outer segment consists of discs anchoring opsin molecules that belong to the seven transmembrane protein class. There, conversion of light to an electrical signal starts by a photochemical reaction initiating the visual transduction cascade. The outer segment is connected to the inner segment by a non-motile cilium. The inner segment is made up of ellipsoid and myoid. The ellipsoid is packed with mitochondria supplying the photoreceptor with energy whereas the myoid connects the metabolically active part of the photoreceptor cell to the nucleus. In vertebrates such as teleosts, that undergo morphological dark and light adaptation in the outer retina, the myoid is able to contract and elongate very dynamically during adaptation processes. The most apical part of the photoreceptor consists of the nucleus belonging to the outer nuclear layer, the axon and the synaptic ending (reviewed in Mustafi et al., 2009). To relay information along the visual pathway, photoreceptors form synapses with bipolar cells in the outer plexiform layer which in turn form synapses with ganglion cells in the inner plexiform layer. Horizontal and amacrine cells belonging to the inner nuclear layer modulate this information flow. The axons of ganglion cells form the optical nerve carrying the visual information from the retina to the tectum (Figure 4).

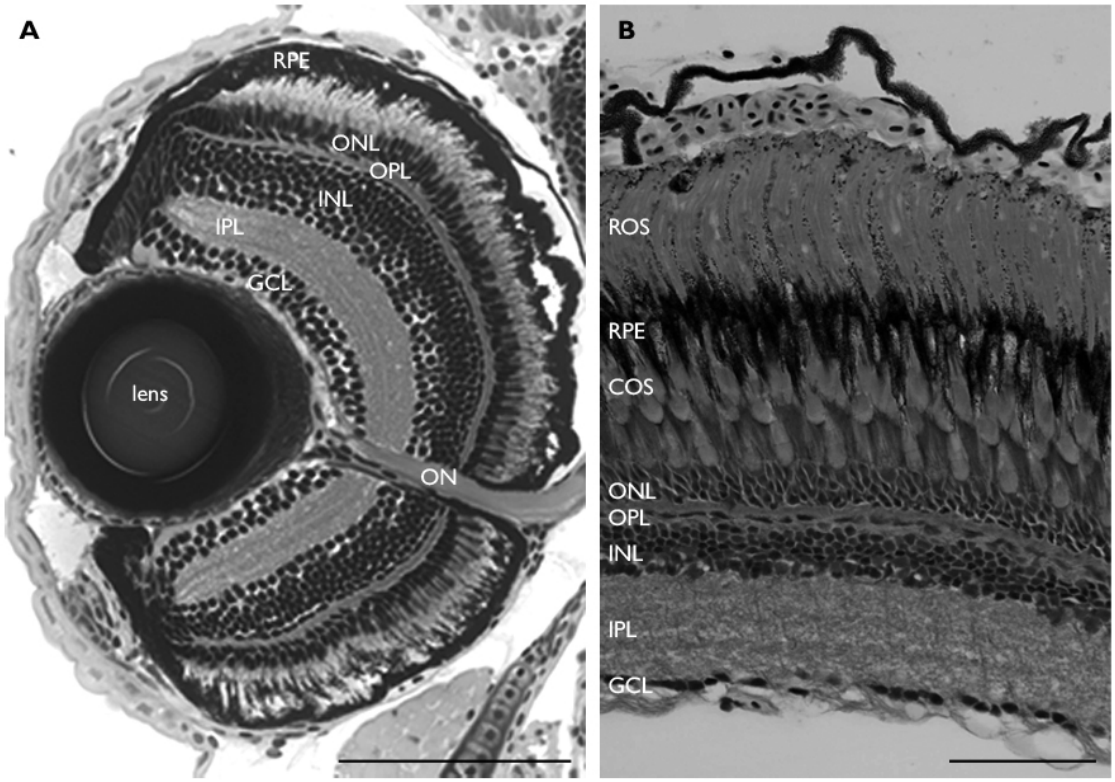

Figure 4 Light micrographs of radial sections of a larval zebrafish eye at 5dpf **(A)** and an adult zebrafish retina **(B)**. COS, cone outer segment; GCL, ganglion cell layer; INL, inner nuclear layer; IPL, inner plexiform layer; ON, optical nerve; ONL, outer nuclear layer; OPL, outer plexiform layer; RPE, retinal pigment epithelium; ROS, rod outer segment; Scale bars: A = 100µm; B = 50µm

The zebrafish retina contains four different cone types with absorption maxima at 570nm (red), 480nm (green), 415nm (blue) and 362nm (UV) (Robinson et al., 1993). Nevertheless, there are more than only four different cone opsins expressed in zebrafish cones. So far, two red (LWS-1 and LWS-2), four green (RH2-1 through RH2-4), a single blue (SWS1) and a single ultraviolet (SWS2) opsin have been identified in zebrafish (Chinen et al., 2003). The four zebrafish cone types not only differ in terms of opsin expression but also in morphology. Whereas UV cones are shorter than the other three cone types, red and green cones form so called double cones characterized by an attached inner segment. The functional consequences of this pairing remain uncertain, possible roles include contribution to motion detection (Schaerer and Neumeyer, 1996), polarization sensitivity (Novales Flamarique et al., 1998), optical (Richter and Simon, 1974) or electrical coupling (Marchiafava et al., 1985). In most teleosts the four cone types are arranged in a regular and repetitive way resulting in a mosaic-like pattern (Figure 5). Different types of cone mosaics have been described varying in terms of double cone axis and the relative position of a certain cone type within the pattern array (Eigenmann and Shafer, 1900; Engström, 1963; Lyall, 1957). The cones of the zebrafish retina are arranged

in a typical row mosaic characterized by alternating rows of double cones with parallel axes and a row of alternate blue and UV cones (Engström, 1960).

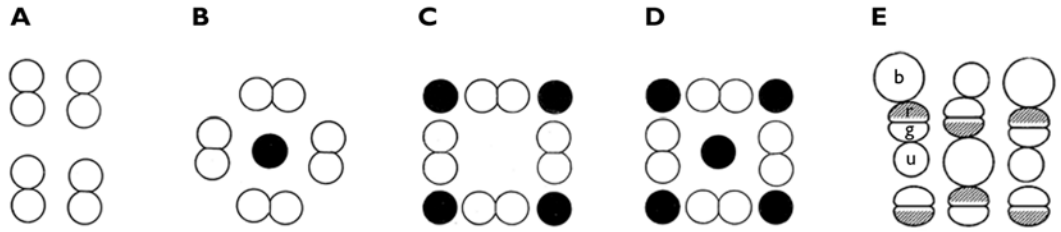

Figure 5 Cone mosaic types found in fish **(A)** Row mosaic. **(B-D)** Square mosaics. White circles: double cones; black circles: single cones; modified from Eigenmann and Shafer, 1900. **(E)** Row mosaic as found in zebrafish. b: blue cone, r/g: red-green double cone, u: uv cone; modified from (Tohya et al., 1999)

Before light hits the retina it passes the anterior segment of the eye. Part of this non-neuronal tissue is the optical apparatus which refracts the incident light. Thereby, the visual image is transmitted and focused. Although the optical apparatus comprises of the cornea, the anterior chamber, the lens and the vitreous cavity, in aquatic species the lens is the only refractive element. The teleost lens is spherical and rigid unable to change its circular curvature. To bring the image in focus teleosts alter the position of the lens instead of its shape. Teleosts and all other bony fish are special among vertebrates in terms of their relaxed mode of accommodation as they are adjusted for near vision in the relaxed accommodative state. Hence, without contribution to accommodation objects lying in short distance are in sharp focus (Douglas and Djamgoz, 1990; Wehner and Gehring, 1990). In order to accommodate to infinity the lens is moved back (from nasal to temporal) by contraction of the retractor lentis muscle (Beer, 1894). However, zebrafish do most likely not move their lens at all as this muscle appears to be vestigial in zebrafish (Gray et al., 2009).

1.3 When Worlds Collide: Neuroscience and Art

Leonardo da Vinci (1452-1519) is probably known as the most famous universal genius being professionally involved in both science and humanities. As a painter and anatomist Leonardo dissected human bodies by himself when he drew the corresponding anatomical illustrations, which were of equally high artistic as well as scientific quality. Times changed since Renaissance as nowadays trained scientific illustrators usually draw what scientists have previously explored. In this case artist and scientist complement one another with each partner fulfilling their specific task. In other words, the role of the artist is often restricted to be an illustrator while the scientist does the research. When artists meet scientists to collaborate it often ends in the stair case of the scientific institute where another sculpture representing the DNA helix is part of the metal stair railing and artistically edited science photographs decorate gray concrete walls. For more advanced interpretations and transfers of scientific elements to art however, a deeper insight into a particular research topic is necessary. This requirement can only be met when artists have the opportunity to be a temporary resident in a scientific lab thus obtaining a more complete view of the different research aspects (Webster, 2005). In Switzerland the Artists-in-Labs program brings artists and scientists together allowing a mutual and productive collaboration to take place (www.artistsinlabs.ch).

Interdisciplinary collaborations between neuroscience and art hold special potential as both deal with perception. From the mechanistic perspective of neuroscience, the nervous system is regarded as a highly sophisticated tool which enables animals, including humans, to perceive the outer world and interact with the environment. Depending on the specific equipment of this toolbox, the very same object is perceived in many different ways. What we call visible spectrum of colour cannot be seen at all by colour-blind species whereas most birds and fish can additionally perceive UV light which is in turn invisible to the human eye. Thus, even at the level of sensory processing perception is subjective (Brown and Lindsey, 2004). Several artists suffering from colour asthenopia has been established (Lanthony, 1999) such as the Australian expressionist painter Clifton Pugh who was red blind (Cole and Harris, 2009; Figure 6). Although these artists perceive the colours of their own paintings differently than most of the viewers they are still universally perceived as art.

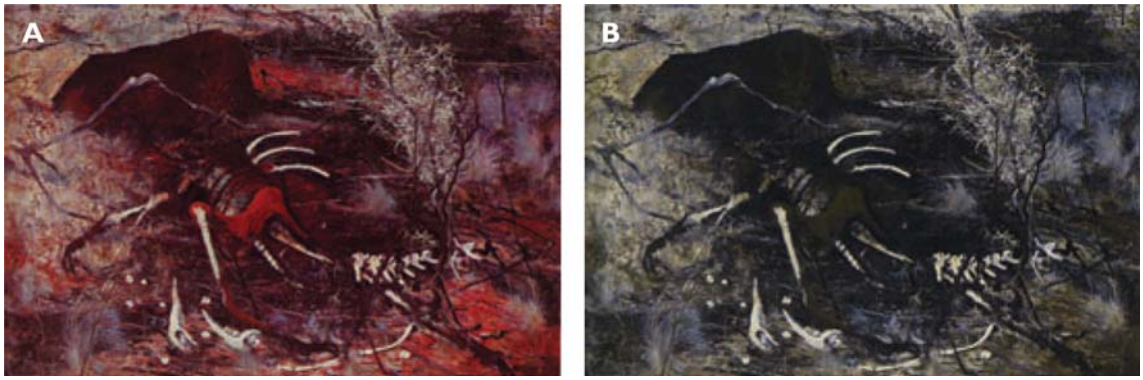

Figure 6 (A) A painting by Clifton Pugh. **(B)** The same painting digitally transformed to the colour appearance for a protanope (modified from Cole and Harris, 2009)

Even assuming that the neurobiological basis of human senses is practically identical, the subjectivity cannot be withdrawn. Depending on experience, cultural education or personality perception of art is different. And even on the level of a single individual perception depends on the present emotional state. The interplay of art and neuroscience has great potential. There is stimulating breeding ground when art meets neuroscience. It is more than transporting knowledge out of a neurobiological laboratory by means of a piece of art a layperson feels to fully conceive. As important as the visible product is the evolution of mutual interaction during the whole process. Art and neuroscience is a cross-pollinating duo more attraction should be paid on.

1.4 References

Beer, T. (1894). Accomodation des Fischauges. Pflugers Arch *58*, 523-650.

Brockerhoff, S. E., Hurley, J. B., Janssen-Bienhold, U., Neuhauss, S. C., Driever, W., and Dowling, J. E. (1995). A behavioral screen for isolating zebrafish mutants with visual system defects. Proc Natl Acad Sci U S A *92*, 10545-10549.

Brockerhoff, S. E., Hurley, J. B., Niemi, G. A., and Dowling, J. E. (1997). A new form of inherited red-blindness identified in zebrafish. J Neurosci *17*, 4236-4242.

Brown, A. M., and Lindsey, D. T. (2004). Color and language: worldwide distribution of Daltonism and distinct words for "blue". Vis Neurosci *21*, 409-412.

Chinen, A., Hamaoka, T., Yamada, Y., and Kawamura, S. (2003). Gene duplication and spectral diversification of cone visual pigments of zebrafish. Genetics *163*, 663-675.

Cole, B. L., and Harris, R. W. (2009). Colour blindness does not preclude fame as an artist: celebrated Australian artist Clifton Pugh was a protanope. Clin Exp Optom *92*, 421-428.

Davenport, S. L. H., and Omenn, G. S. (1977). The Heterogeneity of Usher Syndrome. Int Conf Birth Defects, Vth, Montreal.

Douglas, R. H., and Djamgoz, M. B. (1990). The visual system of fish. Chapman and Hall, London.

Dowling, J. E. (1987). The retina: an approachable part of the brain. Cambridge: Harvard University Press.

Doyon, Y., McCammon, J. M., Miller, J. C., Faraji, F., Ngo, C., Katibah, G. E., Amora, R., Hocking, T. D., Zhang, L., Rebar, E. J.*, et al.* (2008). Heritable targeted gene disruption in zebrafish using designed zinc-finger nucleases. Nat Biotechnol *26*, 702-708.

Eigenmann, C. H., and Shafer, G. D. (1900). The mosaic of single and twin cones in the retina of fishes. Am Nat *34*, 109-118.

Emran, F., Rihel, J., and Dowling, J. E. (2008). A behavioral assay to measure responsiveness of zebrafish to changes in light intensities. J Vis Exp.

Engström, K. (1960). Cone types and cone arrangement in the retina of some cyprinids. Acta Zoologica *41*, 277-295.

Engström, K. (1963). Cone types and cone arrangements in teleost retinae. Acta Zoologica *44*, 179-243.

Ernest, S., Rauch, G. J., Haffter, P., Geisler, R., Petit, C., and Nicolson, T. (2000). Mariner is defective in myosin VIIA: a zebrafish model for human hereditary deafness. Hum Mol Genet *9*, 2189-2196.

Granato, M., van Eeden, F. J., Schach, U., Trowe, T., Brand, M., Furutani-Seiki, M., Haffter, P., Hammerschmidt, M., Heisenberg, C. P., Jiang, Y. J.*, et al.* (1996). Genes controlling and mediating locomotion behavior of the zebrafish embryo and larva. Development *123*, 399-413.

Gray, M. P., Smith, R. S., Soules, K. A., John, S. W., and Link, B. A. (2009). The aqueous humor outflow pathway of zebrafish. Invest Ophthalmol Vis Sci *50*, 1515-1521.

Haffter, P., Granato, M., Brand, M., Mullins, M. C., Hammerschmidt, M., Kane, D. A., Odenthal, J., van Eeden, F. J., Jiang, Y. J., Heisenberg, C. P.*, et al.* (1996). The identification of genes with unique and essential functions in the development of the zebrafish, Danio rerio. Development *123*, 1-36.

Haffter, P., and Nusslein-Volhard, C. (1996). Large scale genetics in a small vertebrate, the zebrafish. Int J Dev Biol *40*, 221-227.

Heisenberg, C. P., Brand, M., Jiang, Y. J., Warga, R. M., Beuchle, D., van Eeden, F. J., Furutani-Seiki, M., Granato, M., Haffter, P., Hammerschmidt, M.*, et al.* (1996). Genes involved in forebrain development in the zebrafish, Danio rerio. Development *123*, 191-203.

Hodel, C., and Neuhauss, S. C. (2008). Computer-based analysis of the optokinetic response in zebrafish larvae. CSH Protocols *2008*, prot4961.

Huang, Y. Y., and Neuhauss, S. C. (2008). The optokinetic response in zebrafish and its applications. Front Biosci *13*, 1899-1916.

Lanthony, P. (1999). [Blindness in painters]. J Fr Ophtalmol *22*, 700-708.

Logan, D. W., Burn, S. F., and Jackson, I. J. (2006). Regulation of pigmentation in zebrafish melanophores. Pigment Cell Res *19*, 206-213.

Lyall, A. H. (1957). Cone arrangements in teleost retinae. Quarterly Journal of Microscopical Science *98*, 189-201.

Marchiafava, P. L., Strettoi, E., and Alpigiani, V. (1985). Intracellular recording from single and double cone cells isolated from the fish retina (Tinca tinca). Exp Biol *44*, 173-180.

McCallum, C. M., Comai, L., Greene, E. A., and Henikoff, S. (2000). Targeting induced local lesions IN genomes (TILLING) for plant functional genomics. Plant Physiol *123*, 439-442.

Meng, X., Noyes, M. B., Zhu, L. J., Lawson, N. D., and Wolfe, S. A. (2008). Targeted gene inactivation in zebrafish using engineered zinc-finger nucleases. Nat Biotechnol *26*, 695-701.

Mullins, M. C., Hammerschmidt, M., Haffter, P., and Nusslein-Volhard, C. (1994). Large-scale mutagenesis in the zebrafish: in search of genes controlling development in a vertebrate. Curr Biol *4*, 189-202.

Mustafi, D., Engel, A. H., and Palczewski, K. (2009). Structure of cone photoreceptors. Prog Retin Eye Res *28*, 289-302.

Nasevicius, A., and Ekker, S. C. (2000). Effective targeted gene 'knockdown' in zebrafish. Nat Genet *26*, 216-220.

Neuhauss, S. C. (2003). Behavioral genetic approaches to visual system development and function in zebrafish. J Neurobiol *54*, 148-160.

Neuhauss, S. C., Biehlmaier, O., Seeliger, M. W., Das, T., Kohler, K., Harris, W. A., and Baier, H. (1999). Genetic disorders of vision revealed by a behavioral screen of 400 essential loci in zebrafish. J Neurosci *19*, 8603-8615.

Nicolson, T., Rusch, A., Friedrich, R. W., Granato, M., Ruppersberg, J. P., and Nusslein-Volhard, C. (1998). Genetic analysis of vertebrate sensory hair cell mechanosensation: the zebrafish circler mutants. Neuron *20*, 271-283.

Novales Flamarique, I., Hawryshyn, C. W., and Harosi, F. I. (1998). Double-cone internal reflection as a basis for polarization detection in fish. J Opt Soc Am A Opt Image Sci Vis *15*, 349-358.

Orger, M. B., and Baier, H. (2005). Channeling of red and green cone inputs to the zebrafish optomotor response. Vis Neurosci *22*, 275-281.

Porteus, M. H., and Carroll, D. (2005). Gene targeting using zinc finger nucleases. Nat Biotechnol *23*, 967-973.

Purves, D., Augustine, G. J., Fitzpatrick, D., Katz, L. C., LaManita, A., McNamara, J. O., and Williams, S. M. (2001). Neuroscience. Sinauer Associates, Inc Publisher, Sunderland, Massachusetts.

Richter, A., and Simon, E. J. (1974). Electrical responses of double cones in the turtle retina. J Physiol *242*, 673-683.

Rinner, O., Rick, J. M., and Neuhauss, S. C. (2005). Contrast sensitivity, spatial and temporal tuning of the larval zebrafish optokinetic response. Invest Ophthalmol Vis Sci *46*, 137-142.

Robinson, J., Schmitt, E. A., Harosi, F. I., Reece, R. J., and Dowling, J. E. (1993). Zebrafish ultraviolet visual pigment: absorption spectrum, sequence, and localization. Proc Natl Acad Sci U S A *90*, 6009-6012.

Schaerer, S., and Neumeyer, C. (1996). Motion detection in goldfish investigated with the optomotor response is "color blind". Vision Res *36*, 4025-4034.

Schonthaler, H. B., Franz-Odendaal, T. A., Hodel, C., Gehring, I., Geisler, R., Schwarz, H., Neuhauss, S. C., and Dahm, R. (2010). The zebrafish mutant bumper shows a

hyperproliferation of lens epithelial cells and fibre cell degeneration leading to functional blindness. Mech Dev *127*, 203-2019.

Seiler, C., Finger-Baier, K. C., Rinner, O., Makhankov, Y. V., Schwarz, H., Neuhauss, S. C., and Nicolson, T. (2005). Duplicated genes with split functions: independent roles of protocadherin15 orthologues in zebrafish hearing and vision. Development *132*, 615-623.

Sollner, C., Rauch, G. J., Siemens, J., Geisler, R., Schuster, S. C., Muller, U., and Nicolson, T. (2004). Mutations in cadherin 23 affect tip links in zebrafish sensory hair cells. Nature *428*, 955-959.

Solnica-Krezel, L., Schier, A. F., and Driever, W. (1994). Efficient recovery of ENU-induced mutations from the zebrafish germline. Genetics *136*, 1401-1420.

Streisinger, G., Walker, C., Dower, N., Knauber, D., and Singer, F. (1981). Production of clones of homozygous diploid zebra fish (Brachydanio rerio). Nature *291*, 293-296.

Summerton, J. (1999). Morpholino antisense oligomers: the case for an RNase H-independent structural type. Biochim Biophys Acta *1489*, 141-158.

Summerton, J., and Weller, D. (1997). Morpholino antisense oligomers: design, preparation, and properties. Antisense Nucleic Acid Drug Dev *7*, 187-195.

Tohya, S., Mochizuki, A., and Iwasa, Y. (1999). Formation of cone mosaic of zebrafish retina. J Theor Biol *200*, 231-244.

Usher, C. H. (1914). On the inheritance of retinitis pigmentosa, with notes of cases. R Lond Ophthalmol Hosp Rep *19*, 130- 236.

Webster, S. (2005). Science and society: art and science collaborations in the United Kingdom. Nat Rev Immunol *5*, 965-969.

Wehner, R., and Gehring, W. (1990). Zoologie. Georg Thieme Verlag Stuttgart.

Wienholds, E., Schulte-Merker, S., Walderich, B., and Plasterk, R. H. (2002). Target-selected inactivation of the zebrafish rag1 gene. Science *297*, 99-102.

Wienholds, E., van Eeden, F., Kosters, M., Mudde, J., Plasterk, R. H., and Cuppen, E. (2003). Efficient target-selected mutagenesis in zebrafish. Genome Res *13*, 2700-2707.

2. FISHING FOR A SECOND *POB* PARALOGUE IN ZEBRAFISH

Corinne Hodel[1], Matthias Gesemann[1], Kara Dannenhauer[1] and Stephan C.F. Neuhauss[1]

[1] University of Zurich, Institut of Zoology and Institut of Molecular Life Science, Winterthurerstrasse 190, 8057 Zurich

Research report on a completed study.

Sequence has been reported on NCBI (Accession number: HM044316).

Personal contribution

Project idea; writing of the manuscript; cloning of the full-length sequence together with K.D; bioinformatics together with M.G.

2.1 Introduction

Zebrafish are tetrachromats having red, green, blue and UV sensitive cones. Every cone type harbours a distinct opsin differing in terms of the absorption maxima (Robinson et al., 1993). A red-blind zebrafish mutant strain has been isolated in a classical forward genetics screen by measuring the optokinetic response (OKR) under red illumination. As the OKR is normal in white light but not in red light, the mutant strain was named *partial optokinetic response b* (*pob)* (Brockerhoff et al., 1997). The mutated gene in *pob* encodes an unknown transmembrane protein (Taylor et al., 2005). Thus, Pob is a protein other than red opsin which is essential for red cone function. Interestingly, in zebrafish its expression pattern is not restricted to red cones as the mutant phenotype would imply. Rather, Pob is expressed in the inner segment and synapses of all four cone types, the brain and even in other tissues. Intracellularly, Pob partially colocalizes with the trans-Golgi and the endoplasmatic reticulum (ER). Moreover, it has been found in small vesicles flanking the ER (Taylor et al., 2005). As the Pob protein comprises a putative signal anchor, transmembrane and protein-sorting motifs a role in protein sorting and transport is very likely (Bonifacino and Traub, 2003).

The encoded 30kDa protein Pob is the highly conserved orthologue of the human and murine transmembrane protein 111 (TMEM111) (Hu et al., 2000; Stryke et al., 2003; Zambrowicz et al., 2003). The function of the mammalian TMEM111 is unknown. However, a recent study discussed the role of TMEM111 in vesicle-mediated transport from ER to Golgi, in secretory pathways in the ER and in protein translation (Nayak et al., 2009). The finding that TMEM111 is part of the transport and secretory processes in the endomembrane system supports the predicted role of Pob in zebrafish (Taylor et al., 2005).

Here we report the existence of a second *pob* paralogue in zebrafish. We compare both nucleotide and amino acid sequences with related *pob* human and mouse orthologues and discuss potential functions of the new zebrafish Pob protein.

2.2 Material & Methods

2.2.1 *in silico* identification of a second *pob* paralogue

The zebrafish mRNA sequence *pob* (NM_213505) was used to search the *Danio rerio* genome database (http://www.ncbi.nlm.nih.gov/genome/seq/BlastGen/BlastGen.cgi?taxid=7955) for related sequences. In addition to the genomic counterpart of the NM_213505 sequence, a highly homologues but clearly not identical sequence (BX957236) was identified. This sequence was entered in Genescan Web Server (http://genes.mit.edu/GENSCAN.html) in order to automatically identify exon/intron boundaries. In addition to this computational analysis a manual search for consensus sequences of 5' and 3' splice sites has been performed (Patel and Steitz, 2003). By these means all exons and therefore the coding sequence can be identified. The alignments of both *pob* genes and both Pob proteins reveal the nucleotide and amino acid identity, respectively.

2.2.2 Cloning of the second *pob* paralogue and identification of EST clones

mRNA from 10-20 TÜ larvae at 5dpf was isolated using the RNeasy kit (Quiagen; Hombrechtikon, Switzerland). A cDNA template for the subsequent polymerase chain reaction (PCR) amplification of the second *pob* gene was generated using the SuperScript® First Strand kit (Invitrogene; Basel, Switzerland). Amplification of overlapping PCR products was achieved using oligonucelotide primers listed in Table 1. They were designed with Oligo Primer Analysis Software (Molecular Biology Insights; Cascade, USA) according to the *in silico* identified sequence. The PCR product was directly subcloned into TOPO pCR 2.1 or TOPO pCR II cloning vector (Invitrogene; Basel, Switzerland) and sequenced with M13(-20) forward and M13 reverse primer (Invitrogene; Basel, Switzerland).

In order to confirm the manually annotated sequence, three independent PCR products were sequenced and subsequently cross-referenced with the following zebrafish expressed sequence tag (EST) clones found in the non-human, non-mouse ESTs database (http://blast.ncbi.nlm.nih.gov/Blast.cgi): AI618648, AW018563, CB352265, CK127855, CK707222, CT601255, CT601256, CT603809, DN765017, EB924610, EB968651, EE695375, EE697163, EG577801, EH556545, EH577644.

Table 1: Oligonucleotide primers used for cloning of the second *pob* gene

Position relative to start codon	Primer Sequence 5' to 3'
- 148 to -1 27 sense	CGCATGTTCATACAGAAATG
0793 to 0811 antisense	GCAATCGCTGGTTCATATC
0678 to 0696 sense	GATCGTGGAGCATAAATGG
1412 to 1392 antisense	CAGTGTTTCTCAACCGTGTTC

2.2.3 Protein domain analysis

Signal sequence prediction and domain analysis were done using the SignalP (http://www.cbs.dtu.dk/services/SignalP/), TMPRED (http://www.ch.embnet.org/software/TMPRED_form.html), TMHMM (http://www.cbs.dtu.dk/services/TMHMM/) and SMART (http://smart.embl-heidelberg.de/) programs. [DE]XXXL[LI] and YXXØ motifs have been identified manually; X is any amino acid, Ø is any hydrophobic amino acid. The molecular weight of Pob1b protein was calculated using EditSeq (DNASTAR; Madison, USA).

2.3 Results

2.3.1 The zebrafish genome harbours two *pob* genes

The first *pob* gene has been shown to be mutated in the red-blind mutant *pob*. It has been mapped to linkage group 6 (Taylor et al., 2005). We found a second *pob* paralogue *in silico* on linkage group 8 by searching the *Danio rerio* genome database and the non-human, non-mouse ESTs database for related but not identical sequences of the first paralogue. In a next step we successfully cloned the second *pob* paralogue using RT-PCR. The newly identified *pob* paralogue is now named *pob1b* and the firstly discovered *pob* gene *pob1a*. We confirmed the *pob1b* sequence by sequencing of at least three independently cloned fragments in combination with cross-referencing our sequence to the EST database. We recently deposited the sequence on the NCBI database (Accession

Number: HM044316). We identified within the coding region six single nucleotide polymorphisms (SNPs) on position 40 (c or t), 88 (c or t), 267 (a or g), 300 (a or c), 384 (a or c), 444 (c or t).

Comparison of the exon length between zebrafish, mouse and human *pob* genes reveal a highly conserved exon length (Table 2). Except for the last exon of zebrafish *pob1b* all exons of the analyzed species have exactly the same number of nucleotides. In contrast, the intron length is highly different (data not shown).

Table 2: Exon length (number of base pairs) of *pob* paralogues and their orthologues

Exon number	*pob1a dr*[A]	*pob1b dr*	*pob mm*[B]	*pob hs*[C]
1	155	155	155	155
2	58	58	58	58
3	94	94	94	94
4	105	105	105	105
5	82	82	82	82
6	80	80	80	80
7	83	83	83	83
8	129	105	129	129

dr, Danio rerio; hs, Homo sapiens; mm, Mus musculus; NCBI Accession numbers of source sequences: [A]NM_213505 [B]NM_175101 [C]NM_018447

As the preserved exon length implies, *pob* genes are highly conserved. Nucleotide identity (Table 3) ranges from 71% between zebrafish *pob1b* and human *pob* to 92% between mouse and human *pob*, whereas amino acid identities ranges from 79% between zebrafish Pob1b and mouse Pob to even 99% between mouse and human Pob.

Table 3: Amino acid identity (bold values in %) and nucleotide identity (italic values in %)

	pob1a *dr*	pob1b *dr*	pob *mm*	pob *hs*
pob1a *dr*		**80**	**89**	**89**
pob1b *dr*	*73*		**79**	**79**
pob *mm*	*76*	*72*		**99**
pob *hs*	*77*	*71*	*92*	

2.3.2 Protein function defining structures are the same in both zebrafish Pob proteins

pob1b was translated to amino acid sequence. Five of the identified SNPs reveal to be silent mutations, whereas the SNP on position 40 (c or t) leads to two alleles differing in amino acid 14 which is either leucine (ctt) or phenylalanine (ttt).

The molecular weight of Pob1b is predicted as 29kDa. The first 31 amino acids comprise a putative signal anchor (Figure 1). Depending on the prediction algorithm two or three transmembrane regions are found spanning from amino acid 14-34 (15-34), 118-136 (115-137) and 163-179 (-). Moreover, one YXXØ motif and one [DE]XXXL[LI] motif has been found.

```
Pob1b  MAGPELLLDS SIR[L/F]WVVLPI VFITFFVGVL RHYITKLIHN EKKVDLQQV SDSQVLLRSRI LRENGKYLPK  70
Pob1a  MAEPELLLDS NIRLWVVLPI VFITFLVGVI RHYVSILLQS DKKLTLEQV SDSQVLIRSRV LRENGKYIPK

       QSFAMRKHYF NNPETGFFKK VKRKVTPKNP MTDPSMLTDM MKGNLTNVLP MILIGGWINW AFSGFLTTKV  140
       QSFLMRKFYF NNQEDGFFKK TKRKVVPPSP MTDPSMLTDM MKGNVTNVLP MILIGGWINW TFSGFVTTKV

       PFPLTLRFKP MLQRGIELVS LDASWVSSAS WYFLNVFGLR SMYTLILGQD NAADQSRIMQ DQMTGAAMAM  210
       PFPLTLRFKP MLQQGIELLS LDASWVSSAS WYFLNVFGLR SMYSLILGQD NGADQSRIMQ EQMSGAAMAM

       PPDPNKAFKS EWEALEIVEH KWALENVEEE LMCQDLNFRE LFN                              253
       PADTNKAFKA EWEALELTDH QWALENVEED LMSKDLDLSG MFSKDLPTGI F                     261
```

Figure 1 Amino acid sequences of both zebrafish Pob proteins and their domains. Putative signal anchor is underlined; YXXØ and [DE]XXXL[LI] motifs are highlighted green; putative

2.4 Discussion

pob1a and *pob1b* are paralogues having a very high nucleotide and amino acid identity and almost completely conserved exon length. There is no definite proof that *pob1a* and *pob1b* rises from the suggested genome duplication event in ray-finned fish (Amores et al., 1998; Postlethwait et al., 1998). However, it is very likely that it has been duplicated after the separation of the fish and mammalian lineage as the mammalian genome only has one *pob* gene. Comparison of the gene sets on linkage group 6 and 8 in proximity of *pob1a* and *pob1b*, respectively can give a hint. If such a syntenic analysis reveals the adjacent genes in the same relative position it is very likely that whole genome duplication is the cause of having two very homologues *pob* genes in the zebrafish genome.

The function of the newly identified Pob1b protein is unknown. However, the same speculation as has been made for Pob1a (Taylor et al., 2005) may be true for Pob1b as both protein sequences harbour the same structural elements. Therefore it is likely that also Pob1b is involved in protein transport and sorting. If so, Pob1b is likely to be expressed in the endomembrane system such as Golgi or ER. When a gene is duplicated three scenarios concerning the function of a duplicated gene are reasonable. The duplicated gene either losses its function (nonfunctionalisation), gains a new function (neofunctionalisation) or the original function is shared by the two paralogues (subfunctionalisation) (Force et al., 1999). As both Pob proteins are supposed to have the same function none of the three mentioned gene fates seem to be suited. Based on protein domain analysis it is very likely that Pob belongs to a complex and interacts with other proteins. Therefore the stoichometric balance has to be regarded as the number of interacting duplicated proteins has to be retained (Aury et al., 2006; Hughes et al., 2007; Semon and Wolfe, 2007).

As it is predicted for the first paralogue the protein contain either two or three putative transmembrane regions depending on the prediction algorithm. The tentative 17 amino acid sequence ASWVSSASWYFLNVFGL contains no charged but 5 polar amino acid (S and N). The remaining 12 amino acids are hydrophobic. The number of transmembrane regions is crucial as it defines whether the C terminus is inside or outside of a cell or of an organelle of the endomembrane system.

The SNP at position 40 of *pob1b* leading to either leucine or phenylalanine at position 14 of the translated amino acid sequence is not expected to influence the property of the Pob1b protein, as both side chains of these amino acids are hydrophobic. Indeed, the amino acid exchange has no influence on the prediction of a putative signal anchor or on putative transmembrane region.

2.5 References

Amores, A., Force, A., Yan, Y. L., Joly, L., Amemiya, C., Fritz, A., Ho, R. K., Langeland, J., Prince, V., Wang, Y. L.*, et al.* (1998). Zebrafish hox clusters and vertebrate genome evolution. Science *282*, 1711-1714.

Aury, J. M., Jaillon, O., Duret, L., Noel, B., Jubin, C., Porcel, B. M., Segurens, B., Daubin, V., Anthouard, V., Aiach, N.*, et al.* (2006). Global trends of whole-genome duplications revealed by the ciliate Paramecium tetraurelia. Nature *444*, 171-178.

Bonifacino, J. S., and Traub, L. M. (2003). Signals for sorting of transmembrane proteins to endosomes and lysosomes. Annu Rev Biochem *72*, 395-447.

Brockerhoff, S. E., Hurley, J. B., Niemi, G. A., and Dowling, J. E. (1997). A new form of inherited red-blindness identified in zebrafish. J Neurosci *17*, 4236-4242.

Force, A., Lynch, M., Pickett, F. B., Amores, A., Yan, Y. L., and Postlethwait, J. (1999). Preservation of duplicate genes by complementary, degenerative mutations. Genetics *151*, 1531-1545.

Hu, R. M., Han, Z. G., Song, H. D., Peng, Y. D., Huang, Q. H., Ren, S. X., Gu, Y. J., Huang, C. H., Li, Y. B., Jiang, C. L.*, et al.* (2000). Gene expression profiling in the human hypothalamus-pituitary-adrenal axis and full-length cDNA cloning. Proc Natl Acad Sci U S A *97*, 9543-9548.

Hughes, T., Ekman, D., Ardawatia, H., Elofsson, A., and Liberles, D. A. (2007). Evaluating dosage compensation as a cause of duplicate gene retention in Paramecium tetraurelia. Genome Biol *8*, 213.

Nayak, R. R., Kearns, M., Spielman, R. S., and Cheung, V. G. (2009). Coexpression network based on natural variation in human gene expression reveals gene interactions and functions. Genome Res *19*, 1953-1962.

Patel, A. A., and Steitz, J. A. (2003). Splicing double: insights from the second spliceosome. Nat Rev Mol Cell Biol *4*, 960-970.

Postlethwait, J. H., Yan, Y. L., Gates, M. A., Horne, S., Amores, A., Brownlie, A., Donovan, A., Egan, E. S., Force, A., Gong, Z.*, et al.* (1998). Vertebrate genome evolution and the zebrafish gene map. Nat Genet *18*, 345-349.

Robinson, J., Schmitt, E. A., Harosi, F. I., Reece, R. J., and Dowling, J. E. (1993). Zebrafish ultraviolet visual pigment: absorption spectrum, sequence, and localization. Proc Natl Acad Sci U S A *90*, 6009-6012.

Semon, M., and Wolfe, K. H. (2007). Consequences of genome duplication. Curr Opin Genet Dev *17*, 505-512.

Stryke, D., Kawamoto, M., Huang, C. C., Johns, S. J., King, L. A., Harper, C. A., Meng, E. C., Lee, R. E., Yee, A., L'Italien, L.*, et al.* (2003). BayGenomics: a resource of insertional mutations in mouse embryonic stem cells. Nucleic Acids Res *31*, 278-281.

Taylor, M. R., Kikkawa, S., Diez-Juan, A., Ramamurthy, V., Kawakami, K., Carmeliet, P., and Brockerhoff, S. E. (2005). The zebrafish pob gene encodes a novel protein required for survival of red cone photoreceptor cells. Genetics *170*, 263-273.

Zambrowicz, B. P., Abuin, A., Ramirez-Solis, R., Richter, L. J., Piggott, J., BeltrandelRio, H., Buxton, E. C., Edwards, J., Finch, R. A., Friddle, C. J.*, et al.* (2003). Wnk1 kinase deficiency lowers blood pressure in mice: a gene-trap screen to identify potential targets for therapeutic intervention. Proc Natl Acad Sci U S A *100*, 14109-14114.

3. MyosinVIIa as a Marker for the Cone Accessory Outer Segment

Corinne Hodel[1,2], Oliver Biehlmaier[2,3], Martina Heidemann[2], Jan Klooster[4], Matthias Gesemann[1,2], Marteen Kamermans[4] and Stephan C.F. Neuhauss[1,2]

[1] University of Zurich, Institut of Molecular Life Science, Winterthurerstrasse 190, 8057 Zurich, Switzerland

[2] University of Zurich, Institut of Zoology, Winterthurerstrasse 190, 8057 Zurich, Switzerland

[3] Current address: Swiss Federal Institute of Technology, Light Microscopy Centre, Schafmattstrasse 18, 8093 Zürich, Switzerland

[4] The Royal Netherlands Academy of Arts and Sciences, Netherlands Institute for Neuroscience, Meibergdreef 47, 1105 BA Amsterdam, The Netherlands.

Draft of a research article in preparation for publication.

Personal contribution

Writing of the manuscript; Scanning electron microscopy; Transmission electron microscopy; Fluorescence immunohistochemistry together with O.B and M.H; cloning of the full-length sequence together with M.H.; bioinformatics together with M.G.

Acknowledgement

We like to thank Franziska Baumann and Kara Dannenhauer for technical assistant with transmission electron microscopy and cloning, respectively.

3.1 Abstract

The accessory outer segment is part of the teleost photoreceptor. It appears to be the cytoplasmic prolongation of the connecting cilium running along the photoreceptor's outer segment. The basal part of an accessory outer segment contains actin filaments and microtubules. Accessory outer segment and outer segment are connected through a very thin cytoplasmic bridge. Here, we demonstrate that MyosinVIIa is a marker for the zebrafish cone accessory outer segment as its retinal expression pattern is restricted to this teleost-specific structure. Surprisingly, MyosinVIIa is not expressed in the RPE where it has been found in all other vertebrates analysed so far. We identified a second *myosinVIIa* paralogue which could be expressed in the retinal pigment epithelium. Moreover, we investigated the ultrastructure of the zebrafish's cone accessory outer segment.

3.2 Introduction

The light sensing cells in the vertebrate eye are the ciliary cone and rod photoreceptors. Basically, such a photoreceptor cell can be divided into separate compartment, consisting of the outer and inner segment, the soma and the synaptic terminal. The inner and outer segments are connected by a non-motile cilium which axoneme prolongs into the outer segment. Hence, the photoreceptor outer segment appears to be a modified primary cilium. The cilium's basal body characteristically composed of nine sets of triplet microtubules originates from the most apical edge of the inner segment. Teleost photoreceptors are special in terms of connecting cilium length and axoneme continuation beyond the connecting cilium. As the teleost connecting cilium is very short, outer and inner segment are almost in direct contact. The axoneme is not part of the outer segment but rises into an accessory structure extending alongside the outer segment. Historically, this structure is referred as 'accessory element' (Engström, 1963) or 'lateral sac' (Fineran and Nicol, 1974). Nowadays, the term 'accessory outer segment' has prevailed.

The accessory outer segment (AOS) was firstly described by Engström (1961) in gadidae as a cilium-like structure with a fine netlike cytoplasm containing fine tubules, most likely microtubules. It was found to originate from the inner segment of photoreceptors and run along the outer segment. AOS and cone outer segment are connected by a thin plasma bridge enclosed by a continuous membrane (Engström, 1963; Fineran and Nicol, 1974; Nagle et al., 1986; Yacob et al., 1977). The AOS has been described as a "slender sac of cytoplasm" (Douglas and Djamgoz, 1990) containing microtubules in the most basal part (Nagle et al., 1986; Pagh-Roehl et al., 1991; Yacob et al., 1977). The AOS has not been found in all teleost rod photoreceptors. In gadidae there is a rod AOS but "very difficult to observe" (Engström, 1961). The AOS of guppy rods is embedded within the rod outer segment instead of connected via a plasma bridge as found for the cone AOS in guppy and other species (Engström, 1963; Fineran and Nicol, 1974; Nagle et al., 1986; Yacob et al., 1977). Parrot fish do not have a rod AOS at all (Fineran and Nicol, 1974). Most vertebrates have double cones (eutheria are exceptional) characterized by two cones attached to each other at the inner segment (Rowe, 2000). Both partners appear to have an own AOS lying laterally 90° to the double cone axis on the same side (Engström, 1961; Januschka et al., 1987).

"All the cones (as also the rods) are found to have an elongated 'accessory element' of varying shape and of quite unknown function, which is to be found along the outer segment." stated Engström (1961) after having discovered the AOS. Regrettably, 50 years later AOS functions are still unknown. As in certain species AOS and retinal pigment epithelium (RPE) are in close contact a physiological relationship such as metabolic exchange was considered (Burnside et al., 1993; Yacob et al., 1977). Moreover, a role in photoreceptor stability, retinomotor movement, reservoir of high energy metabolites or transport between inner and outer segment have been suggested but never experimentally proofed (Collin et al., 1996; Fineran and Nicol, 1974; Januschka et al., 1987; Yacob et al., 1977).

In this study, we show that retinal expression of MyosinVIIa (Myo7a) in adult zebrafish is restricted to the AOS which has not yet described in *Danio rerio*. Myo7a is an unconventional myosin belonging to the myosin super family. Myosins are motor molecules, which move along actin filaments. The heads, where ATP and actin binding sites are located, are structurally conserved, whereas the tails are highly divergent (Ernest et al., 2000). Myo7a mutations in humans lead to the Usher syndrome 1B (USH1B) characterized by sensorineural vision and hearing loss. It is an autosomal recessive disease, which impairs both the retina and the organ of Corti thereby causing retinitis pigmentosa and hearing defects, respectively (Usher, 1914). In mammals, Myo7a is

expressed in cochlear and vestibular sensory hair cells of the inner ear and in photoreceptor cilia and RPE (el-Amraoui et al., 1996; Hasson et al., 1995; Liu et al., 1997; Weil et al., 1996; Wolfrum et al., 1998). The *myo7a* mouse mutant *shaker-1* (Gibson et al., 1995) does not show any degeneration of photoreceptors as found in human USH1B patients. The morphology of cilium in *shaker-1* appears normal, whereas the ciliary transport function is impaired (Liu et al., 1999). As a result, opsin accumulates in the inner segment due to a slower transport rate through the cilium. RPE analysis of *shaker-1* revealed an abnormal phagocytic process of photoreceptor outer segment disks by the RPE (Gibbs et al., 2003). Moreover, pigment granules in the *shaker-1* retina do not extend into the apical projections of the RPE, neither in dark adapted nor in light adapted retinas (Liu et al., 1998).

In zebrafish, *myo7a* has been identified as the defective gene in the *mariner* mutant (Ernest et al., 2000). *mariner* belongs to the *circler* mutants and swim – according to the name - in circles. This phenotype is due to defects in sensory hair cells (Nicolson et al., 1998; Seiler et al., 2005). *myo7a* RNA has been found in the inner ear and in the neuromasts, but not in the eye (Ernest et al., 2000). This is in contrast to other vertebrates where *myo7a* has been localised to photoreceptor cilia and RPE (el-Amraoui et al., 1996; Hasson et al., 1995; Liu et al., 1997; Weil et al., 1996; Wolfrum et al., 1998).

As mentioned above, in this study we show that Myo7a is expressed in the zebrafish eye. Our data based on a zebrafish specific antibody restrict the retinal Myo7a expression in zebrafish to the cone AOS. As this structure is not yet described in zebrafish, we performed an ultrastructural analysis of the adult zebrafish cone AOS. Our data are contradictory to another zebrafish retinal expression study investigated with an antibody against a human Myo7a epitope which nicely recognises Myo7a in zebrafish retinal extract on western blot (Lin-Jones et al., 2009). By means of fluorescence immunohistochemistry, they found Myo7a in cone inner segments, rod inner segments, cone AOS, cone axons, and cone synapses. Moreover, they describe a weaker labelling in horizontal, amacrine, and ganglion cells.

Additionally, it appears that Myo7a is not expressed in the RPE where it has been found in all other vertebrates analysed so far. We identified a second *myo7a* paralogue which could be expressed in the RPE.

3.3 Material & Methods

3.3.1 Fluorescence immunohistochemistry

Adult wild-type or albino zebrafish were sacrificed, the eye cup was removed and immediately fixed (without lens) in 4% paraformaldehyde for 40 minutes at room temperature. After washing with 150mM phosphate-buffered saline (pH 7.4) the eye cup was cryoprotected in 30% sucrose at 4°C over night, embedded in Tissue-Tek (Sakura Finetek Germany GmbH, Staufen, Germany) and frozen in liquid nitrogen. 16µm section were cut, mounted on slides (SuperFrost®Plus, Menzel-Gläser, Braunschweig, Germany) and air dried at 37°C before freezing at -20°C. Before the staining procedure slides were thawed at 37°C and washed with 150mM phosphate-buffered saline (pH 7.4). In order to avoid background staining the slides were treated with a blocking solution (20% normal goat serum, 2% bovine serum albumin in 150mM phosphate-buffered saline (pH 7.4) containing 0.3% Tween-20) for at least 30 minutes at room temperature. The primary antibodies diluted in blocking solution were applied over night at 4°C. Microtubules were stained with a monoclonal mouse α-acetylated tubulin antibody (1:150, Sigma, Buchs, Switzerland). Myo7a was stained with a peptide polyclonal rabbit α-MyosinVIIa (1:350, custom made by Eurogentec S.A., Seraing, Belgium) directed against a C-terminus peptide at position 2004-2017 (CYRVKFEDDKSHFPS). Washing with 150mM phosphate-buffered saline (pH 7.4) was followed by incubation with secondary antibodies (Alexa Fluor®, Invitrogen, Basel, Switzerland) diluted in 150mM phosphate-buffered saline (pH 7.4). The slides were washed and coverslipped with Mowiol and viewed with an Olympus BX61 fluorescence microscope.

3.3.2 Electron microscopy

For scanning electron microscopy the eye cup was conserved in freshly prepared fixative (1% paraformaldehyde, 100mM phosphate buffer, 3% saccharose, 0.15mM $CaCl_2$-solution and 2.5% glutaraldehyde) over night at 4°C and washed with 100mM sodium cacodylate buffer. Postfixation with 2% osmium for 30 minutes at room temperature was followed by washing with 100mM sodium cacodylate buffer and a graded ethanol series ending with a H_2O-free absolute ethanol step. The specimen was transferred to the critical point drying device (BAL-TEC AG, Balzers, Liechtenstein; today Leica Microsystems, Heerbrugg, Switzerland). After several medium changes between dry ethanol and fluid CO_2

at around 10°C the specimen was dried above the critical point of CO_2 (31°C, 73,8 bar). Before the dried specimen was mounted on carbon pads it was randomly broken by means of a razor blade or a tungsten wire. In order to avoid charging of the specimen when exposed to electrons the surface has been covered with a 10-20nm thick platinum or gold coat by means of a sputter coater (Balzers Union AG, Balzers, Liechtenstein; today Leica Microsystems, Heerbrugg, Switzerland). The specimen was analysed with a Zeiss SUPRA 50 VP scanning electron microscope (Carl Zeiss AG, Feldbach, Switzerland).

For standard transmission electron microscopy the same fixation was used as for scanning electron microscopy. Specimens were then washed with 100mM phosphate buffer before postfixation in 1% osmium tetroxide for 80 minutes at room temperature took place. The eye cups were washed with 100mM phosphate buffer and then with ddH_2O before contrasted with 1% uranyl acetate for 1 hour at 4°C. Dehydration was done in a graded ethanol series and a propylene oxide step. After preinfiltration in an epon/propylene oxid mixture the eye cups were embedded in pure epon and polymerized at 65°C for 24–48 hours. Ultrathin section were contrasted with lead and analyzed with a Philips CM208 transmission electron microscope (Philips Schweiz AG, Zurich, Switzerland). Transmission electron microscopical immunohistochemistry has been done as detailed described in an author's publication (Klooster et al., 2009). Briefly, retinal sections were incubated with the anti-rabbit α-MyosinVIIa antibody as described in the 'fluorescence immunohistochemistry' section. After incubation with horseradish peroxidise and Tris–HCl diaminobenzidine (DAB) solution the reaction was enhanced by gold-substituted silver peroxidise.

3.3.3 *in silico* identification and cloning of the second zebrafish *myosinVIIa* gene

The *Danio rerio* genome database (http://www.ncbi.nlm.nih.gov/genome/seq/BlastGen/BlastGen.cgi?taxid=7955) was search for related sequences of the zebrafish mRNA sequence *myo7a* (AJ404001). The output of interest was the genomic sequence (NW_001878211) containing parts of highly homology to the query. Exon/intron boundaries have been identified automatically (http://genes.mit.edu/GENSCAN.html) and by a manual search for consensus sequences of 5' and 3' splice sites (Patel and Steitz, 2003). By these the coding sequence of the second paralogue has been identified.

mRNA from 10-20 TÜ 5dpf larvae was isolated using the RNeasy kit (Quiagen; Hombrechtikon, Switzerland) and reversed transcribed using SuperScript® First Strand kit (Invitrogene; Basel, Switzerland). The resultant single strand cDNA was polymerase

chain reaction (PCR) amplified with Taq polymerase (Sigma-Aldrich; St. Louis, USA) using oligonucleotide primers (Table 1) designed with Oligo Primer Analysis Software (Molecular Biology Insights; Cascade, USA) according to the *in silico* identified sequence. The PCR product was directly subcloned into TOPO pCR 2.1or TOPO pCR II cloning vector (Invitrogene; Basel, Switzerland) and sequenced with M13(-20) forward and M13 reverse primer (Invitrogene; Basel, Switzerland).

Table 1: Oligonucleotide primers used for cloning of the second *myo7a* gene

Position relative to start codon	**Primer Sequence 5' to 3'**
0042 to 0061 sense	CAGAACAGACCATGAGTTTG
0632 to 649 sense	GCCGGTTTGGAAAATATG
1283 to 1300 sense	CCGTTCGCAGGTCTATAG
1671 to 1692 sense	GGTGCACTATGAAACTAAAGG
1743 to 1763 antisense	AACTTGTTTTTGGATGAATGG
2782 to 2802 sense	CAGATGGAGAGAGAAAAAAAG
2832 to 2850 antisense	CAGGAATCCGAACATCTTG
3212 to 3233 antisense	CCCAACGTCTCATAGATTTTAG
3329 to 3348 sense	TGGTGTCCCTCACATTAAAG
4120 to 4139 antisense	CGATACTCTCCGAATTTGAC
4281 to 4299 sense	GGAGAAATGGGCTCAGATG
4692 to 4710 antisense	CACCACAAACTTTGACCTG
4901 to 4920 sense	TCACCAGGCCACAGTATGAT
6017 to 6035 antisense	GATTTGTCCTCCTCGAACC

3.4 Results & Discussion

3.4.1 MyosinVIIa is expressed in the accessory outer segment of all four cone types

As the retinal expression pattern of Myo7a in zebrafish has only been studied with an antibody against the human orthologue, we raised polyclonal peptide-antibodies against the zebrafish Myo7a protein. Peptide designing was based on the protein sequence published by Ernest and colleagues (2000). We performed immunohistochemical experiments to assess the protein distribution in the adult zebrafish retina by means of fluorescence and transmission electron microscopy.

Antibody staining by means of fluorescence microscopy reveals a prominent staining in the outer retina (Figure 1). The labelling originates in the region of the connecting cilium of every cone photoreceptor and spans alongside the outer segment. The labelled structure is the cone accessory outer segment (AOS), which is not yet described in zebrafish but common in other teleost species. Compared to the outer segment, the AOS is reduced. It is clearly thinner and slightly shorter than the outer segment. As both, AOS and outer segment run in parallel they appear attached to each other.

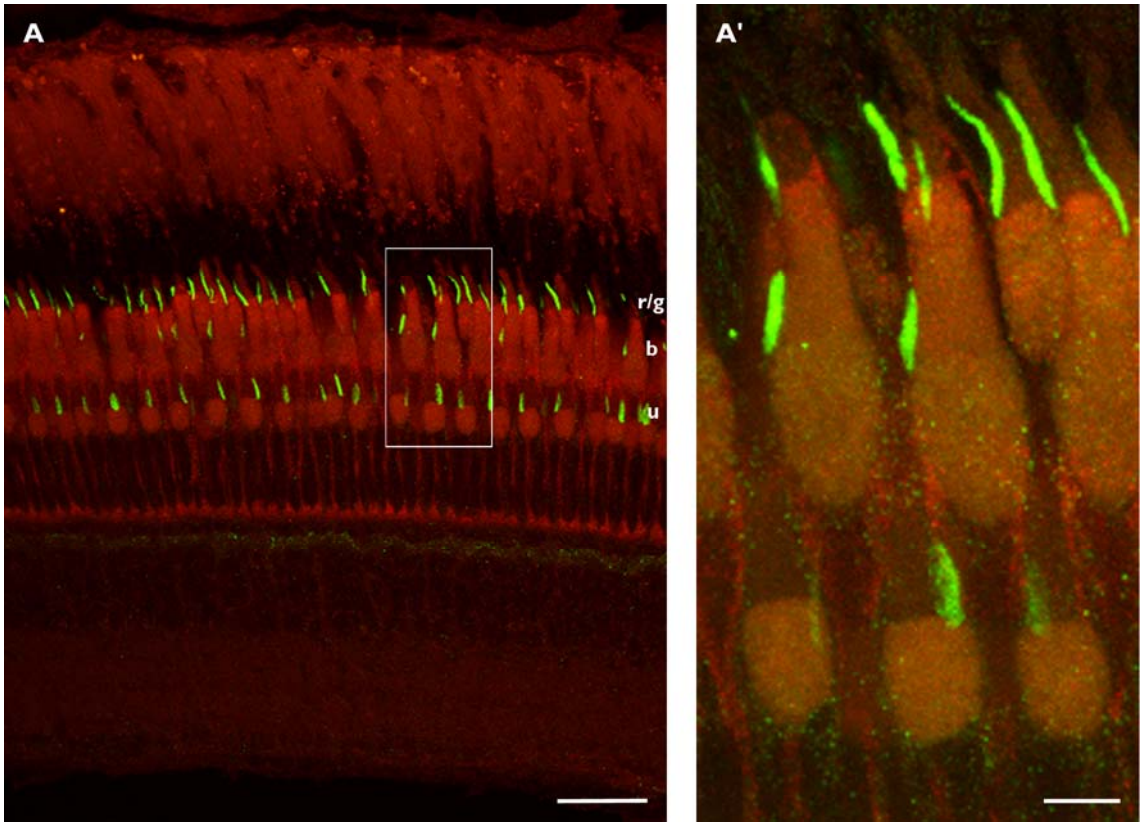

Figure 1 Fluorescence immunohistochemistry staining of Moy7a (green) in a radial section of an adult zebrafish retina (red: autofluorescence). **(A)** Myo7a is localised to the accessory outer segment of all four cone types (r/g = red/green double cones; b = blue cones; u = uv cones). **(A')** Optical zoom of the outer retina where Myo7a has been located. Scale bars: A=25µm, A'=5µm.

In mammalian species Myo7a has been found in the connecting cilium of photoreceptors (el-Amraoui et al., 1996; Hasson et al., 1995; Liu et al., 1997; Weil et al., 1996; Wolfrum et al., 1998). In teleosts the cilium is too small to resolve with light microscopy. Hence, it is not possible to judge by means of fluorescence microscopy whether Myo7a expression is restricted to the AOS or if the staining extends to the connecting cilium. In order to ultrastructurally determine protein expression we performed transmission electron microscopical immunohistochemistry with the same Myo7a antibody as we used for the fluorescence microscopical approach.

Immunogold transmission electron microscopical studies clearly confirm the staining pattern found by means of fluorescence immunohistochemistry. The colloidal gold particles are clearly located in the AOS (Figure 2A). We also found a staining in the connecting cilium (Figure 2B). However, the particle density in the connecting cilium is much lower than in the AOS. Moreover, the gold particles within the connecting cilium are arranged in a gradient having highest density near the AOS and fading out towards the inner segment.

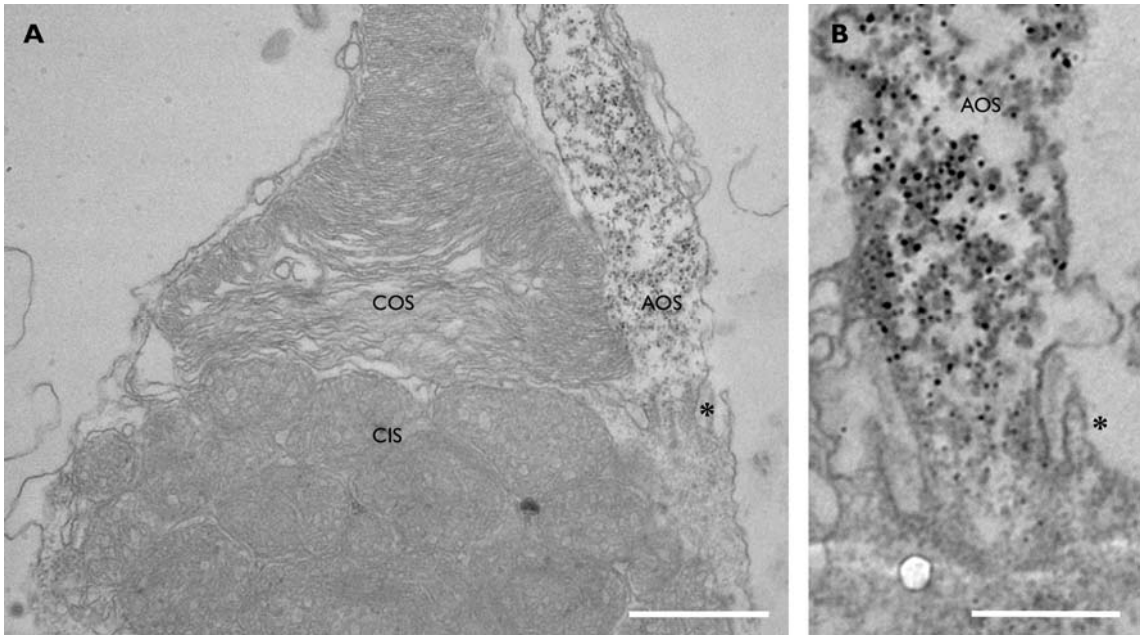

Figure 2 Electron microscopical immunohistochemistry of adult zebrafish retina using the Myo7a antibody **(A)** The cold particles seen as tiny black dots are mostly localised to the AOS and to a lesser extent to the connecting cilium (*) **(B)** Optical magnification of the connecting cilium (*) and the basal part of the AOS showing an intense staining in the AOS and a gradient of gold particles within the connecting cilium. Scale bars: A=1µm, B=0.5µm. AOS, accessory outer segment; CIS, cone inner segment; COS, cone outer segment

3.4.2 Morphology of the zebrafish accessory outer segment

To our knowledge the zebrafish AOS has not yet been described. For this reason we examine its ultrastructural morphology by means of transmission electron microscopy (TEM) and scanning electron microscopy (SEM).

Radial TEM sections reveal that the AOS continues from the connecting cilium (see Figure 2). The transition between AOS and connecting cilium is gradual. The microtubules found in the connecting cilium fade out into the AOS and not into the outer segment. There is no cytoplasmic part in the outer segment of a zebrafish cone as the discs spanning all along the entire width of a radially sectioned outer segment (Figure 3A). This is a major difference between teleost and mammalian cone outer segments. In mammals the ciliary axoneme and its adjacent cytoplasm extends into the outer segment (Mustafi et al., 2009). It is very likely that the AOS of teleost and the ciliary axoneme of the mammalian outer segment are homologues structures. It appears that the thin cytoplasmic bridge connecting the AOS and outer segment has been enlarged over time so that the AOS became incorporated into the outer segment. The separation of the AOS from the outer segment can also be seen in tangential TEM sections (Figure 3B). The AOS is enclosed by a

membrane, which is part of the cell membrane as there is a cytoplasmic connection between the AOS and the outer segment. The AOS membrane is curved leading to an enlarged surface. Moreover, the AOS is in close contact with the RPE membrane running along the curved AOS membrane. The features of the zebrafish AOS described until now are very common for teleost AOS described so far in the literature.

The axoneme of the connecting cilium appears extend only slightly into the AOS it is rather almost restricted to the connecting cilium (see Figure 2). Cross sections of the AOS are also devoid of microtubules (Figure 3B). Colocalisation studies with antibodies against Myo7a and against acetylated alpha-tubulin reveal an absence of microtubules in the AOS as well (Figure 3C). This is in contrast to the AOS of other species where microtubules have been found at least in the basal part of the AOS (Nagle et al., 1986; Pagh-Roehl et al., 1991; Yacob et al., 1977). The alpha-tubulin of microtubules found in teleost cones are variously modified; acetylated, tyrosinated and detyrosinated tubulins have been identified (Pagh-Roehl et al., 1991). In order to be able to label all microtubule types within a cone an antibody against beta-tubulin could be used as the beta-unit of a microtubule is normally not modified. Moreover, a closer look on serial cross sections from the connecting cilium through the AOS can answer the question to which extend the axoneme prolongs into the AOS after having leaved the connecting cilium. In addition to microtubules, it has been found that the basal part of the AOS also contains actin (Chaitin and Burnside, 1989; Nagle et al., 1986). Preliminary data of staining with phalloidin suggest that there is no actin in the AOS (data not shown). Notably, Myo7a as all other Myosin proteins comprises an ATP- and actin-binding site and its role is constituted by walking along the actin filament in an ATP dependent manner (Udovichenko et al., 2002). Phalloidin binds to filamentous actin rather than to soluble globular actin. Therefore, it can not be completely excluded that there is no actin at all in the AOS. Nevertheless, Myosin proteins are supposed to bind to actin filaments and not to the soluble globular actin (Alberts et al., 2002).

In summary the zebrafish cone AOS is the cytoplasmic prolongation of the connecting cilium running along the outer segment connected only via a thin cytoplasmic bridge to the outer segment. AOS and RPE are in close contact. Preliminary studies reveal that the AOS appear to neither contain microtubules nor actin filaments.

In order to get a three dimensional idea of the AOS ultrastructure we performed SEM studies. These SEM pictures confirm the surface enlargement (Figure 3D and D') found in TEM cross sections (see Figure 3B). Besides, every zebrafish cone is surrounded by calycal processes (Figure 3E) which are supposed to have supporting functions (Lin-Jones and Burnside, 2007; Pagh-Roehl et al., 1992). The connecting cilium is very short as

it can already be see in the radial TEM section. Strikingly, each partner of a red-green double cone has its own AOS which is strictly laterally located and both are located at the same side (Figure 3F and F'). This has also been found in other teleosts (Engström, 1961; Januschka et al., 1987).

Figure 3 (next page) Ultrastructural analysis of zebrafish's cone accessory outer segment by means of transmission (A-B) and scanning (D-F) electron microscopy and fluorescence microscopy (C). **(A)** Radial section of an adult zebrafish retina showing that the COS is devoid of an cytoplasmic part as the AOS is not part of the COS. **(B)** There are no microtubules found in a AOS cross section. AOS and COS are connected via a cytoplasmic bridge (*). Hence, the AOS is enclosed by the cell membrane continuing to the COS. The AOS is in close contact with the RPE. **(C)** Colocalisation of Myo7a (red) and acetylated tubulin (green) reveals that the AOS is devoid of acetylated tubulin. **(D-D')** The surface of the AOS is highly enlarged (compare to B). **(E)** In contrast to the diameter of the numerous calycal processes (the tip of one process is indicated by an arrow head in the inset), the diameter of the AOS (start and end of two AOSs are marked with arrows) is larger. **(F)** The AOSs of double cones (arrow heads) are laterally located on the same side. Scale bars: A=1µm, B=0.2µm, C=20µm, D=0.75µm, D'=0.2µm, E=7.5µm, F=1µm, F'=1µm. AOS, accessory outer segment; CC, connecting cilium; CIS, cone inner segment; COS, cone outer segment; ONL, outer nuclear layer; ROS, rod outer segment; RPE, retinal pigment epithelium

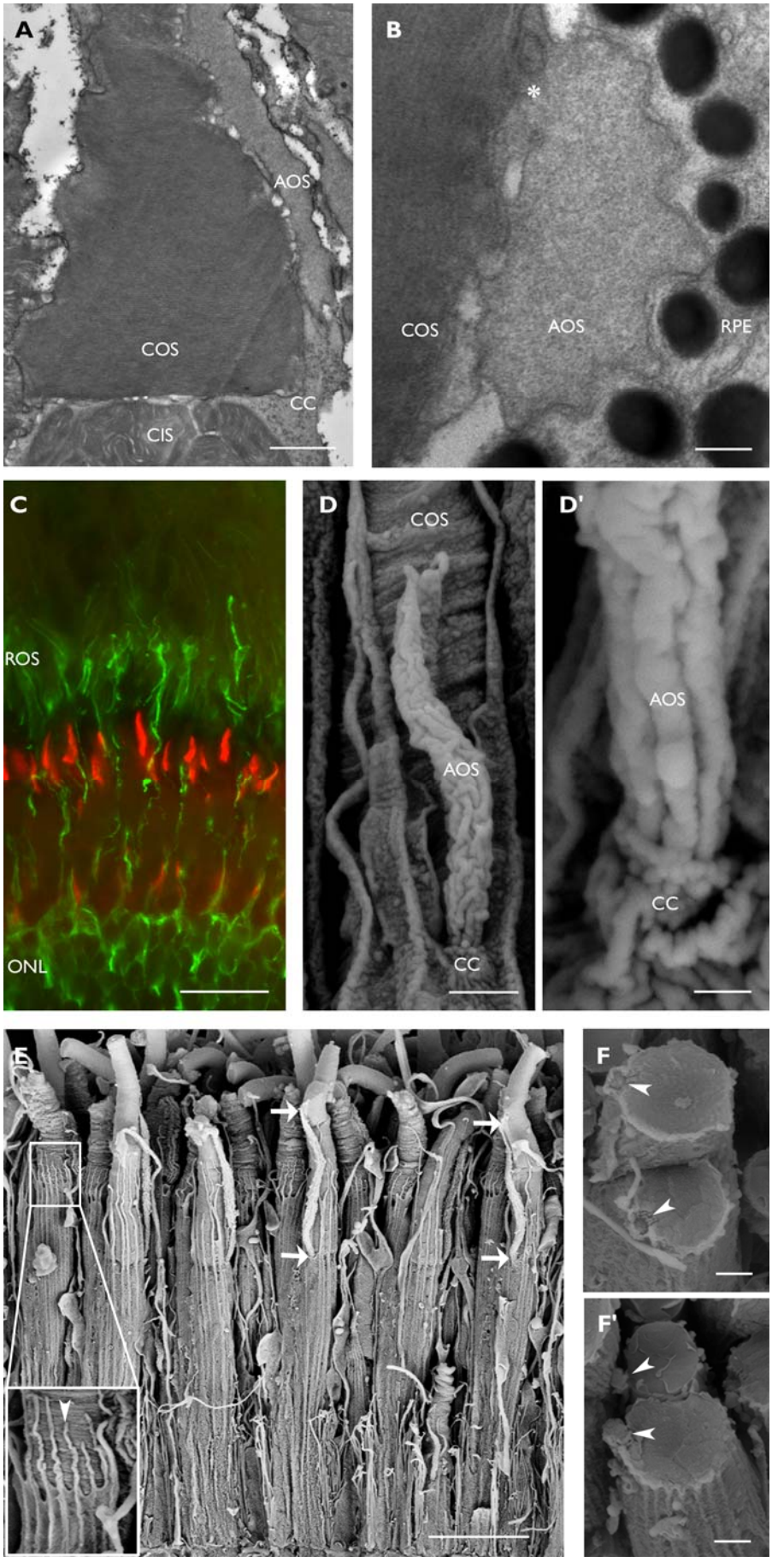
A
AOS
COS
CC
CIS
B
*
COS
AOS
RPE
C
ROS
ONL
D
COS
AOS
CC
D'
AOS
CC
E
F
F'

3.4.3 Identification of a second *myosinVIIa* paralogue in zebrafish

As in all species analysed so far Myo7a has always been found in the RPE (el-Amraoui et al., 1996; Hasson et al., 1995; Liu et al., 1997; Weil et al., 1996; Wolfrum et al., 1998) we were surprising not to detect zebrafish Myo7a in this structure (Figure 1A, 3C). However, it is known that in contrast to mammals, teleost genome underwent at least one additional duplication during evolution. Hence there is the possibility that the zebrafish genome might harbour a second *myo7a* paralogue, which could be expressed in the RPE. Indeed, bioinformatically we identified a second *myo7a* paralogue on linkage group 21 which we named *myo7a2*. Accordingly, we refer to the firstly discovered paralogue on linkage group 18 (Ernest et al., 2000) whose protein expression pattern in zebrafish retina is described in this study as *myo7a1*. As expected (Ernest et al., 2000) the translated amino acid sequence is very conserved (Table 2).

Table 2: Amino acid identities

	Myo7a1 *dr*	Myo7a *mm*	Myo7a *hs*
Myo7a2 *dr*	83%	78%	79%
Myo7a1 *dr*	-	83%	84%

3.5 Outlook

To our knowledge the zebrafish specific Myo7a antibody used in this study is the first maker selectively labels cone AOS. It is of great interest whether this antibody also recognizes the epitope of other teleost Myo7a proteins and thus can be proclaimed as a general AOS marker. Of course, we will assess the specificity of the antibody by western blotting. As Myo7a is supposed to bind actin filaments we will comprehensively investigate actin expression in zebrafish AOS. In addition to fluorescence staining we will also look for the distribution of actin filaments in TEM sections. Thereby it is important to

take into account that actin filament preservation needs a special fixation (McDonald, 1984). We did not find acetylated tubulin in the zebrafish AOS. Localization of the microtubule entirety can be achieved by TEM serial cross sections and by using an antibody against the beta-tubulin subunit which is found in all microtubules.

Surprisingly we did not find a Myo7a staining in the zebrafish RPE where the mammalian Myo7a has been located (el-Amraoui et al., 1996; Hasson et al., 1995; Liu et al., 1997; Weil et al., 1996; Wolfrum et al., 1998). Therefore, it is very likely that the second zebrafish *myo7a* paralogue is expressed in this structure. By means of real time PCR with cDNA from isolated eyes we will investigate whether *myo7a2* is expressed in the zebrafish eye. Depending on the outcome we will analysed the eye expression pattern of *myo7a2* by means of *in situ* hybridization and antibody staining.

3.6 References

Alberts, B., Johnson, A., Lewis, J., Raff, M., Keith, R., and Walter, P. (2002). Molecular biology of the cell. Garland Science, New York.

Burnside, B., Wang, E., Pagh-Roehl, K., and Rey, H. (1993). Retinomotor movements in isolated teleost retinal cone inner-outer segment preparations (CIS-COS): effects of light, dark and dopamine. Exp Eye Res *57*, 709-722.

Chaitin, M. H., and Burnside, B. (1989). Actin filament polarity at the site of rod outer segment disk morphogenesis. Invest Ophthalmol Vis Sci *30*, 2461-2469.

Collin, S. P., Collin, H. B., and Ali, M. A. (1996). Ultrastructure and organisation of the retina and pigment epithelium in the cutlips minnow, Exoglossum maxillingua (Cyprinidae, Teleostei). Histol Histopathol *11*, 55-69.

Douglas, R. H., and Djamgoz, M. B. (1990). The visual system of fish. Chapman and Hall, London.

el-Amraoui, A., Sahly, I., Picaud, S., Sahel, J., Abitbol, M., and Petit, C. (1996). Human Usher 1B/mouse shaker-1: the retinal phenotype discrepancy explained by the presence/absence of myosin VIIA in the photoreceptor cells. Hum Mol Genet *5*, 1171-1178.

Engström, K. (1961). Cone types and cone arrangement in the retina of some gadids. Acta Zoologica *42*, 227-243.

Engström, K. (1963). Cone types and cone arrangements in teleost retinae. Acta Zoologica *44*, 179-243.

Ernest, S., Rauch, G. J., Haffter, P., Geisler, R., Petit, C., and Nicolson, T. (2000). Mariner is defective in myosin VIIA: a zebrafish model for human hereditary deafness. Hum Mol Genet *9*, 2189-2196.

Fineran, B. A., and Nicol, J. A. (1974). Studies on the eyes of New Zealand parrot-fishes (Labridae). Proc R Soc Lond B Biol Sci *186*, 217-247.

Gibbs, D., Kitamoto, J., and Williams, D. S. (2003). Abnormal phagocytosis by retinal pigmented epithelium that lacks myosin VIIa, the Usher syndrome 1B protein. Proc Natl Acad Sci U S A *100*, 6481-6486.

Gibson, F., Walsh, J., Mburu, P., Varela, A., Brown, K. A., Antonio, M., Beisel, K. W., Steel, K. P., and Brown, S. D. (1995). A type VII myosin encoded by the mouse deafness gene shaker-1. Nature *374*, 62-64.

Hasson, T., Heintzelman, M. B., Santos-Sacchi, J., Corey, D. P., and Mooseker, M. S. (1995). Expression in cochlea and retina of myosin VIIa, the gene product defective in Usher syndrome type 1B. Proc Natl Acad Sci U S A *92*, 9815-9819.

Januschka, M. M., Burkhardt, D. A., Erlandsen, S. L., and Purple, R. L. (1987). The ultrastructure of cones in the walleye retina. Vision Res *27*, 327-341.

Klooster, J., Yazulla, S., and Kamermans, M. (2009). Ultrastructural analysis of the glutamatergic system in the outer plexiform layer of zebrafish retina. J Chem Neuroanat *37*, 254-265.

Lin-Jones, J., and Burnside, B. (2007). Retina-specific protein fascin 2 is an actin cross-linker associated with actin bundles in photoreceptor inner segments and calycal processes. Invest Ophthalmol Vis Sci *48*, 1380-1388.

Lin-Jones, J., Sohlberg, L., Dose, A., Breckler, J., Hillman, D. W., and Burnside, B. (2009). Identification and localization of myosin superfamily members in fish retina and retinal pigmented epithelium. J Comp Neurol *513*, 209-223.

Liu, X., Ondek, B., and Williams, D. S. (1998). Mutant myosin VIIa causes defective melanosome distribution in the RPE of shaker-1 mice. Nat Genet *19*, 117-118.

Liu, X., Udovichenko, I. P., Brown, S. D., Steel, K. P., and Williams, D. S. (1999). Myosin VIIa participates in opsin transport through the photoreceptor cilium. J Neurosci *19*, 6267-6274.

Liu, X., Vansant, G., Udovichenko, I. P., Wolfrum, U., and Williams, D. S. (1997). Myosin VIIa, the product of the Usher 1B syndrome gene, is concentrated in the connecting cilia of photoreceptor cells. Cell Motil Cytoskeleton *37*, 240-252.

McDonald, K. (1984). Osmium ferricyanide fixation improves microfilament preservation and membrane visualization in a variety of animal cell types. J Ultrastruct Res *86*, 107-118.

Mustafi, D., Engel, A. H., and Palczewski, K. (2009). Structure of cone photoreceptors. Prog Retin Eye Res *28*, 289-302.

Nagle, B. W., Okamoto, C., Taggart, B., and Burnside, B. (1986). The teleost cone cytoskeleton. Localization of actin, microtubules, and intermediate filaments. Invest Ophthalmol Vis Sci *27*, 689-701.

Nicolson, T., Rusch, A., Friedrich, R. W., Granato, M., Ruppersberg, J. P., and Nusslein-Volhard, C. (1998). Genetic analysis of vertebrate sensory hair cell mechanosensation: the zebrafish circler mutants. Neuron *20*, 271-283.

Pagh-Roehl, K., Wang, E., and Burnside, B. (1991). Posttranslational modifications of tubulin in teleost photoreceptor cytoskeletons. Cell Mol Neurobiol *11*, 593-610.

Pagh-Roehl, K., Wang, E., and Burnside, B. (1992). Shortening of the calycal process actin cytoskeleton is correlated with myoid elongation in teleost rods. Exp Eye Res *55*, 735-746.

Patel, A. A., and Steitz, J. A. (2003). Splicing double: insights from the second spliceosome. Nat Rev Mol Cell Biol *4*, 960-970.

Rowe, M. P. (2000). Inferring the retinal anatomy and visual capacities of extinct vertebrates. Palaeontologia Electronica *3*, art. 3: 43 pp.

Seiler, C., Finger-Baier, K. C., Rinner, O., Makhankov, Y. V., Schwarz, H., Neuhauss, S. C., and Nicolson, T. (2005). Duplicated genes with split functions: independent roles of protocadherin15 orthologues in zebrafish hearing and vision. Development *132*, 615-623.

Udovichenko, I. P., Gibbs, D., and Williams, D. S. (2002). Actin-based motor properties of native myosin VIIa. J Cell Sci *115*, 445-450.

Usher, C. H. (1914). On the inheritance of retinitis pigmentosa, with notes of cases. R Lond Ophthalmol Hosp Rep *19*, 130- 236.

Weil, D., Levy, G., Sahly, I., Levi-Acobas, F., Blanchard, S., El-Amraoui, A., Crozet, F., Philippe, H., Abitbol, M., and Petit, C. (1996). Human myosin VIIA responsible for the Usher 1B syndrome: a predicted membrane-associated motor protein expressed in developing sensory epithelia. Proc Natl Acad Sci U S A *93*, 3232-3237.

Wolfrum, U., Liu, X., Schmitt, A., Udovichenko, I. P., and Williams, D. S. (1998). Myosin VIIa as a common component of cilia and microvilli. Cell Motil Cytoskeleton *40*, 261-271.

Yacob, A., Wise, C., and Kunz, Y. W. (1977). The accessory outer segment of rods and cones in the retina of the guppy, Poecilia reticulata P. (Teleostei). An electron microscopical study. Cell Tissue Res *177*, 181-193.

4. THE ZEBRAFISH MUTANT *BUMPER* SHOWS A HYPER-PROLIFERATION OF LENS EPITHELIAL CELLS AND FIBRE CELL DEGENERATION LEADING TO FUNCTIONAL BLINDNESS

Helia B. Schonthaler [a,b,1,3], Tamara A. Franz-Odendaal [c,3], Corinne Hodel [b,3], Ines Gehring [a], Robert Geisler [a,2], Heinz Schwarz [a], Stephan C.F. Neuhauss [b], Ralf Dahm [a,d,1,*]

[a] Max Planck Institute for Developmental Biology, Department of Genetics, Spemannstr. 35, D-72076 Tübingen, Germany

[b] Institute of Zoology, University of Zurich, CH-8057 Zurich, Switzerland

[c] Department of Biology, Mount Saint Vincent University, 166 Bedford Highway, Halifax, NS, Canada B3M 2J6

[d] Department of Biology, University of Padova, Via U. Bassi 58/B, I-35121 Padova, Italy

[1] Present address: Spanish National Cancer Research Centre (CNIO), C/Melchor Ferna´ndez Almagro 3, E-28029 Madrid, Spain.

[2] Present address: Institute of Toxicology and Genetics, Karlsruhe Institute of Technology, Hermann-von-Helmholtz-Platz 1, 76344 Eggenstein-Leopoldshafen, Germany.

[3] These authors contributed equally to this work.

[*] Corresponding author

Article published in *Mechanism of Development, 2010, 127:3-4,203-219*

Personal Contribution

Experiments for Figure 3, Figure 5 and Figure 7 as well as for the Supplementary Figure 2; writing of the corresponding Material & Methods as well as Results & Discussion sections; providing of fixated embryos to Supplementary Figure 1; assistance with proofing the entire manuscript

MECHANISMS OF DEVELOPMENT 127 (2010) 203–219

available at www.sciencedirect.com

ScienceDirect

journal homepage: www.elsevier.com/locate/modo

MECHANISMS OF DEVELOPMENT

The zebrafish mutant *bumper* shows a hyperproliferation of lens epithelial cells and fibre cell degeneration leading to functional blindness

Helia B. Schonthaler [a,b,1,3], *Tamara A. Franz-Odendaal* [c,3], *Corinne Hodel* [b,3], *Ines Gehring* [a], *Robert Geisler* [a,2], *Heinz Schwarz* [a], *Stephan C.F. Neuhauss* [b], *Ralf Dahm* [a,d,*,1]

[a] *Max Planck Institute for Developmental Biology, Department of Genetics, Spemannstr. 35, D-72076 Tübingen, Germany*
[b] *Institute of Zoology, University of Zurich, CH-8057 Zurich, Switzerland*
[c] *Department of Biology, Mount Saint Vincent University, 166 Bedford Highway, Halifax, NS, Canada B3M 2J6*
[d] *Department of Biology, University of Padova, Via U. Bassi 58/B, I-35121 Padova, Italy*

ARTICLE INFO

Article history:
Received 23 April 2009
Received in revised form
25 January 2010
Accepted 26 January 2010
Available online 1 February 2010

Keywords:
Zebrafish (*Danio rerio*)
Embryonic development
Eye
Vision
Lens fibre cell differentiation
Tumour-like hyperproliferation
Head skeleton

ABSTRACT

The development of the eye lens is one of the classical paradigms of induction during embryonic development in vertebrates. But while there have been numerous studies aimed at discovering the genetic networks controlling early lens development, comparatively little is known about later stages, including the differentiation of secondary lens fibre cells. The analysis of mutant zebrafish isolated in forward genetic screens is an important way to investigate the roles of genes in embryogenesis. In this study we describe the zebrafish mutant *bumper* (*bum*), which shows a transient, tumour-like hyperproliferation of the lens epithelium as well as a progressively stronger defect in secondary fibre cell differentiation, which results in a significantly reduced lens size and ectopic location of the lens within the neural retina. Interestingly, the initial hyperproliferation of the lens epithelium in *bum* spontaneously regresses, suggesting this mutant as a valuable model to study the molecular control of tumour progression/suppression. Behavioural analyses demonstrate that, despite a morphologically normal retina, larval and adult *bum*$^{-/-}$ zebrafish are functionally blind. We further show that these fish have defects in their craniofacial skeleton with normal but delayed formation of the scleral ossicles within the eye, several reduced craniofacial bones resulting in an abnormal skull shape, and asymmetric ectopic bone formation within the mandible. Genetic mapping located the mutation in *bum* to a 4 cM interval on chromosome 7 with the closest markers located at 0.2 and 0 cM, respectively.

1. Introduction

The zebrafish (*Danio rerio*) is well established as a model organism to study vertebrate embryogenesis and large-scale mutagenesis screens have led to the identification of genes controlling the development of specific organs and cell types. Whereas the formation of the retina (reviewed in Fadool and Dowling (2008), Glass and Dahm (2004), Malicki et al. (2002))

* Corresponding author. Address: Department of Biology, University of Padova, Via U. Bassi 58/B, I-35121 Padova, Italy. Tel.: +39 049 827 6229; fax: +39 049 827 6300.
E-mail address: ralf.dahm@bio.unipd.it (R. Dahm).
[1] Present address: Spanish National Cancer Research Centre (CNIO), C/Melchor Fernández Almagro 3, E-28029 Madrid, Spain.
[2] Present address: Institute of Toxicology and Genetics, Karlsruhe Institute of Technology, Hermann-von-Helmholtz-Platz 1, 76344 Eggenstein-Leopoldshafen, Germany.
[3] These authors contributed equally to this work.
0925-4773/$ - see front matter
doi:10.1016/j.mod.2010.01.005

and the development of visual function (Easter and Malicki, 2002; Schmitt and Dowling, 1994) have been extensively investigated in zebrafish, the embryonic development and adult morphology of the zebrafish lens have only recently been described in detail (Dahm et al., 2007); see also (Greiling and Clark, 2008; Vihtelic, 2008; Soules and Link, 2005). Similarly, there are comparatively fewer studies examining the genetic factors controlling the development of the lens in zebrafish and a number of these relied on reverse genetics techniques (morpholino knock-down or over-expression experiments) targeting known genes (see e.g. Nakayama et al., 2008; Evans et al., 2007; Shi et al., 2006, 2005; Zinkevich et al., 2006; Cheng et al., 2004). The number of described zebrafish mutants with lens defects is therefore still limited (see e.g. Lee and Gross, 2007; Gross et al., 2005; Vihtelic and Hyde, 2002; Vihtelic et al., 2001; reviewed in Glass and Dahm (2004)).

In this study we provide the first characterisation of one of the zebrafish mutants with a reported lens phenotype that were isolated in the first large-scale ENU mutagenesis screen for mutations affecting embryonic and early larval development in the zebrafish (Haffter et al., 1996; Driever et al., 1996). The description of the *bumper* (*bum*) mutant phenotype in the initial publication is restricted to a brief note in the appendix of the publication summarizing the phenotypic descriptions of the mutants with aberrant forebrain development and merely states that in $bum^{-/-}$ the lenses begin to degenerate on the fourth day of development (Heisenberg et al., 1996). To date, there have been no subsequent studies aimed at obtaining a more comprehensive phenotypic analysis of this mutant. The only other study involving *bum* larvae was a subsequent behavioural screen of 400 zebrafish mutants to identify genes affecting visual performance in zebrafish (Neuhauss et al., 1999). While identifying a visual impairment for $bum^{-/-}$ mutant larvae in optokinetic response (OKR), optomotor-response (OMR) and visual background adaptation (VBA) assays as well as determining that the retinotectal projection was normal, this study did not quantitatively characterise the visual behaviour phenotype and does not include any direct data on the mutant.

In order to better assess the $bum^{-/-}$ mutant phenotype, we performed detailed histological and functional analyses of the eye and vision. These revealed that this mutant shows a transient hyperproliferation of the lens epithelium. Moreover, while the primary lens fibre cells form normally, the differentiation of secondary lens fibre cells is severely impaired with the cells apparently swelling, detaching and disintegrating. This results in a lens of significantly reduced size, which can be ectopically located in the neural retina and a severe visual impairment of mutant fish.

The restriction of the fibre cell defect to secondary lens fibre cells is interesting because the two types of lens fibres found in vertebrates – primary and secondary – have a different developmental origin. In mammalian and avian species, the lens detaches from the surface ectoderm as a hollow lens vesicle, which is lined by a single layer of undifferentiated epithelial cells. While the epithelial cells at the lens' anterior surface (facing the cornea) persist throughout life, the cells lining the lens' posterior surface (facing the prospective retina) elongate towards the anterior to fill the vesicle (see e.g. Dahm et al., 2007 and references therein). These cells, which during the early development of the lens obliterate the lens vesicle's lumen, are termed primary lens fibre cells. The situation in zebrafish is different in that the lens delaminates from the surface ectoderm as a solid cell mass and the primary fibre cells elongate not in a linear but in a circular fashion from the initial lens cell mass (Dahm et al., 2007).

Subsequent lens growth in mammals, birds as well as in zebrafish occurs via the differentiation of additional fibre cells from epithelial cells located near the lens' equator. These secondary fibre cells elongate towards both the anterior and posterior lens poles. This elongation continues until they contact the tips of secondary fibre cells originating from the opposite equatorial region of the lens and form the anterior and posterior sutures, respectively (Taylor et al., 1996). Both types of lens fibre cells, primary and secondary, persist throughout life and the nature of lens development means that they remain in those regions of the lens where they were initially formed.

While the two mechanisms leading to the differentiation of primary and secondary lens fibre cells are morphologically and molecularly similar, the two processes are nevertheless distinct (reviewed in Dahm et al. (2007), Taylor et al. (1996), Dahm (1999), Kuszak (1995)). The $bum^{-/-}$ mutant with its phenotype which is restricted to the secondary lens fibre cells thus offers an opportunity to gain new, mechanistic insights into the processes that distinguish the differentiation of primary and secondary lens fibre cells.

The developing lens placode and lens have also been shown to influence the development of other tissues in the embryo, for example, the optic cup in mice (West-Mays et al., 1999; Ashery-Padan et al., 2000) and chicken (Hyer et al., 2003), the cornea in chicken (Beebe and Coats, 2000) as well as the sclera in chicken (Coulombre and Coulombre, 1964) and the Mexican tetra (*Astyanax mexicanus*) (Yamamoto et al., 2003). In this context it is very interesting to note that tissues other than the lens, such as the retina and the cornea, appear to form normally in $bum^{-/-}$ mutants.

While it is well established that the eye is an important component in determining the formation of the head skeleton, little is known about the contribution of the lens in this process. In this context, the development of the ocular skeleton (scleral ossicles and scleral cartilage) which is situated within the eye has recently been described in teleosts (Franz-Odendaal et al., 2007), opening up the possibility of investigating the effects of the lens on the developing ocular skeleton. We therefore determined whether the degenerating lens in $bum^{-/-}$ affects the developing head skeleton by whole-mount staining zebrafish for cartilage and bone. These analyses revealed that the overall shape of the skull is altered, with several reduced craniofacial elements, and that asymmetric ectopic ossifications are present within the mandible. Surprisingly, the ocular skeleton is normal in adults.

2. Results and discussion

2.1. *Lens phenotype in bumper*

When first identified as part of a large-scale ENU mutagenesis screen, the zebrafish mutant *bumper* (*bum*) was classified as showing a degenerating lens starting at 4 days post-fertil-

isation (dpf) (Heisenberg et al., 1996). This study did, however, not provide any details on the phenotype nor show any data. As a first step towards the characterisation of the mutant phenotype, we therefore performed a detailed analysis of the morphology of the eyes in embryonic (36 hpf and 2 dpf; see Suppl. Fig. 1) and larval *bum*$^{-/-}$ zebrafish (3, 4 and 5 dpf; see Figs. 1, 2 and 4A–G, respectively) as well as in adult *bum*$^{-/-}$ individuals (Fig. 4H, I). These analyses revealed a number of unique aspects of the *bum*$^{-/-}$ phenotype, starting at 3 days post-fertilisation (cf. Suppl. Fig. 1 and Fig. 1, respectively). In contrast to wild-type eyes, which display large lenses of homogenous appearance that are located centrally in the eye cup, *bum*$^{-/-}$ eyes show a range of lens abnormalities with respect to the size and position of the lens within the eye (Figs. 1–5) as well as the control of proliferation and differentiation of lens cells. Importantly, the ocular phenotype in *bum*$^{-/-}$ appears to be restricted to the lens epithelium and the secondary lens fibre cells (Figs. 1, 2, 4 and 5), while the primary fibres form normally and the development of other tissues of the eye, including the neural retina and cornea, is not affected (Figs. 1, 2, 4 and 5).

When analysing semi-thin and ultrathin sections of the eyes of 3–5 dpf *bum*$^{-/-}$ larvae by light and transmission electron microscopy, respectively, we observed several cellular and subcellular malformations of the lens. The most prominent of these is a significant hyperproliferation of the anterior lens epithelium, which can first be observed at 3 dpf (Fig. 1). In contrast to wild-type lens epithelia, which consistently form a monolayer of cells (see Fig. 1B, D, F (3 dpf) and Fig. 2C, C′ (4 dpf)), the lens epithelia in *bum*$^{-/-}$ larvae are invariably multilayered (Fig. 1C, E, G, G′). This phenotype becomes more pronounced at 4 dpf (Fig. 2B, D, E; see also Fig. 5). The hyperproliferation of the lens epithelium in *bum*$^{-/-}$ results in a disorganised mass of cells which fills the chambers of the anterior part of the eye.

Closer inspection of the cells in the 3 and 4 dpf *bum*$^{-/-}$ epithelia revealed two important aspects of these cell masses. First, they comprise morphologically undifferentiated cells, indicating a tumour-like growth of the lens epithelium in the mutant (Figs. 1E, G, G′ (3 dpf) and 2D, E (4 dpf)). Second, they contain a number of pyknotic nuclei and structures that appear to be remnants of perished cells (Figs. 1G′ (3 dpf) and 2D, E (4 dpf)), suggesting a frequent occurrence of apoptotic and/or necrotic cell death. The latter observation was confirmed by the large numbers of apoptotic cells seen in 4 dpf *bum*$^{-/-}$ larvae stained with Acridine Orange, a dye that labels the nuclei of cells undergoing apoptosis (Fig. 3).

This elimination of cells in the *bum*$^{-/-}$ lens epithelium may explain why the hyperproliferative cell masses are reduced in size or even no longer present at subsequent stages of development (see Figs. 4B–D (5 dpf) and 5). Importantly, we never observed tumours in the eyes (or other organs) of the *bum*$^{-/-}$ mutant individuals we raised to adulthood and kept for >2 years ($n > 50$; see also Figs. 4H and 6), further indicating that the hyperproliferation of lens epithelium is a transient phenomenon. This observation is particularly interesting in the context that there are no reports of human lens tumours in the medical literature, suggesting the existence of a mechanism to suppress persistent neoplasia in this tissue. The *bum*$^{-/-}$ mutant, with its initial hyperproliferation of the lens epithelium, may thus prove a valuable model to investigate these mechanisms and to gain new insights into tumour suppression.

In addition to the hyperproliferation of the lens epithelium, also the differentiation of lens fibre cells shows defects in *bum*$^{-/-}$ larvae. Lens fibre cell differentiation is morphologically indistinguishable between sibling and mutant larvae until 2 dpf (Suppl. Fig. 1). At 3 dpf, however, the first phenotype becomes apparent. While the differentiation of the secondary fibre cells themselves still appears to occur normally at this stage (Fig. 1H, I), mutant lenses show the first signs of deformations at their outer cortices (Fig. 1J). This phenotype becomes more pronounced at 4 dpf (Fig. 2H).

Moreover, at 4 dpf we occasionally observed secondary fibre cells with a significantly less electron-dense cytoplasm embedded in layers of fibre cells that show the much darker appearance characteristic of differentiated lens fibres in electron micrographs (Fig. 2G). The homogenous, electron dense appearance of lens fibre cells at later stages of cell differentiation is a reflection of the expression of high levels of soluble cytoplasmic proteins, most notably crystallins, which contribute significantly to the optical properties of the lens fibre cells' cytoplasm (Bloemendal et al., 2004). The light appearance of the cytoplasm of these occasional fibre cells in the mutant lens suggests that they either fail to express the high protein levels characteristic of differentiated wild-type lens fibres or that the protein content of their cytoplasm is diluted. In this context it is interesting to note that we observed that the outermost fibre cells in the *bum*$^{-/-}$ mutant lens appear to show signs of swelling (cells labelled "s" in Fig. 2G, H). This phenotype becomes substantially stronger at later stages of development (see below). Importantly, neither a swelling of secondary lens fibre cells nor the presence of fibre cells with a lighter cytoplasm were ever detected in wild-type lenses at any of the stages examined (see Figs. 1D (3 dpf), 2F (4 dpf) and 4F, G (5 dpf)).

In addition to the lighter appearance of their cytoplasm, we also observed that at least some of the differentiating secondary lens fibre cells in 4 dpf mutant larvae retain nuclei of morphologically normal appearance beyond the stage where organelles are normally degraded during lens cell differentiation (arrowhead labelled "N" and inset in Fig. 2G). This indicates that the elimination of organelles is impaired in these cells. The programmed degradation of all membrane-bound organelles, such as the nucleus (Dahm and Prescott, 2002; Dahm et al., 1998; Bassnett, 1997) and mitochondria (Dahm et al., 1998; Bassnett, 1992), is a hallmark of fibre cell differentiation and a prerequisite of lens transparency (reviewed in Dahm (1999), Bassnett (2002)). Together with the less electron-dense cytoplasm, the failure of these cells to undergo this degradation suggests a general deregulation of the differentiation process in *bum*$^{-/-}$. Interestingly, we never observed primary fibre cells in which this organelle elimination had not occurred, suggesting that the molecular mechanisms underlying the degradation of organelles in the two types of lens fibres may have distinct components.

We also observed that the lobe-like protrusions of fibre cells from the main fibre cell mass that were first seen in 3 dpf lenses (Fig. 1J) became more pronounced at 4 dpf (Fig. 2H). The wild-type lens is one of the most precisely or-

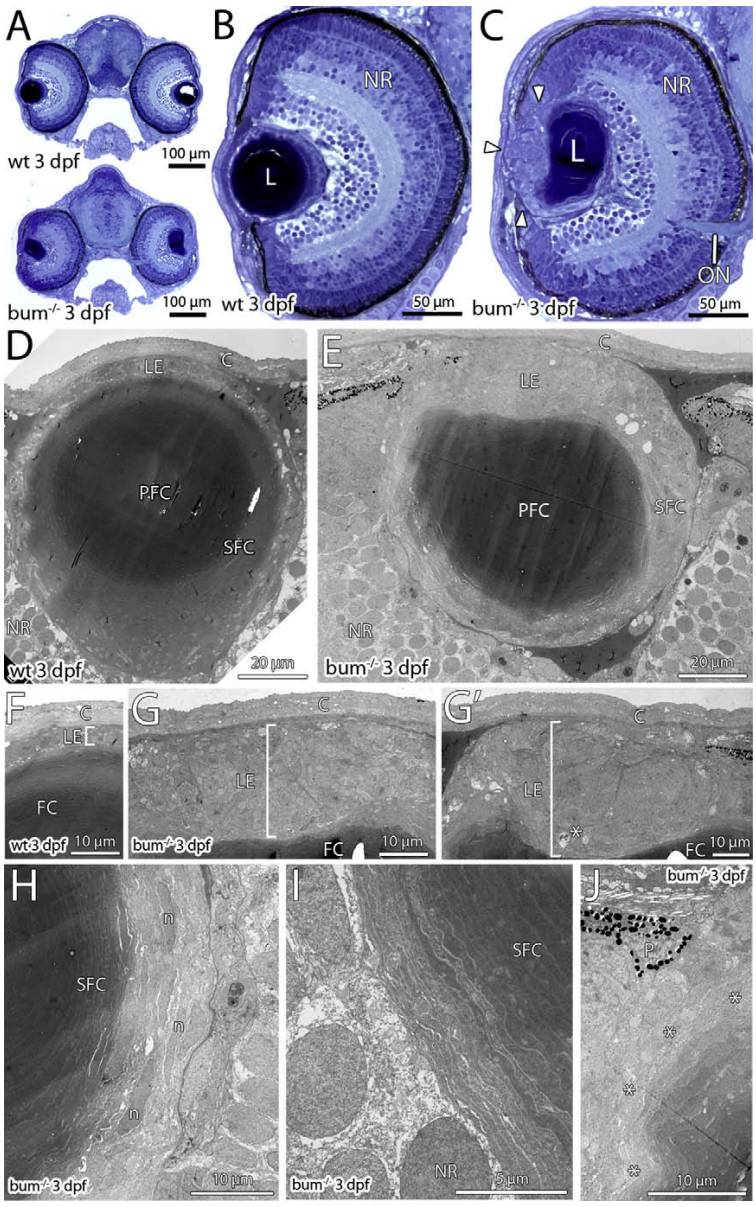

Fig. 1 – The lens in 3 dpf *bum*$^{-/-}$ zebrafish shows the onset of a hyperproliferation of the anterior epithelium. (A–C) Toluidine blue-stained transversal semi-thin sections through the central part of the eyes of 3 dpf sibling (wild-type, wt; top picture in A and B) and *bum*$^{-/-}$ mutant zebrafish larvae (bottom picture in A and C). (A) Cross-sections of entire heads, (B and C) higher magnifications of individual eyes. Note the onset of a hyperproliferation of the anterior lens epithelium in the mutant (C; white arrowheads). The overall morphology of the eye however, including the layers of the neural retina (NR), is normal in *bum*$^{-/-}$ mutant larvae (compare B and C). (D–J) Thin-section electron microscopy images of transversal sections through the central part of the eyes of 3 dpf sibling (D, F) and *bum*$^{-/-}$ (E, G–J) zebrafish larvae. (D, E) Overviews showing the morphology of the entire lens. (F, G) Higher magnifications of the anterior lens epithelia in sibling (F) and *bum*$^{-/-}$ (G, G′) zebrafish larvae. Note that the epithelium (brackets) forms a monolayer in the wild-type larvae, but is expanded to several cell layers in the mutants. Occasionally, apoptotic cells can be observed in the mutant lens epithelium (asterisk in G′). (H, I) Higher magnifications of the lens' bow region in *bum*$^{-/-}$ mutant zebrafish larvae showing the differentiating secondary lens fibre cells, which at this stage do not yet show the massive degenerative changes observed at later developmental stages (see Figs. 2 and 4). (J) Slight deformation of the outer cortex of a *bum*$^{-/-}$ mutant lens anterior of the lens' equator. Asterisks denote superficial secondary lens fibre cells that show the first signs of cellular swelling. *Abbreviations:* C, cornea; PFC, primary lens fibre cells; L, lens; LE, lens epithelium; n, secondary lens fibre cell nuclei; NR, neural retina; ON, optic nerve; P, pigment granules of the iris; PFC, primary lens fibres; SFC, secondary lens fibre cells.

dered and regularly shaped tissues in the vertebrate body with the fibre cells forming concentric shells and the fibres within each shell running in parallel to one another (Dahm et al., 2007); (Taylor et al., 1996; Kuszak, 1995). The reason for the partial breakdown of this arrangement in the *bum*$^{-/-}$ lens is currently unclear. It could be due to pressure exerted by the hyperproliferating epithelial cells (see also the massive deformation of the fibre mass near the anterior lens pole indicated by # signs in Fig. 2D, E at 4 dpf) and/or a defect in the formation of the lens capsule, which was not examined in this study.

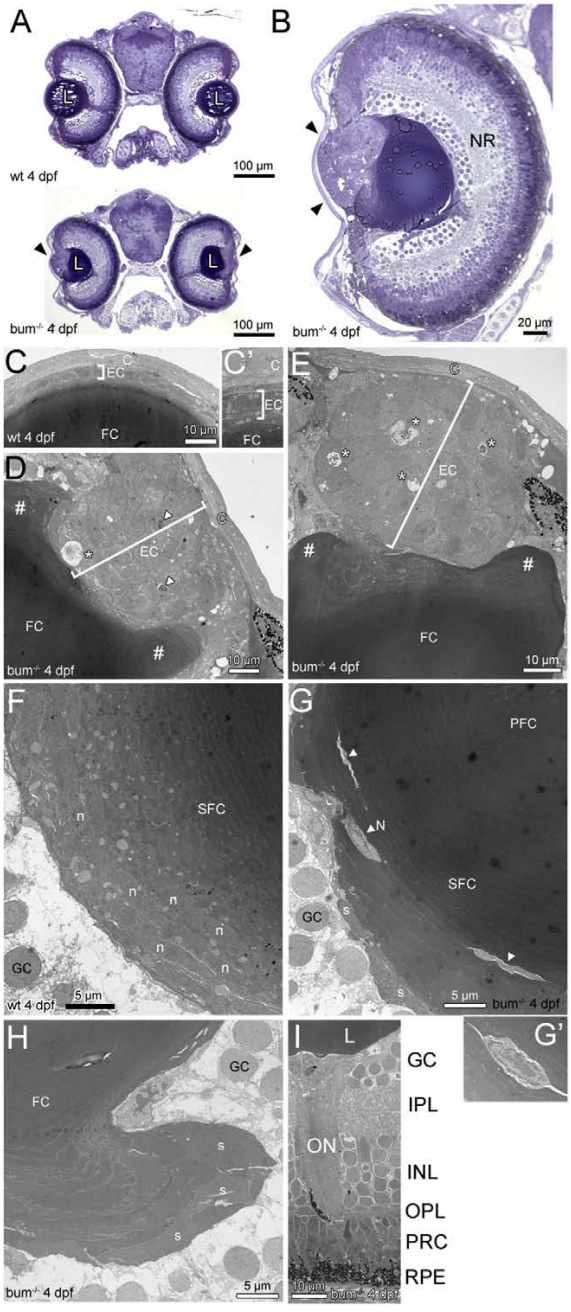

The *bum*$^{-/-}$ phenotype at 5 dpf displays several interesting developments over earlier developmental stages. In wild-type larvae, the lenses are large and well-developed at this stage (Fig. 4A). In the *bum*$^{-/-}$ mutant by contrast, the lenses can be significantly reduced in size (Fig. 4B). They are occasionally

Fig. 2 – The lens in 4 dpf *bum*$^{-/-}$ zebrafish shows a massive hyperproliferation of the anterior epithelium and the onset of a maldifferentiation of secondary fibre cells. (A, B) Toluidine blue-stained transversal semi-thin sections through the central part of the eyes of 4 dpf sibling (wild-type, wt; top picture in A) and *bum*$^{-/-}$ zebrafish larvae (bottom picture in A and B). (A) Cross-sections of entire heads, (B) A higher magnification of an individual eye. Note the hyperproliferation of the anterior lens epithelium in the mutant (black arrowheads), which does not affect the differentiation of the primary and early developing secondary fibre cells (collectively termed "FC" here as they cannot be differentiated at the magnification shown in B). The overall morphology of the head (A) and eye (B), including the development of the layers of the neural retina (NR), are normal in *bum*$^{-/-}$ mutant larvae. (C–I) Thin-section electron microscopy images of transversal sections through the central part of the eyes of 4 dpf *bum*$^{-/-}$ zebrafish larvae. (C–E) Anterior part of the eyes of 4 dpf sibling (C; higher magnification C′) and *bum*$^{-/-}$ mutant (D, E) zebrafish larvae. Note that while wild-type larvae consistently have a monolayered lens epithelium (brackets in C, C′), the mutants display a massively hyperproliferating lens epithelium (brackets in D, E). Moreover, the mutant lens epithelium frequently comprises pyknotic nuclei (arrowheads in D) and empty spaces containing cell debris (asterisks in D and E). The # signs indicate the massive deformation of the fibre mass near the anterior lens pole. (F, G) Bow regions posterior of lens equator encompassing the early differentiating lens secondary fibre cells in 4 dpf sibling (F) and *bum*$^{-/-}$ mutant (G) zebrafish larvae. In the mutant lenses note the presence of cytoplasm with a much lighter appearance (arrowheads and inset G′), sometimes still containing nuclei (N, inset), embedded in layers of secondary fibre cells that appear to have differentiated normally. Also note the swelling of some of the outermost fibre cells (s), which is however not yet as pronounced as at later developmental stages (see Fig. 4). (H) Lobe-like protrusion of secondary lens fibre cells near the posterior pole of a *bum*$^{-/-}$ mutant lens. Note that some of the fibre cells, particularly in the outermost layers, appear to be swollen (s). (I) Part of the central retina showing normal development of the layers of the neural retina, the optic nerve and the retinal pigment epithelium. Abbreviations: C, cornea; EC, lens epithelial cells; FC, (primary and secondary) fibre cells; GC, retinal ganglion cells; INL, inner nuclear layer; IPL, inner plexiform layer; L, lens; N, remaining nucleus in a late-stage differentiating secondary lens fibre cell; n, nuclei in a early-stage differentiating secondary lens fibre cells; NR, neural retina; ON, optic nerve; OPL, outer plexiform layer; PFC, primary lens fibre cells; PRC, photoreceptor cells; RPE, retinal pigment epithelium; SFC, secondary lens fibre cells.

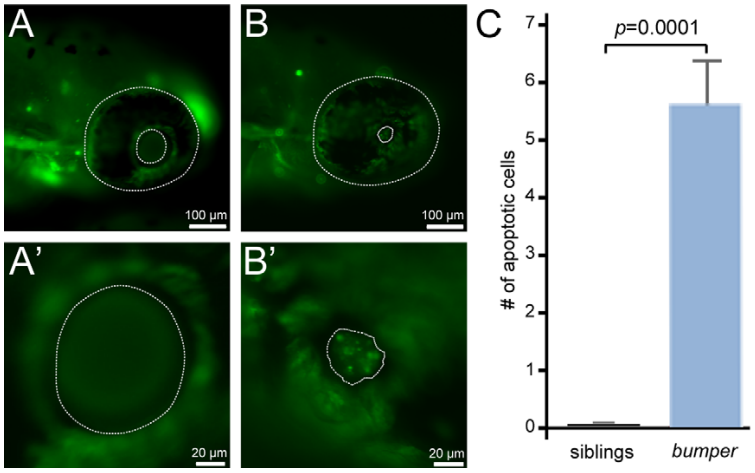

Fig. 3 – Mutant *bum*$^{-/-}$ lenses display significantly increased levels of apoptotic cell death in the anterior lens region at 4 dpf. (A, B) External views of the heads (A, B) and eyes (A′, B′) of 4 dpf sibling (wild-type, wt; A, A′) and *bum*$^{-/-}$ larvae (B, B′) showing Acridine Orange fluorescence to reveal cells undergoing apoptosis. The outer margins of the eyes (outer dotted lines in A and B) and the inner margins of the pupils (inner dotted lines in A and B; dotted lines in A′ and B′) are indicated. Note the reduced and irregular pupil diameter in the *bum*$^{-/-}$ mutant larvae. While the wild-type lenses do not show Acridine Orange-positive cells (A′), mutant lenses regularly contain numerous fluorescent cells (B). (C) Statistical analysis of the number of apoptotic cells in 4 dpf sibling (left) and *bum*$^{-/-}$ mutant larvae (right) showing highly significant numbers of apoptotic cells in the mutant lenses (but not in the wild-type), which suggests a mechanism for the regression of the lens tumours in *bum*$^{-/-}$. Error bars represent the standard error of the mean (SEM).

also located ectopically, e.g. within the dorsal ganglion cell layer and the inner plexiform layer of the neural retina as evident in the eye on the right-hand side in Fig. 4B. Furthermore, the massive hyperproliferation of the lens epithelium seen at 4 dpf (Fig. 2) is not as pronounced anymore at 5 dpf and these mutant lenses occasionally even display an epithelial monolayer as seen in the wild-type lens (Fig. 4C, D; inset in D).

As the spontaneous reduction in the epithelial cell masses seen between 4 and 5 dpf might have important implications for the understanding of tumour progression (e.g. the transition from an initial hyperproliferation to sustained tumour growth), we quantified the decrease in epithelial thickness (Fig. 5). These analyses show a very significant decline in the thickness of the mutant epithelium from day 4 (Fig. 5A) to day 5 (Fig. 5B). These findings suggest that the hyperproliferation of the lens epithelium in *bum*$^{-/-}$ is reversed at this developmental stage. This reversal may be due to two factors: a decline in proliferation rates (not assessed in this study) and/or an increase in cell death (see Fig. 3). Importantly however, the reduction in hyperproliferation seems to be sustained as we never observed ocular (or any other) tumours in adult (>2 years old) *bum*$^{-/-}$ zebrafish ($n > 50$; see also Figs. 4H and 6). This suggests this mutant as an interesting model to identify the molecular mechanisms that normally prevent the development of tumours in the eye lens as well as those underlying tumour progression/suppression in general.

Closer examination of the lens phenotype in 5 dpf *bum*$^{-/-}$ mutant larvae in semi-thin sections also revealed that these mutants have a severe defect in secondary lens fibre cell differentiation. In all eyes examined, the outer region of the lens showed varying degrees of degeneration, resulting in small and often misshapen lenses (Fig. 4B–E). Regularly, the outer layers of fibres appeared to have become detached from one another resulting in large vacuolar spaces between adjacent fibre cells (Fig. 4C–E). As observed at 4 dpf (Fig. 2), the primary lens fibre cells appear to have developed normally and the lens' nucleus is morphologically indistinguishable from wild-type lenses (compare the appearance of the central regions of the lenses in Fig. 4A (wild-type) with Fig. 4B, C (mutant) and see Fig. 4D, E). As in the wild-type (Fig. 4A), the lens nucleus in 5 dpf *bum*$^{-/-}$ larvae stains uniformly with dyes such as toluidine blue (Fig. 4B, C), indicating that the cells comprising this region have eliminated their intracellular organelles, most notably their nuclei which are readily visualised with this technique or would be visible in electron micrographs (see Fig. 4D).

The phenotype of the secondary lens fibres becomes more apparent at higher magnifications in thin-section transmission electron microscopy images (Fig. 4D, E). These images reveal that in 5 dpf *bum*$^{-/-}$ larvae the secondary fibres, instead of adopting the flattened, band- or fibre-like shape characteristic of lens fibre cells soon after having differentiated from the surface epithelium (see Fig. 4F, G for age-matched wild-type sibling lenses), become enlarged (asterisks in Fig. 4E). Note that this swelling of the fibres already sets in only a few cells deep into the fibre mass, i.e. at a stage when the cells are still differentiating (Fig. 4E). These swollen differentiating secondary lens fibre cells also appear to be atypically arranged and are not aligned as parallel fibres forming the concentric shells observed in normal vertebrate lenses (Taylor et al., 1996), including that of the zebrafish (Dahm et al., 2007).

One or two cell layers deeper into the lens, the fibre cells become detached from each other and appear to fragment or burst open, leaving large empty spaces between residual fibre cell fragments (labelled "v" in Fig. 4D, E). By contrast, the deeper (primary) lens fibre cells appear to have differentiated normally and possess a homogenous, electron-dense cytoplasm, indicative of the high protein concentrations normally found in the cytoplasm of differentiated fibre cells (Fig. 4D, E). It is, however, worth noting that, in contrast to our observation on 4 dpf *bum*$^{-/-}$ lenses (Fig. 2), the abnormally differentiating secondary lens fibre cells in the 5 dpf *bum*$^{-/-}$ lens seem to eliminate their intracellular organelles (Fig. 4E).

It is interesting that, despite the dramatic effect of the mutation on the differentiation of secondary lens fibre cells, the primary fibres forming very early during lens development appear to have differentiated normally. Differences in

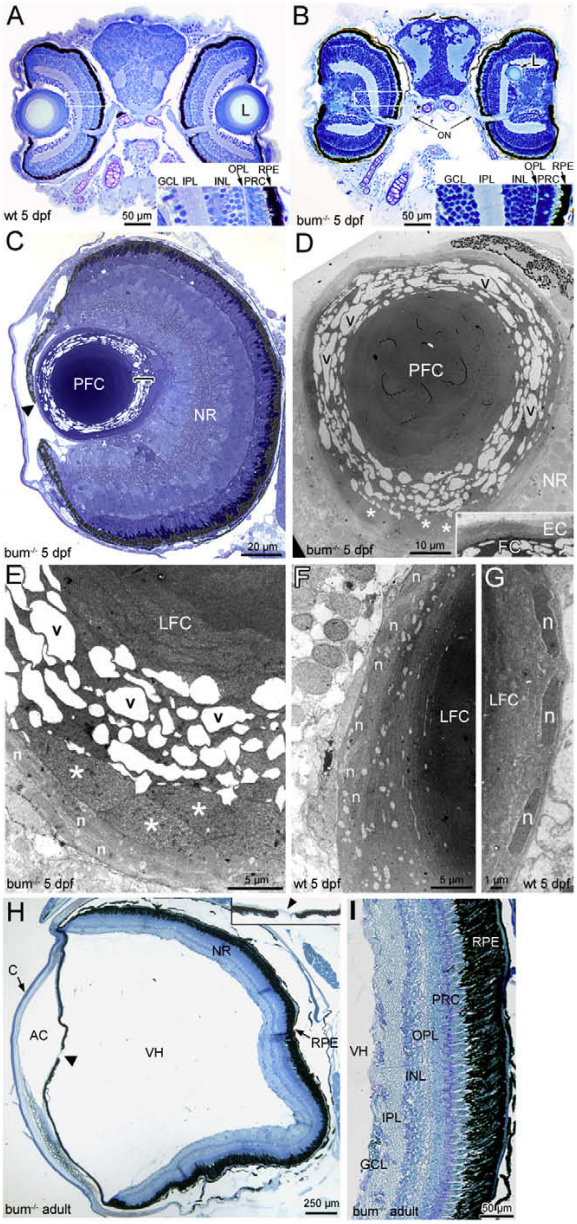

Fig. 4 – The lens in 5 dpf *bum*$^{-/-}$ zebrafish shows a severe degeneration of secondary lens fibre cells and can be ectopically located in the neural retina. (A–F) Histology of the eyes in larval (A–G) and adult *bum*$^{-/-}$ zebrafish (H, I). (A, B) Toluidine blue-stained transversal sections through the central part of the eyes of 5 dpf sibling (wild-type, wt; A) and *bum*$^{-/-}$ (B) zebrafish larvae. Insets in bottom-right corners show magnifications of the boxed areas in the retinas of the eyes shown on the left in A and B, respectively. (C) Semi-thin section of a *bum*$^{-/-}$ eye at 5 dpf. The higher magnification of the lens reveals that in the outer lens cortex, the secondary lens fibre cells appear detached from each other with large empty spaces between them (see bracket indicating this region at the lens' posterior pole). The central lens nucleus, however, seems to be composed of morphologically normal primary lens fibre cells. Note that part of the iris reaches beyond the centre of the lens (black arrowhead) leaving only a small, lopsided pupil opening. (D–G) Thin-section electron microscopy images of 5 dpf *bum*$^{-/-}$ (D, E) and wild-type lenses (F–G). The images of mutant lenses show that the initial stages of fibre cell differentiation occur normally with the cells (and their nuclei) adopting a flattened shape during cellular elongation. Soon after the onset of differentiation (3–4 cells into the lens), however, the differentiating secondary lens fibre cells appear to swell, increasing in thickness by a factor of up to ten (asterisks). A further 1–2 cells deeper into the lens, the secondary fibre cells appear to detach from each other and/or fragment. This results in large empty, vacuolar spaces (v) between fibre cell fragments. The fibre cells of the lens nucleus by contrast appear to have differentiated normally. Such swelling, detachment and fragmentation of secondary lens fibres is never observed in age-matched wild-type sibling lenses (F, G). (H, I) Morphology of the adult eye in *bum*$^{-/-}$ as revealed in transverse sections through the central part of the eye. Except for the conspicuous absence of the lens and an almost closed pupil opening (arrowhead and inset in H), the morphology of the eye in *bum*$^{-/-}$ mutant zebrafish is comparable to that of wild-type individuals, with a neural retina displaying all characteristic layers, a retinal pigment epithelium interdigitating with the well-developed photoreceptor outer segments, as well as a normally formed anterior chamber, vitreous humour cavity and cornea. A higher magnification of part of the retina of an adult *bum*$^{-/-}$ mutant zebrafish shows normal retinal layering (I). Abbreviations: AC, anterior chamber; C, cornea; EC, lens epithelial cells; GCL, ganglion cell layer; INL, inner nuclear layer; IPL, inner plexiform layer; L, lens; LFC, lens fibre cells; n, nuclei of differentiating secondary lens fibre cells; NR, neural retina; ON, optic nerve exiting the retina; OPL, outer plexiform layer; PFC, primary lens fibre cells; PRC, photoreceptor cells; RPE, retinal pigment epithelium; v, vacuolar spaces; VH, vitreous humour.

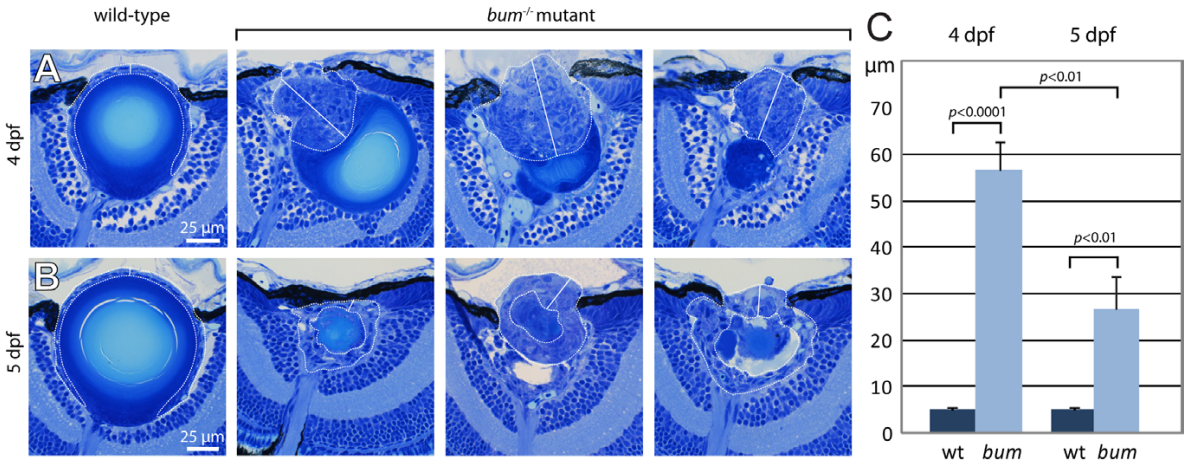

Fig. 5 – The hyperproliferation of the lens epithelium regresses between 4 and 5 dpf in *bum*$^{-/-}$ mutant larvae. (A–B) Histological sections of sibling (wild-type, wt) and *bum*$^{-/-}$ mutant eyes at 4 dpf (A) and 5 dpf (B). The lens epithelial cells are encircled (curved dotted lines) and the lines along which the thickness of the lens epithelium was measured are indicated (straight solid lines). Note that the epithelium in the wild-type lenses always comprises a single layer of cells (epithelial monolayer), whereas in the mutant lenses it can be very significantly expanded (three representative examples are shown for each developmental stage). (C) Quantitative measurements of the thicknesses of wild-type ($n = 10$) and *bum*$^{-/-}$ mutant lens epithelia ($n = 10$ for 4 dpf; $n = 9$ for 5 dpf). Mutant epithelia are on average approx. 10-fold and 5-fold thicker than wild-type epithelia at 4 and 5 dpf, respectively. Notably, there is a statistically significant decrease of 53% in the thickness between mutant lens epithelia from 4 to 5 dpf. Error bars represent the standard error of the mean (SEM).

the differentiation of primary and secondary lens fibres have previously been described (reviewed in Dahm (1999), Dahm et al. (2007)). The molecular mechanism(s) underlying these differences are, however, still largely unknown. The *bum* mutant might thus offer interesting insights into the molecular differences between these two processes.

Note that the pupil diameter in *bum*$^{-/-}$ eyes at 5 dpf is already noticeably reduced as compared to the wild-type eyes (compare panel A (wild-type) with panels B and C (mutant) in Fig. 4; see also Fig. 5). This feature of the mutant phenotype, combined with the absence of the anterior part of the lens protruding into the anterior eye chamber (compare panel A (wild-type) with panels B and C (mutant) in Fig. 4), greatly facilitates the reliable identification of mutant individuals at this developmental stage.

Despite the severity of the lens phenotype in *bum*$^{-/-}$ individuals – the hyperproliferation of the lens epithelium, the compromised secondary lens fibre cell differentiation and the deformation of the lens fibre cell mass – the development of the other tissues in the *bum*$^{-/-}$ eye appears to be largely unaffected. In particular, the retina and the cornea, which are in close contact with the lens throughout development, appear to be unaffected in a major way. The mutant retina, for instance, displays all the layers seen in the wild-type, including, from the centre of the eye to its periphery, a ganglion cell layer, an inner plexiform layer, an inner nuclear layer, an outer plexiform layer, a photoreceptor cell layer and a retinal pigment epithelium (Figs. 1A–C (3 dpf); 2A, B (4 dpf); 4A–C (5 dpf) and Fig. 4H, I (adult)). Moreover, as seen in the wild-type, the optic nerve exits the eye and seems to be projecting normally to the brain (Figs. 1A, C; 2B). Also the cornea appears morphologically normal at all stages examined (Figs. 1A–G′ (3 dpf); 2A–E (4 dpf); 4A, D (5 dpf) and Fig. 4H (adult)). These findings indicate that the ocular phenotype in the *bum*$^{-/-}$ mutant is lens-specific. It should, however, be noted that compared to the wild-type adult retina (Suppl. Fig. 2), the thickness of retinal layers in adult *bum*$^{-/-}$ eyes appears reduced. This is likely a secondary effect resulting from the lack of (or reduction in) visual input in the adult mutant, which lack a pupil (Fig. 6), and the subsequent decreased need for processing of visual information, which might result in fewer cells and neuronal connections in the *bum*$^{-/-}$ retina.

In view of the fact that the lens is considered a major contributor to the shape of the developing eye, it is notable that at 5 dpf the overall size of the eyes is only slightly affected by the reduction in lens size in *bum*$^{-/-}$ larvae (Fig. 4A, B). This is in contrast to later stages where the eyes of *bum*$^{-/-}$ zebrafish are more strongly reduced compared to age-matched wild-type individuals. Especially, in adult zebrafish, which normally have prominent lateral eyes (Fig. 6A), the eyes are significantly smaller in *bum*$^{-/-}$ mutant individuals (Fig. 6B; see also Fig. 8B, E below).

Sectioning of the eyes of adult *bum*$^{-/-}$ zebrafish revealed the absence of a lens in the mutant (Fig. 4H). This indicates that the small lenses which initially form in *bum*$^{-/-}$ larvae remain too small to be detected when preparing serial sections or are lost as development proceeds. While we cannot formally rule out the presence of very small, residual lenses (as observed at early larval stages; see e.g. Fig. 4B), the lack of large, transparent lenses centrally located in the eyes of adult *bum*$^{-/-}$ zebrafish means that the functions normally fulfilled by this structure are absent in the mutant.

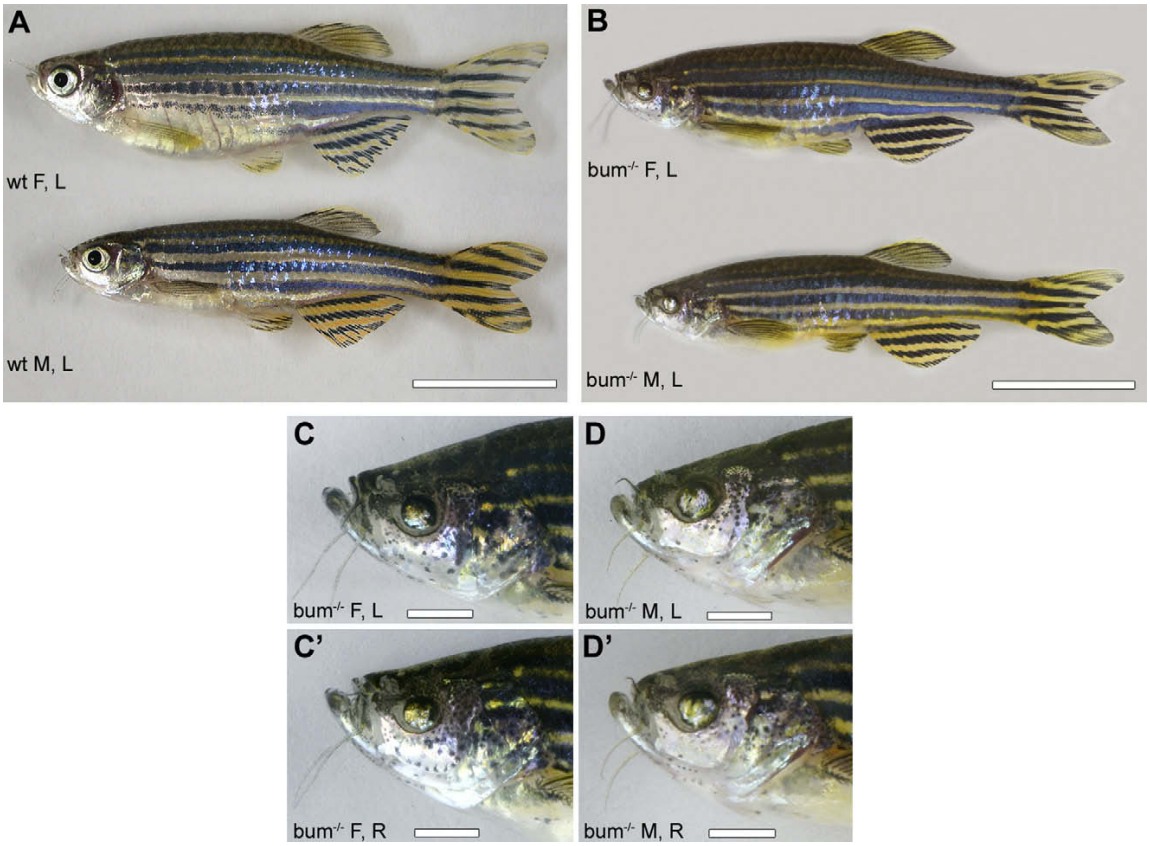

Fig. 6 – *bum*$^{-/-}$ mutant zebrafish survive to adulthood but show smaller eyes lacking a pupil. (A–D) External views of adult sibling (wild-type; wt) and homozygous *bum*$^{-/-}$ zebrafish. (A) Lateral views of the left (L) side of the bodies of a female (F) and a male (M) adult sibling zebrafish. (B) Lateral views of the left side of the body of a female and a male homozygous *bum*$^{-/-}$ adult zebrafish revealing a bilateral reduction in eye size and a complete lack of a pupil in the mutant. (C, C′) Magnifications of the left (L) and right (R) sides of the head of the female homozygous *bum*$^{-/-}$ zebrafish shown in B. (D, D′) Magnifications of the left (L) and right (R) sides of the head of the male homozygous bumper zebrafish shown in B. Note that adult sibling and *bum*$^{-/-}$ individuals are of comparable size and, except for the eyes, overall morphology. Scale bars: A, B: 1 cm, C–D′: 2 mm.

Adult *bum*$^{-/-}$ eyes are further characterised by a virtually closed pupil. Instead of the iris forming a large, circular opening as observed in wild-type eyes (Fig. 6A), the iris in adult *bum*$^{-/-}$ eyes appears continuous (Fig. 6C–D′) or with only small unpigmented areas (Fig. 4H and inset in 4H; arrowheads point to a short melanin-free area in the continuous iris). This morphology would allow for only very little light to be able to penetrate into the eyes of *bum*$^{-/-}$ individuals. Surprisingly, the cornea (Fig. 4H) as well as the retina (Fig. 4I) and the other parts of the eye (Fig. 4H) appear to have developed normally in *bum*$^{-/-}$ zebrafish despite the severe degeneration/absence of the lens. The overall size of the eye in adult *bum*$^{-/-}$ mutant zebrafish (Fig. 6B–D) is, however, substantially reduced as compared to the wild-type (Fig. 6A).

2.2. *Visual behaviour of bum*

Despite a retina with wild-type morphology, *bum*$^{-/-}$ mutant larvae and adult fish display morphological and behavioural phenotypes that indicate a lack of visual function. For instance, when kept under bright light conditions, the dorsal and lateral surfaces of adult *bum*$^{-/-}$ zebrafish are significantly darker than those of age-matched siblings (Fig. 7A, B), indicating that *bum*$^{-/-}$ zebrafish fail to undergo visual background adaptation (VBA). This is a mechanism by which zebrafish can adjust the brightness of their skin to environmental light levels by changing the distribution of melanosomes in the skin's melanocytes. In bright light conditions, the melanin granules are concentrated in a small, perinuclear volume resulting in most of the melanocytes' cytoplasm being melanin-free. As a consequence the fish's skin will appear lighter. By contrast under conditions of low light levels, the melanin granules are dispersed throughout the melanocytes thus covering most of the skin area and resulting in a darker appearance. As VBA in zebrafish is mediated by visual input through the eyes (Sugimoto, 2002; Baker, 1993), the absence of this response in *bum*$^{-/-}$ individuals is an indication that these fish are strongly impaired in light perception.

This observation is corroborated by observations of the visual behaviour of *bum*$^{-/-}$ adult zebrafish. In contrast to wild-

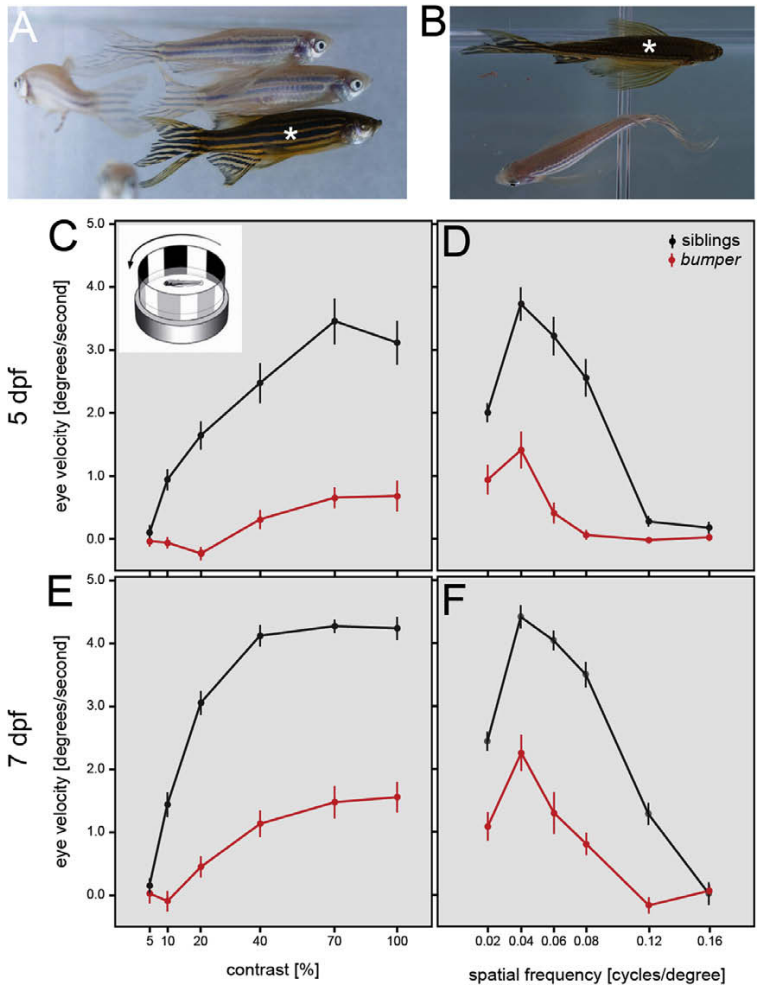

Fig. 7 – *bum*$^{-/-}$ zebrafish are severely visually impaired. (A–B) Lateral (A) and dorsal (B) views of adult *bum*$^{-/-}$ mutant zebrafish and sibling (wild-type) zebrafish swimming together. Note the significantly darker overall appearance of the mutant fish (asterisks; lower individual in A and upper individual in B, respectively) compared to their siblings when kept under bright light conditions. (C–F) Optokinetic response of *bum*$^{-/-}$ mutants and siblings at 5 dpf (C, D) and 7 dpf (E, F). Both contrast sensitivity (C, E) and visual acuity (D, F) are affected by the mutation. In both paradigms the eye velocity as a measure of visual performance is lower in *bum*$^{-/-}$ mutant larvae compared to their siblings. The inset in C shows a schematic representation of the experimental set-up.

type zebrafish, which actively and in a directed fashion swim towards food (e.g. flakes of dry food or *Artemia*) even from considerable distances, *bum*$^{-/-}$ individuals aimlessly scout their tanks until, almost by accident, they touch a food item with their head at which point they rapidly turn to ingest it. This behaviour was frequently observed in >4 separate tanks of adult *bum*$^{-/-}$ zebrafish each containing at least 15 individuals.

2.3. *Contrast sensitivity and visual acuity are affected by the mutation in bum*

In order to obtain more quantitative data on the visual ability of *bum*$^{-/-}$ zebrafish, we performed optokinetic response tests to assess visual performance (Rinner et al., 2005). We compared the visual performance of *bum*$^{-/-}$ larvae with that of age-matched (wild-type) siblings in two experimental paradigms. In the first experiment, we tested contrast sensitivity by varying the contrast of the projected stripes (Fig. 7C, E). This test revealed a highly significant reduction in contrast sensitivity in *bum*$^{-/-}$ mutants compared to their siblings at 5 dpf [$F(1;19) = 34.92$, $p < 0.001$] as well as at 7 dpf [$F(1;19) = 89.91$, $p < 0.001$]. At all contrast levels, the eye velocity in *bum*$^{-/-}$ mutants was significantly lower compared to siblings with the exception of 5% contrast, where both groups show spontaneous baseline activity as observed in the absence of movement in the surround (data not shown).

The second test used to assess for visual acuity involved varying the spatial frequency of the moving stripes. The visual acuity of *bum*$^{-/-}$ mutants is also affected by the mutation in this test (Fig. 7D, F). The average eye velocity of 5 and 7 day

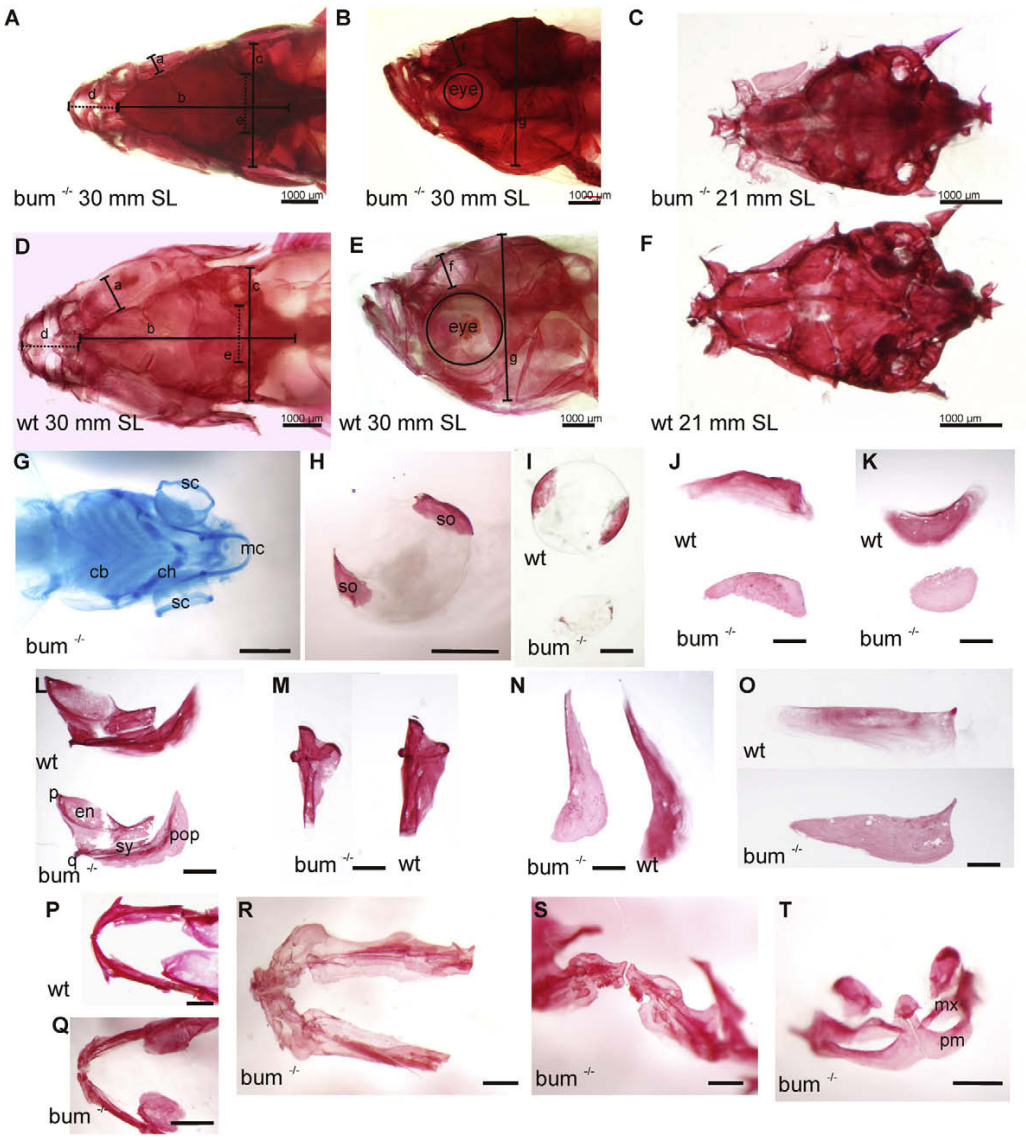

Fig. 8 – Skeletal analyses by whole-mount staining reveal craniofacial defects and a normal ocular skeleton. Alizarin red staining, except for G, which is stained with Alcian blue. (A–C) *bum*$^{-/-}$, (D–F) wild-type (wt). Comparative linear dimensions are shown and indicated by a–g. (A) dorsal view, *bum*$^{-/-}$ 30 mm SL; (B) lateral view, *bum*$^{-/-}$ 30 mm SL; (C) dorsal view after removal of jaws, eyes and opercular complex, *bum*$^{-/-}$ 21 mm SL; (D) dorsal view, wt 30 mm SL; (E) lateral view, wt 30 mm SL; (F) dorsal view after removal of jaws, eyes and opercular complex, wt 21 mm SL; (G) *bum*$^{-/-}$ 10 mm SL, Alcian blue-stained; (H) scleral ossicles, *bum*$^{-/-}$ 30 mm SL; (I) scleral ossicles of wt 21 mm SL, top, and *bum*$^{-/-}$ 21 mm SL, below; (J) supraorbital bone of wt 21 mm SL, top, and *bum*$^{-/-}$ 21 mm SL, below; (K) suborbital bone of wt 21 mm SL, top, and *bum*$^{-/-}$ 21 mm SL, below; (L) lateral bones including pterygoid complex, preopercle, symplectic, and quadrate bones, wt 21 mm SL, top, and *bum*$^{-/-}$ 21 mm SL, below; (M) hyomandibular, wt 21 mm SL, right, and *bum*$^{-/-}$ 21 mm SL, left; (N) subopercle, wt 21 mm SL, right, and *bum*$^{-/-}$ 21 mm SL, left; (O) interopercle, wt 21 mm SL, top, and *bum*$^{-/-}$ 21 mm SL, below; (P) mandible, wt 30 mm SL; (Q) mandible, *bum*$^{-/-}$ 30 mm SL; (R) mandible, *bum*$^{-/-}$ 28 mm SL; (S) mandible, *bum*$^{-/-}$ 30 mm SL; (T) maxilla complex, *bum*$^{-/-}$ 30 mm SL. Abbreviations: cb, ceratobranchials; ch, ceratohyal cartilage; en, entopterygoid; mc, Meckel's cartilage; mx, maxilla; p, palatine; pm, premaxilla; q, quadrate; sc, scleral cartilage; so, scleral ossicles; sy, symplectic. Scale bars: 500 μm unless otherwise indicated.

old *bum*$^{-/-}$ mutants compared to their siblings is highly significantly reduced [$F(1;18) = 31.10$, $p < 0.001$ or $F(1;18) = 53.65$, $p < 0.001$, respectively] for any spatial frequency tested except for 0.16 cycles (Fig. 7D, F). This spatial frequency is below the cut-off frequency detected by wild-type individuals and therefore no eye movement is evoked. Interestingly, both larval groups showed an increase in visual performance in both experimental paradigms with age, reflecting the ongoing maturation of the visual system also in *bum*$^{-/-}$ mutant larvae. It should, however, be noted that *bum*$^{-/-}$ mutant zebrafish show a very limited visual ability in the tests we performed.

Importantly, the mutation in *bum* does not affect a vital organ or cell type as homozygous *bum*$^{-/-}$ mutant zebrafish are viable (Fig. 6). Moreover, it does not affect fertility (we succeeded in breeding homozygous *bum*$^{-/-}$ mutants over several generations). While the absence of visual function would constitute a significant decrease in fitness for individuals living in the wild, eyes are a non-essential organ in the artificial setting of a laboratory, especially when *bum*$^{-/-}$ individuals are kept separate from wild-type zebrafish and thus are not competing for food. Given that adult *bum*$^{-/-}$ zebrafish are viable and display no obvious difference in survival rates when compared with wild-type zebrafish, this strain is suited for experiments in which *bum*$^{-/-}$ and wild-type zebrafish are kept in the same environment to assess their respective fitness and thus assess the evolutionary advantage of vision in a vertebrate species. In blind tetra (cavefish), the reduction of the eye has lead to several constructive changes which include expanded circumorbital bones (shown here for *bum*$^{-/-}$ as well; see below) as well as increased taste buds and neuromasts, presumably to compensate for the lost visual ability (see Franz-Odendaal and Hall, 2006, for discussion). Although it would be extremely interesting to investigate whether these changes also occur in *bum*$^{-/-}$, our behavioural data (described above) would suggest that no compensation has occurred.

2.4. *Skeletal analyses reveal craniofacial defects and a normal ocular skeleton*

In addition to the lens and other ocular phenotypes described above, skeletal anomalies were observed in the craniofacial region of *bum*$^{-/-}$ zebrafish, whereas the trunk skeleton appeared normal in all specimens examined. In wild-type zebrafish the eye occupies a large space within the skull. In *bum*$^{-/-}$, however, many (but not all) of the craniofacial skeletal elements are altered in size and/or shape. Overall the skull appears to be reduced in all three axes – anterior-posteriorly, laterally and dorso-ventrally – compared to wild-type specimens (Fig. 8A–F). Specifically, the length of the skull roof (distance b in Fig. 8A, D), its overall width (distance c) and the depth (distance g) of the skull are reduced in *bum*$^{-/-}$ compared to wild-type individuals (Suppl. Table 1). Statistical analyses show that all three measures are significantly different (length: $t(-5.57, 12)$, $p = 0.0001$; width: $t(-3.54, 12)$, $p = 0.004$; depth: $t(-1.79, 9)$, $p = 0.10$). Interestingly, the distance between the subtemporal fossa (distance e in Fig. 8A, D) is similar suggesting that this defect is not a simple re-scaling of the skull dimensions.

Cartilage and bone elements of the olfactory region are also normal in *bum*$^{-/-}$. In 2 out of 6 adult *bum*$^{-/-}$ zebrafish, the dentary bone has ectopic asymmetric ossifications while the maxilla and premaxilla of these specimens are only mildly affected (Fig. 8P–T). For example, the dorsal process of the premaxilla in one specimen is slightly shorter on the left versus the right side. One specimen also has a severely folded opercule bone on the left side. The hyoid and branchial arches are normal, while the pterygoid complex and hyomandibular bones are slightly smaller in *bum*$^{-/-}$ compared to wild-type specimens of the same size (Fig. 8G, L, M).

Apart from the overall differences in skull shape, some of the orbital bones are altered in shape, size or position (Fig. 8J, K, N, O). The supraorbital bone (dissected in Fig. 8J), which usually covers the dorsal aspect of the eyeball (distance in Fig. 8A, D), instead extends ventrally to partially cover the orbit, thereby further reducing the lateral dimensions of the skull. Surprisingly despite adult *bum*$^{-/-}$ zebrafish having a non-functional eye which is significantly reduced in size in the adult (Figs. 6 and 7), the ocular skeleton is preserved with normal scleral cartilage (Fig. 8G) in juveniles. This element later ossifies periskeletally from the scleral cartilage template to form two normal scleral ossicles (Fig. 8H, I). This ossification occurs much later than scleral cartilage induction and lens development (Franz-Odendaal et al., 2007), however in *bum*$^{-/-}$ subadult specimens, we observed delayed ossification of the scleral ossicles (Fig. 8I, top wild-type, bottom, *bum*$^{-/-}$). These findings suggest that the developmental programme responsible for induction of the ocular skeleton is unchanged despite lens degeneration. This is in contrast to lens ablation experiments done in the sighted Mexican tetra (*Astyanax mexicanus*), where ablating the lens prevents scleral ossicle formation, leaving only the scleral cartilage template (Yamamoto et al., 2003). The infraorbital bones of *bum*$^{-/-}$ are also slightly expanded (not shown).

One reason why the ocular skeleton is preserved in *bum*$^{-/-}$ but not in cavefish could be differences in the process of lens degeneration. In *bum*$^{-/-}$, the primary lens fibres and the other eye tissues (iris, cornea, retina) develop normally. The secondary lens fibres however, degenerate soon after forming resulting in a reduced size of the lens. In the cavefish, lens fibres do not form and the cornea does not differentiate, however, the retina does differentiate and the resulting optic cup is smaller (Jeffery and Martasian, 1998); Fig. 2D in Yamamoto and Jeffery (2000). This suggests that the degenerating secondary lens fibres are not required for normal development of the ocular skeleton in zebrafish. Alternatively, this could be a species difference.

Recently, Albertson and Yelick reported distinct skeletal defects including facial asymmetries, irregular cranial suturing and ectopic bone formation in zebrafish with an *fgf8* haploinsufficiency (*ace*^{ti282a}/*fgf8* heterozygotes) (Albertson and Yelick, 2007). The ectopic bone formation in these heterozygotes was limited to the mandible, as in *bum*$^{-/-}$, shown here, and was observed in 30% of homozygous recessive *ace*^{ti282a} mutants. The frontal region of the skull was expanded in both length and height relative to the posterior region. These authors hypothesize that the bone defects observed may relate to mechanisms that underlie bone growth and remodelling since FGFs are known to play major roles in skeletal development (e.g. Colvin et al., 1996; Deng et al., 1996 and others). The reason why the mandible region (and not other skel-

etal elements) is susceptible to ectopic bone growth is unclear at present but could point to as yet unknown epigenetic factors involved in teleost ossification. Further experiments to identify the mutation in *bum*$^{-/-}$ and whether it functions in the same genetic network as FGFs would need to be conducted in order to understand the observed craniofacial defects.

2.5. *Genetic mapping of the mutation in bumper*

To identify the genetic defect underlying the *bum*$^{-/-}$ phenotype, we mapped the mutation on the zebrafish genome. Pooled DNA of 48 *bum*$^{-/-}$ and 48 sibling 5 dpf larvae, respectively, was tested with 192 SSLP markers resulting in a linkage of the mutation to chromosome 7 between markers z4706 (located 28.3 cM north of the mutation) and z13880 (26.0 cM south of the mutation; data not shown). To narrow down the critical interval of the mutated locus, we tested additional SSLP markers located in this genomic region. Analysis of between 516 and 684 meioses identified z8604 and z7958 as the closest SSLP markers with distances of 0.2 and 3.7 cM, respectively (Fig. 9A). Analysis of 510 meioses for the marker z15069 revealed no recombination events, indicating very close linkage to this SSLP marker (asterisk in Fig. 9A).

As the phenotype observed in *bum*$^{-/-}$ larvae suggests a defect in secondary lens fibre cell differentiation and in the development of the head skeleton, we screened the genomic region between the SSLP markers z8604 and z7958 for genes that, when mutated, might explain the phenotype (Fig. 9B). This approach resulted in three candidate genes: *hspa12b*, a heat-shock protein; *slc8a4b*, a member of a solute carrier family; and *cct7*, a chaperonin containing TCP1, subunit 7 (eta). *hspa12b* and *cct7* appeared as attractive candidates as heat-shock proteins/chaperones have been shown to play crucial roles in the development and function of the vertebrate lens (Akerfelt et al., 2007; Banh et al., 2006), including in zebrafish (Mao and Shelden, 2006; Krone et al., 2003; Blechinger et al., 2002), and have been demonstrated to be important for lens fibre cell differentiation in this species (Evans et al., 2007, 2005). *slc8a4b* was chosen as a candidate gene due to the crit-

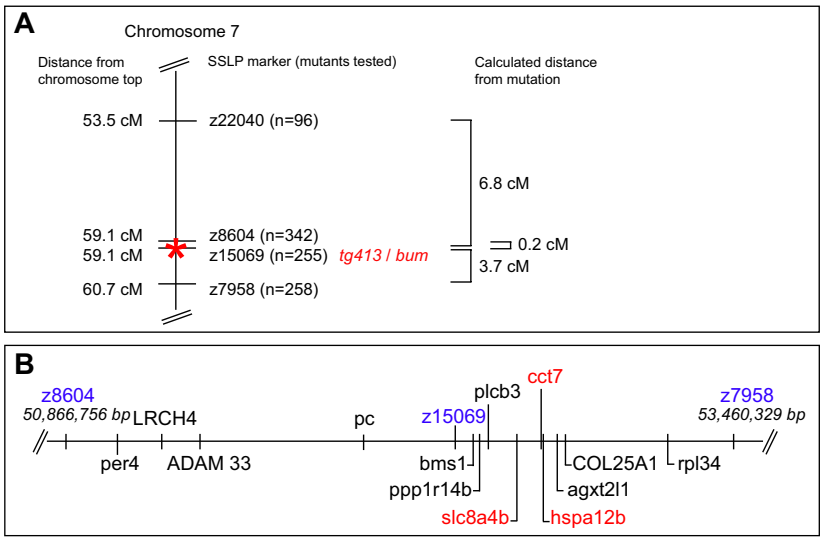

Fig. 9 – The mutation in *bumper* maps to chromosome 7. (A) Genetic mapping of *bum* resulted in close linkage to SSLP markers z8604, z15069 and z7958 on chromosome 7. Distances from the mutation are given in centimorgan (cM). Figures in brackets refer to the number of *bum*$^{-/-}$ larvae analysed. Note that the 255 *bum*$^{-/-}$ larvae tested for the SSLP marker z15069 did not show a recombination event resulting in a distance to the mutation (asterisk) of 0 cM. The locations of the SSLP markers from the top of chromosome 7 are indicated in cM as predicted by the MGH genetic map of the zebrafish genome. (B) Schematic representation of the region of the zebrafish genome comprising the three SSLP markers (blue) closest to the *bum* mutation as predicted by the ENSEMBL zV7 assembly. The representation shows known genes or genes with known homology to genes characterised in other organisms as well as their locations. Genes in sense orientation are shown above the line representing part of chromosome 7, those in antisense orientation below. Genes sequenced as part of this study are indicated in red. Note that the distances between the markers differ between the ENSEMBL assembly (B) and those on the genetic map (A). The abbreviated gene names stand for: per4, period homolog 4; LRCH4, Leucine-rich repeat and calponin homology domain-containing protein 4 (Leucine-rich repeat neuronal protein 4, Leucine-rich neuronal protein); ADAM 33, ADAM 33 Precursor (A disintegrin and metalloproteinase domain 33); pc, pyruvate carboxylase; bms1, breast cancer metastasis-suppressor 1; ppp1r14b, protein phosphatase 1, regulatory (inhibitor) subunit 14B; plcb3, novel protein similar to human phospholipase C beta (PLCB) (fragment); slc8a4b, solute carrier family 8 (sodium/calcium exchanger), member 4b; cct7, chaperonin containing TCP1, subunit 7 (eta); hspa12B, heat-shock protein 12B; agxt2l1, Alanine-glyoxylate aminotransferase 2-like 1; COL25A1, Collagen alpha-1(XXV) chain (CLAC-P) (Alzheimer disease amyloid-associated protein; AMY); rpl34, 60S ribosomal protein L34.

ical role of ion channels in lens physiology (reviewed in Mathias and Rae (2004)) and the observed phenotype, i.e. the swelling of the secondary fibres soon after the onset of differentiation, could be explained by an osmotic imbalance in these cells.

We prepared cDNA from 5 dpf old *bum*$^{-/-}$ and sibling larvae and sequenced all of these genes. Analysis of the full-length coding sequences of the *hspa12b*, the *cct7* and the *slc8a4b* genes did, however, not reveal a mutation that would alter the amino acid sequence of the corresponding proteins (see Suppl. Figs. 3–5, respectively). This suggests that either the mutation in *bum*$^{-/-}$ affects a different gene or that it is not located in the coding region of one of either of these genes, but in regulatory sequences such as promoter regions. In the latter case, only extensive sequencing of large regions of the DNA flanking the candidate genes might reveal possible mutations, which would subsequently have to be validated in, for example, reporter assays.

3. Materials and methods

3.1. Fish husbandry and breeding

The zebrafish (*Danio rerio*) used in this study were of the Tübingen (TU) strain (Dahm et al., 2005; Geisler, 2002). General fish husbandry was as described (Brand et al., 2002). Embryos and larvae up to 5 days post-fertilisation (dpf) were kept in E3 medium (5 mM NaCl, 0.17 mM KCl, 0.33 mM $CaCl_2$, 0.33 mM $MgSO_4$ and 10^{-5}% methylene blue in distilled water) at 28 °C and staged according to morphological markers as published (Dahm, 2002; Kimmel et al., 1995). For external and behavioural analyses, living larvae and adult fish were anesthetized in 0.01% Tricaine® (3-aminobenzoic acid ethylester, Sigma) and mounted in 3% methyl cellulose (w/v) in E3 medium (Brand et al., 2002).

The zebrafish mutant *bumper* (*bum*; tg413, originally referred to as tg413b) (Heisenberg et al., 1996) was initially identified in a large-scale ENU mutagenesis screen using zebrafish with the TU background carried out at the Max Planck Institute for Developmental Biology in 1994–1995 (Haffter et al., 1996).

3.2. Histology and whole-mount staining

Zebrafish embryos and larvae at different stages of development as well as adult zebrafish were fixed in a solution of 4% (w/v) paraformaldehyde and 2.5% (v/v) glutaraldehyde in 75 mM phosphate buffer (pH 7.4) for 1 h at room temperature (RT) and stored at 4 °C overnight. For light microscopy, the fixed embryos and larvae were dehydrated in a graded series of ethanol (30%, 50%, 70%, 90%, 96% and 2 × 100% for 15 min each). Subsequently, the samples were infiltrated with Technovit® 7100 (Heraeus-Kulzer, Wehrheim/TS, Germany) including hardener I through the following steps: 1× in 2:1 100% ethanol/Technovit for 30 min, 1× in 1:1 100% ethanol/Technovit for 30 min, 1× in 100% Technovit for 45 min and 1× in 100% Technovit for 1 h. All steps were carried out at RT under gentle agitation. The infiltrated samples were transferred into freshly made Technovit 7100 containing both hardener I and II, properly orientated in moulds and left overnight to polymerize. Sections of 1–4 μm thickness were cut on a microtome (Reichert, Austria) using glass knifes. The sections were subsequently transferred onto a drop of 15% ethanol on SuperFrost® Plus slides (Menzel-Glaser, Germany) and left to dry on a heated plate at approx. 50 °C for 15 min. For general histology, the dried sections were stained with 0.5% toluidine blue (Fluka) in 1% sodium tetraborate for 10 s. Excess staining solution was washed off with tap water and the sections left to dry again at approx. 50 °C for 15 min. For imaging and long-term storage, dried slides were mounted in Epon and examined in an Axiophot microscope (Zeiss, Germany) equipped with a digital camera. For the histological analyses, >10 individuals were used for the larval stages and 5 adult individuals were analysed.

For the visualisation of apoptotic cells in the lens, living 4 dpf zebrafish larvae were incubated in 0.5% (w/v) Acridine Orange (Sigma, Germany) in E3 medium without methylene blue for 90 min. at 28 °C. The incubated larvae were then washed three times with E3 medium and examined with an Olympus BX61 fluorescence microscope (Olympus, Germany). The number of apoptotic bodies within the lens of 8 siblings and 8 mutant larvae were manually counted and statistically analysed using SPSS (SPSS, USA). Image processing and graph designing was performed with Adobe Photoshop and Illustrator (Adobe Systems, USA) and SPSS (SPSS, USA).

To visualise the skeleton, adult and juvenile *bum*$^{-/-}$ and wild-type zebrafish were whole-mount stained with Alizarin red and/or Alcian blue (described in Franz-Odendaal et al. (2007)). Briefly fish were fixed overnight in 4% paraformaldehyde at 4 °C, dehydrated, bleached in a mild hydrogen peroxide solution and trypsinized to remove most of the soft tissue. Approx. 15 specimens were stained in this manner. The analyses focused on 8 specimens ranging in size from 15–30 mm SL which showed the most striking skeletal differences. Specimens were examined using a Nikon SMZ1500 stereomicroscope. Some dissection was conducted to display the skeletal phenotypes. Measurements of skeletal elements were taken from digital images using Nikon NIS imaging software. Student *t*-tests were used to compare measures between wild-type and mutant fish. All measures were standardized with standard length. Statistical analyses were conducted using Sigma Plot 10.0 (Systat Software Inc., USA).

3.3. Electron microscopy

For transmission electron microscopy (TEM) of embryonic and larval eyes, the specimens were fixed in five times their volume of 2.5% (v/v) glutaraldehyde and 4% (w/v) paraformaldehyde in 75 mM phosphate buffer (pH 7.4) for at least 24 h. The fixed specimens were then washed three times with PBS and contrasted with 1% OsO_4 in PBS for 90 min. on ice. The samples were subsequently washed once in PBS and three times in distilled water, before being incubated in 1% aqueous uranyl acetate for 1 h. The tissue was then dehydrated in a graded series of ethanol at RT and embedded in Epon (Roth, Karlsruhe, Germany). Ultrathin sections (60–100 nm) were cut on a LKB Ultratome IV (LKB Instruments, Bromma, Sweden), contrasted with lead citrate (Venable and Coggeshall, 1965) and examined using a Philips CM10 transmission electron microscope (Philips Industries, Eindhoven,

The Netherlands) operating at 60 kV. The TEM analyses were performed on 10 individuals.

3.4. Quantitative measurement of lens epithelial cell hyperproliferation

For the measurements of the hyperproliferating lens epithelia, 4 and 5 dpf larvae were fixed in a solution of 4% (w/v) paraformaldehyde in 150 mM phosphate buffer (pH 7.4) overnight at 4 °C. Fixed larvae were dehydrated in a graded series of ethanol (see above) and subsequently infiltrated with Technovit® 7100 (Heraeus-Kulzer, Germany) including hardener I 2× in 1:1 100% ethanol/Technovit for 30 min each and 2× in 100% Technovit for 1 h each. All steps were carried out at RT under gentle agitation. The infiltrated samples were transferred into freshly made Technovit 7100 containing both hardener I and II, properly orientated in moulds and left overnight to polymerize. Sections of 3 μm thickness were cut on a Leica RM 2145 microtome (Leica, Germany) using glass knifes. The sections were transferred onto a drop of ddH_2O on SuperFrost® Plus slides (Menzel-Glaser, Germany) and left to dry on a heated plate at approx. 50 °C for 15 min. For general histology, dried sections were stained with 0.5% toluidine blue (Fluka, Switzerland) in 1% sodium tetraborate (Fluka, Switzerland) for 10 s. Excess staining solution was washed off with tap water and the sections left to dry again at approx. 50 °C for 15 min. For imaging and long-term storage, dried slides were mounted in Entellan (Merck, Germany) and examined in an Olympus BX61 microscope (Olympus, Germany) equipped with a digital camera. Ten sibling and 9–10 mutant larvae were analyzed. The thickness of the lens epithelium was measured using ImageJ (National Institutes of Health, USA) and statistically evaluated and plotted with SPSS (SPSS, USA) and the Excel software (Microsoft, USA). The images were processed using Adobe Photoshop and Illustrator (Adobe Systems, USA).

3.5. Quantitative measurement of visual performance

The optokinetic response (OKR) was quantitatively measured to analyze the visual performance of *bum*$^{-/-}$ mutants. The stimulus triggering an OKR consisted of a 360° moving black-and-white sine-wave grating. Contrast sensitivity and visual acuity of 5 and 7 day old zebrafish larvae were tested by separately changing the contrast and the spatial frequency of the stimulation pattern. The temporal frequency was kept constant at 7.5 degrees per second. The stimulus was generated using the Vision Egg stimulus generation software library (Straw, 2008). It was projected by a LCD projector (Sony, VPL CX1) via a mirror to the inside of a white cylindrical screen with a diameter of 90 mm. The larva to be analyzed was placed in a 35 mm Petri dish and immobilized in a 3% methyl cellulose solution in the centre of the cylinder. The elicited eye movements were recorded by an infrared-sensitive black-and-white CCD camera (Allied Vision Technologies, Guppy F-038B NIR) and evaluated by custom made software based on Labview v7.1 with IMAQ v3.7 extension (National Instruments). A total of 10 sibling and 10 *bum*$^{-/-}$ mutant larvae were analyzed for both paradigms. Statistic analysis and graph design were performed using SPSS v17.0 (SPSS Inc.).

3.6. Genetic mapping of *bum*$^{-/-}$ and sequencing of candidate genes

Map crosses were set up between heterozygous *bum*$^{+/-}$ (Tü background) and wild-type WIK zebrafish. The offspring from these crosses were inbred and homozygous *bum*$^{-/-}$ and sibling F_2 progeny were collected and their DNA extracted. Bulked segregant analysis on 48 *bum*$^{-/-}$ larvae and siblings, respectively, was done using 192 simple sequence length polymorphisms (SSLP markers) distributed over the entire genome (Geisler, 2002). Further fine mapping was performed using the total DNA of additional single homozygous *bum*$^{-/-}$ mutant larvae. The number of mutant larvae tested for each SSLP marker in the fine mapping approach is given in Fig. 7. DNA extraction and PCR were performed as described (Geisler, 2002; Schonthaler et al., 2008). The coding sequences (cds) of the zebrafish genes *hspa12b*, *cct7* and *slc8a4b* were sequenced using primers encompassing the entire cds of the respective cDNAs.

Acknowledgements

The authors are very grateful to Brigitte Sailer (Max Planck Institute for Developmental Biology) for help with the processing of samples for TEM. The authors would also like to thank Daniele Oberti (Institute of Neuroinformatics of the ETH and University Zürich) for help with taking the photographs of swimming adult *bum*$^{-/-}$ and wild-type zebrafish. This work was supported by an EMBO Long-term Fellowship (RD) and by the European Commission as part of the ZF-MODELS Integrated Project in the 6th Framework Programme, Contract No. LSHG-CT-2003-503496 (SCFN, RD, RG), and the Swiss National Science Foundation grant SNF 31-117782 (CH, SCFN).

Appendix A. Supplementary data

Supplementary data associated with this article can be found, in the online version, at doi:10.1016/j.mod.2010.01.005.

REFERENCES

Akerfelt, M., Trouillet, D., Mezger, V., Sistonen, L., 2007. Heat shock factors at a crossroad between stress and development. Ann. NY Acad. Sci. 1113, 15–27.

Albertson, C.R., Yelick, P.C., 2007. Fgf8 haploinsufficiency rsults in distinct craniofacial defects in adult zebrafish. Dev. Biol. 306, 505–515.

Ashery-Padan, R., Marquardt, T., Zhou, X., Gruss, P., 2000. Pax6 activity in the lens primordium is required for lens formation and for correct placement of a single retina in the eye. Genes Dev. 14, 2701–2711.

Baker, B.I., 1993. The role of melanin-concentrating hormone in color change. Ann. NY Acad. Sci. 680, 279–289.

Banh, A., Bantseev, V., Choh, V., Moran, K.L., Sivak, J.G., 2006. The lens of the eye as a focusing device and its response to stress. Prog. Retin Eye Res. 25, 189–206.

Bassnett, S., 1992. Mitochondrial dynamics in differentiating fiber cells of the mammalian lens. Curr. Eye Res. 11, 1227–1232.

Bassnett, S., 1997. Fiber cell denucleation in the primate lens. Invest. Ophthalmol. Vis. Sci. 38, 1678–1687.

Bassnett, S., 2002. Lens organelle degradation. Exp. Eye Res. 74, 1–6.
Beebe, D.C., Coats, J.M., 2000. The lens organizes the anterior segment: specification of neural crest cell differentiation in the avian eye. Dev. Biol. 220, 424–431.
Blechinger, S.R., Evans, T.G., Tang, P.T., Kuwada, J.Y., Warren, J.T., Krone, P.H., 2002. The heat-inducible zebrafish hsp70 gene is expressed during normal lens development under non-stress conditions. Mech. Dev. 112, 213–215.
Bloemendal, H., de Jong, W., Jaenicke, R., Lubsen, N.H., Slingsby, C., Tardieu, A., 2004. Ageing and vision: structure, stability and function of lens crystallins. Prog. Biophys. Mol. Biol. 86, 407–485.
Brand, M., Granato, M., Nüsslein-Volhard, C., 2002. Keeping and raising zebrafish. In: Nüsslein-Volhard, C., Dahm, R. (Eds.), Zebrafish – A Practical Approach. Oxford University Press, Oxford.
Cheng, S., Shakespeare, T., Mui, R., White, T.W., Valdimarsson, G., 2004. Connexin 48.5 is required for normal cardiovascular function and lens development in zebrafish embryos. J. Biol. Chem. 279, 36993–37003.
Colvin, J.S., Bohne, B.A., Harding, G.W., McEwen, D.G., Ornitz, D.M., 1996. Skeletal overgrowth and deafness in mice lacking fibroblast growth factor receptor 3. Nat. Genet. 12, 390–397.
Coulombre, A.J., Coulombre, J.L., 1964. Lens development: fiber elongation and lens orientation. Science 142, 1489–1490.
Dahm, R., 1999. Lens fibre cell differentiation - A link with apoptosis? Ophthalmic Res. 31, 163–183.
Dahm, R., 2002. Atlas of embryonic stages of development in the zebrafish. In: Nüsslein-Volhard, C., Dahm, R. (Eds.), Zebrafish – A Practical Approach. Oxford University Press, Oxford.
Dahm, R., Prescott, A.R., 2002. Morphological changes and nuclear pore clustering during nuclear degradation in differentiating bovine lens fibre cells. Ophthalmic Res. 34, 288–294.
Dahm, R., Gribbon, C., Quinlan, R.A., Prescott, A.R., 1998. Changes in the nucleolar and coiled body compartments precede lamina and chromatin reorganization during fibre cell denucleation in the bovine lens. Eur. J. Cell Biol. 75, 237–246.
Dahm, R., Geisler, R., Nüsslein-Volhard, C., 2005. Zebrafish (*Danio rerio*) genome and genetics, second ed.. In: Meyers, R.A. (Ed.), Encyclopedia of Molecular Cell Biology and Molecular Medicine, vol. 15 Wiley-VCH, Weinheim, pp. 593–626.
Dahm, R., Schonthaler, H.B., Soehn, A.S., van Marle, J., Vrensen, G.F., 2007. Development and adult morphology of the eye lens in the zebrafish. Exp. Eye Res. 85, 74–89.
Deng, C., Wynshaw-Boris, A., Zhou, F., Kuo, A., Leder, P., 1996. Fibroblast growth factor receptor 3 is a negative regulator of bone growth. Cell 84, 911–921.
Driever, W., Solnica-Krezel, L., Schier, A.F., Neuhauss, S.C., Malicki, J., Stemple, D.L., Stainier, D.Y., Zwartkruis, F., Abdelilah, S., Rangini, Z., et al, 1996. A genetic screen for mutations affecting embryogenesis in zebrafish. Development 123, 37–46.
Easter Jr., S.S., Malicki, J.J., 2002. The zebrafish eye: developmental and genetic analysis. Results Probl. Cell Differ. 40, 346–370.
Evans, T.G., Yamamoto, Y., Jeffery, W.R., Krone, P.H., 2005. Zebrafish Hsp70 is required for embryonic lens formation. Cell Stress Chaperones 10, 66–78.
Evans, T.G., Belak, Z., Ovsenek, N., Krone, P.H., 2007. Heat shock factor 1 is required for constitutive Hsp70 expression and normal lens development in embryonic zebrafish. Comp. Biochem. Physiol. A Mol. Integr. Physiol. 146, 131–140.
Fadool, J.M., Dowling, J.E., 2008. Zebrafish: a model system for the study of eye genetics. Prog. Retin Eye Res. 27, 89–110.
Franz-Odendaal, T.A., Hall, B.K., 2006. Modularity and sense organs in the blind cavefish, *Astyanax mexicanus*. Evol. & Dev. 8, 94–100.
Franz-Odendaal, T.A., Ryan, K., Hall, B.K., 2007. Developmental and morphological variation in the teleost craniofacial skeleton reveals an unusual mode of ossification. J. Exp. Zoolog. B Mol. Dev. Evol. 308, 709–721.
Geisler, R., 2002. Mapping and cloning. In: Nüsslein-Volhard, C., Dahm, R. (Eds.), Zebrafish – A Practical Approach. Oxford University Press, Oxford, pp. 175–212.
Glass, A.S., Dahm, R., 2004. The zebrafish as a model organism for eye development. Ophthalmic Res. 36, 4–24.
Greiling, T.M., Clark, J.I., 2008. The transparent lens and cornea in the mouse and zebra fish eye. Semin. Cell Dev. Biol. 19, 94–99.
Gross, J.M., Perkins, B.D., Amsterdam, A., Egana, A., Darland, T., Matsui, J.I., Sciascia, S., Hopkins, N., Dowling, J.E., 2005. Identification of zebrafish insertional mutants with defects in visual system development and function. Genetics 170, 245–261.
Haffter, P., Granato, M., Brand, M., Mullins, M.C., Hammerschmidt, M., Kane, D.A., Odenthal, J., van Eeden, F.J., Jiang, Y.J., Heisenberg, C.P., et al, 1996. The identification of genes with unique and essential functions in the development of the zebrafish, *Danio rerio*. Development 123, 1–36.
Heisenberg, C.P., Brand, M., Jiang, Y.J., Warga, R.M., Beuchle, D., van Eeden, F.J., Furutani-Seiki, M., Granato, M., Haffter, P., Hammerschmidt, M., et al, 1996. Genes involved in forebrain development in the zebrafish, *Danio rerio*. Development 123, 191–203.
Hyer, J., HKuhlman, J., Afif, E., Mikawa, T., 2003. Optic cup morphogenesis requires pre-lens ectoderm but not lens differentiation. Dev. Biol. 259, 351–363.
Jeffery, W.R., Martasian, D.P., 1998. Evolution of eye regression in the cavefish *Astyanax*: apoptosis and the *Pax*-6 gene. Am. Zool. 38, 685–696.
Kimmel, C.B., Ballard, W.W., Kimmel, S.R., Ullmann, B., Schilling, T.F., 1995. Stages of embryonic development of the zebrafish. Dev. Dyn. 203, 253–310.
Krone, P.H., Evans, T.G., Blechinger, S.R., 2003. Heat shock gene expression and function during zebrafish embryogenesis. Semin. Cell Dev. Biol. 14, 267–274.
Kuszak, J.R., 1995. The ultrastructure of epithelial and fiber cells in the crystalline lens. Int. Rev. Cytol. 163, 305–350.
Lee, J., Gross, J.M., 2007. Laminin beta1 and gamma1 containing laminins are essential for basement membrane integrity in the zebrafish eye. Invest. Ophthalmol. Vis. Sci. 48, 2483–2490.
Malicki, J.J., Pujic, Z., Thisse, C., Thisse, B., Wei, X., 2002. Forward and reverse genetic approaches to the analysis of eye development in zebrafish. Vision Res. 42, 527–533.
Mao, L., Shelden, E.A., 2006. Developmentally regulated gene expression of the small heat shock protein Hsp27 in zebrafish embryos. Gene Expr. Patterns 6, 127–133.
Mathias, R.T., Rae, J.L., 2004. The lens: local transport and global transparency. Exp. Eye Res. 78, 689–698.
Nakayama, Y., Miyake, A., Nakagawa, Y., Mido, T., Yoshikawa, M., Konishi, M., Itoh, N., 2008. Fgf19 is required for zebrafish lens and retina development. Dev. Biol. 313, 752–766.
Neuhauss, S.C., Biehlmaier, O., Seeliger, M.W., Das, T., Kohler, K., Harris, W.A., Baier, H., 1999. Genetic disorders of vision revealed by a behavioral screen of 400 essential loci in zebrafish. J. Neurosci. 19, 8603–8615.
Rinner, O., Rick, J.M., Neuhauss, S.C., 2005. Contrast sensitivity, spatial and temporal tuning of the larval zebrafish optokinetic response. Invest. Ophthalmol. Vis. Sci. 46, 137–142.
Schmitt, E.A., Dowling, J.E., 1994. Early eye morphogenesis in the zebrafish, *Brachydanio rerio*. J. Comp. Neurol. 344, 532–542.
Schonthaler, H.B., Fleisch, V.C., Biehlmaier, O., Makhankov, Y., Rinner, O., Bahadori, R., Geisler, R., Schwarz, H., Neuhauss, S.C., Dahm, R., 2008. The zebrafish mutant lbk/vam6 resembles human multisystemic disorders caused by aberrant trafficking of endosomal vesicles. Development 135, 387–399.
Shi, X., Bosenko, D.V., Zinkevich, N.S., Foley, S., Hyde, D.R., Semina, E.V., Vihtelic, T.S., 2005. Zebrafish pitx3 is necessary

for normal lens and retinal development. Mech. Dev. 122, 513–527.
Shi, X., Luo, Y., Howley, S., Dzialo, A., Foley, S., Hyde, D.R., Vihtelic, T.S., 2006. Zebrafish foxe3: roles in ocular lens morphogenesis through interaction with pitx3. Mech. Dev. 123, 761–782.
Soules, K.A., Link, B.A., 2005. Morphogenesis of the anterior segment in the zebrafish eye. BMC Dev. Biol. 5, 12.
Straw, A.D., 2008. Vision egg: an open-source library for realtime visual stimulus generation. Front. Neuroinformatics 2, 4.
Sugimoto, M., 2002. Morphological color changes in fish: regulation of pigment cell density and morphology. Microsc. Res. Tech. 58, 496–503.
Taylor, V.L., al-Ghoul, K.J., Lane, C.W., Davis, V.A., Kuszak, J.R., Costello, M.J., 1996. Morphology of the normal human lens. Invest. Ophthalmol. Vis. Sci. 37, 1396–1410.
Venable, J.H., Coggeshall, R., 1965. A simplified lead staining for use in electron microscopy. J. Cell Biol. 25, 407–408.
Vihtelic, T.S., 2008. Teleost lens development and degeneration. Int. Rev. Cell Mol. Biol. 269, 341–373.
Vihtelic, T.S., Hyde, D.R., 2002. Zebrafish mutagenesis yields eye morphological mutants with retinal and lens defects. Vision Res. 42, 535–540.
Vihtelic, T.S., Yamamoto, Y., Sweeney, M.T., Jeffery, W.R., Hyde, D.R., 2001. Arrested differentiation and epithelial cell degeneration in zebrafish lens mutants. Dev. Dyn. 222, 625–636.
West-Mays, J.A., Zhang, J., Nottoli, T., Hagopian-Donaldson, S., Libby, D., Strissel, K.J., Williams, T., 1999. AP-2 alpha transcription factor is required for early morphogenesis of the lens vesicle. Dev. Biol. 206, 46–62.
Yamamoto, Y., Jeffery, W.R., 2000. Central role for the lens in Cave Fish eye degeneration. Science 289, 631–633.
Yamamoto, Y., Espinasa, L., Stock, D.W., Jeffery, W.R., 2003. Development and evolution of craniofacial patterning is mediated by eye-dependent and -independent processes in the cavefish *Astyanax*. Evol. Dev. 5, 435–446.
Zinkevich, N.S., Bosenko, D.V., Link, B.A., Semina, E.V., 2006. Laminin alpha 1 gene is essential for normal lens development in zebrafish. BMC Dev. Biol. 6, 13.

Appendix A. Supplementary Data

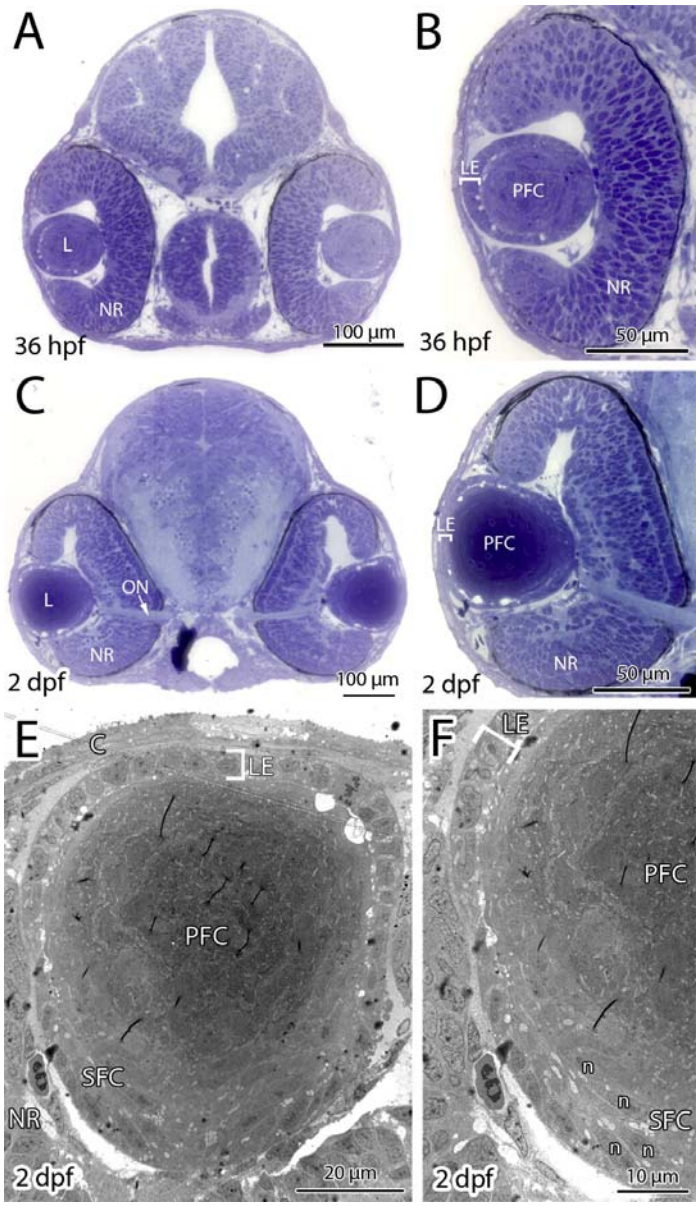

Suppl. Fig. 1. Eye development proceeds normally in *bum*$^{-/-}$ embryos until 2dpf. (A–D) Toluidine blue-stained transversal semi-thin sections through the central part of the eyes of 36hpf (A, B) and 2dpf (C, D) *bum*$^{-/-}$ mutant embryos. A and C show cross-sections of entire heads, B and D shows higher magnifications of individual eyes. (E, F) Thin-section electron microscopy images of transversal sections through the central part of the lens of 2 dpf *bum*$^{-/-}$ zebrafish larvae: overview (E) and higher magnification of the lens' bow region (F) comprising the early differentiating secondary lens fibre cells. These images demonstrate that the hyperproliferation of the anterior lens epithelium and the degenerative changes in the secondary lens fibre cells observed in *bum*$^{-/-}$ mutant larvae at later developmental stages are not apparent at these earlier stages. Brackets in panels B and D–F indicate the monolayer of anterior lens epithelial cells. The overall morphology of the head (A, C) and eye (B, D), including the development of the neural retina are also normal in *bum*$^{-/-}$ mutant larvae. *Abbreviations:* C, cornea; L, lens; LE, lens epithelium; n, elongated nuclei of the differentiating secondary lens fibre cells; NR, neural retina; ON, optic nerve leaving the eye; PFC, primary lens fibre cells; SFC, secondary lens fibre cells.

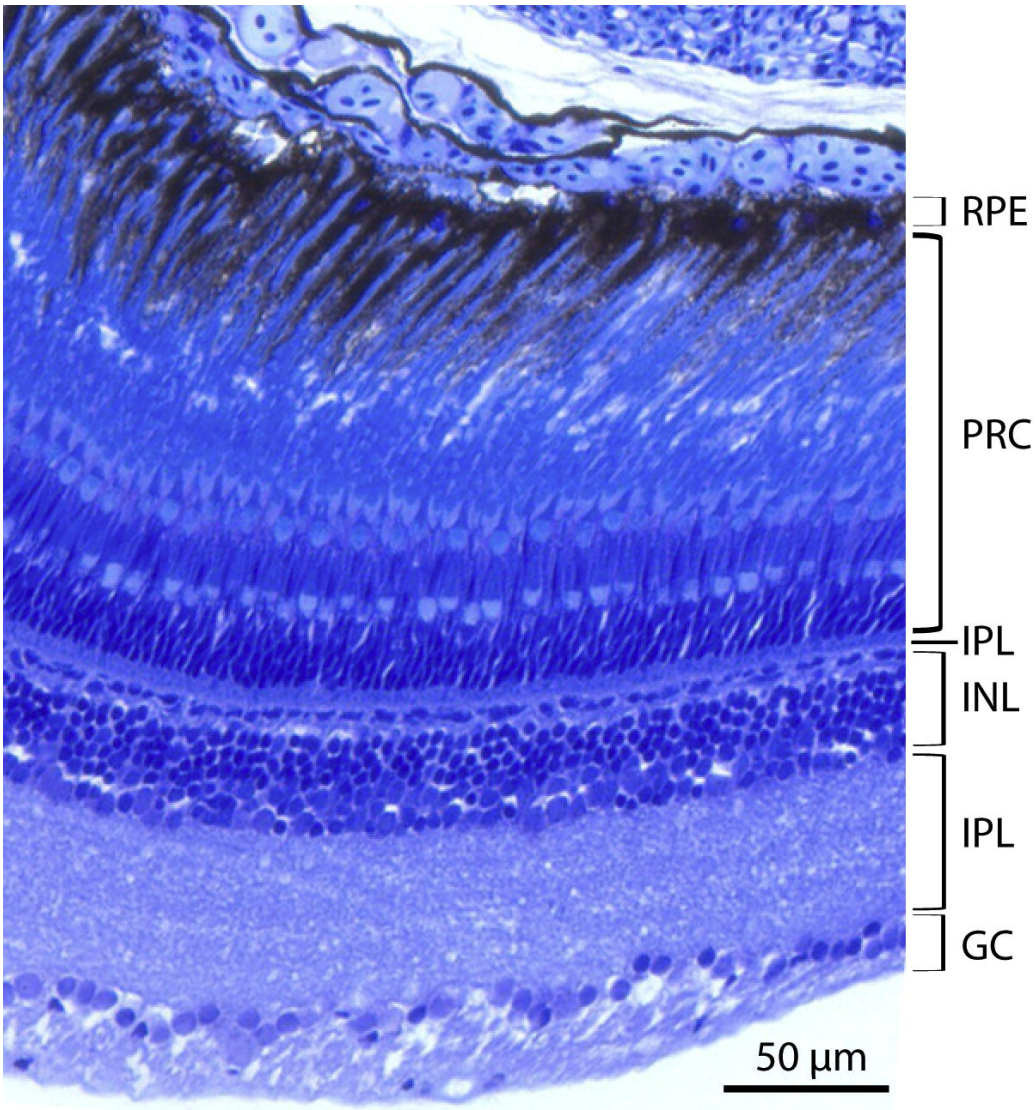

Suppl. Fig. 2. Histological section showing the layers of the adult wild-type zebrafish retina. See Fig. 4I for the retinal morphology in adult *bum*$^{-/-}$ zebrafish. *Abbreviations:* GC, retinal ganglion cells; INL, inner nuclear layer; IPL, inner plexiform layer; OPL, outer plexiform layer; PRC, photoreceptor cells; RPE, retinal pigment epithelium.

A DNA sequence

```
   1 tccaattcct tttggcactt tggacatcaa agactatact ccaagtatcc ttaacaatcg
  61 ggctgtgaaa gtcctgtaat atttacaATG gcagacgtct tgcaactcag tatcaacagt
 121 ctacaggtgc caggtgaaga taaatcagac tctacatctc catcgggttc tccatttcct
 181 tccagaaatg agtgtagtat cactcctctt actccctccc cctctccgag aacagaagtt
 241 agaccacgtt tggctcgtcc attttatgtg gtggtcgcaa tagattttgg caccacctcc
 301 agtggctatg ccttcagttt cattgaagac cctgagacca ttcacatgat gagaaggtgg
 361 gagggaggag accctggtgt agcaaatcag aaaagtccaa cctgtcttct gctgacccct
 421 gacctacgtt tccacagttt tggctttgca gcgcgagaca gttatcatga ccttgacccc
 481 gaggaggcca gacattggct atactttgac aaattcaaaa tgaaaatcca cagcacaagt
 541 gatcttacta tggagactga gctggagtct gttagtggaa gaagagtgca ggccattgag
 601 gtgtttgctc atgccttgag gttctttcga gaacatgctt taaaggaggt gaaggaccag
 661 tcctcctctg tgctggaagg taatgaagta cggtgggtca tcacagttcc tgccgtgtgg
 721 aggcagccag ccaaacagtt catgcgagaa gctgcatatc tggcaggctt agttcctcca
 781 gattctcctg agcagcttct tatagctctt gaaccagagg ctgcatcaat ctactgcagg
 841 aaactgcgtc ttcaccaggt cactgaccta agccagcgtc cagtaactaa tggttttgat
 901 atagacgggt cccgtccatt tgactccagt tttaggcaag cccgtgagca gctccgcaga
 961 gccagacata gccgaacttt tctggtagag agtggtactg gagaattgtg gtctgagatg
1021 cagacaggtg accggtacat tgtagctgac tgtggaggtg ggactgtgga tttgacagtg
1081 catcagattg agcagccaca gggcactctg aaagagcttt acaaagcctc agggggtcct
1141 tatggtgcag ttggtgtgga tcttgccttt gagacaatgt tgtgccaaat ctttggcact
1201 gactttattg acagttttaa agctaaacgt ccagctgctt gggtagatct cactattgca
1261 tttgaagccc gcaaacgtac agcagctcct ggccgtgcca acactttaaa catctcactg
1321 cccttctcct tcattgactt ctacaagcaa caccggggcc agagtgtgga aactgccctg
1381 cgcaagagca atatgaattt tataaagtgg tcatctcaag gaatgctgag actctctacg
1441 gaggccacga acgagctttt tcagccgacc attaacaata tcataaaaca tattgagaac
1501 gtcatgcaga aggaagaagt taagggtgtc cgttttctct tcctggttgg aggattcgca
1561 gagtcaccca tgcttcaacg ggcaattcag aatacactag gacggaactg ccgtataata
1621 attccacatg atgtaggtct aaccatcttg aagggtgcag tccttttgg tctagacccc
1681 actgttgtca gagtacgccg ttgtccgtta acttatggtg ttggggtttt gaaccgcttt
1741 gtagaaggaa gacaccctca tgataagcta ctcatcaagg atggaagaga atggtgcact
1801 gacattctgg accgctttgt aagtgttgat caatctgtgg ccttgggtga ggttgtgagg
1861 cggagctaca ctcctgctag gatgggtcaa cggaagatca tcatcaacat ctactgcagc
1921 gacactgatg acataaccta tattaccgac cctggggtga ggaagtgtgg tgccatcacg
1981 ctagacctac ttgaatcagg ggaagcttca gctagcactg gtgataacga taaaggatca
2041 gcatttgaac gcagggagat tcgcactacc atgcagtttg gtgacactga gatcaaagtc
2101 acagcagttg atgtggcaac tggccgacta gtgcgggcat caattgactt cttgtctaac
2161 TAAttctatt gtggaatgca aggggtttac cccatataat ctcatcgata aatgactaaa
2221 aataatagct ttgaggtcac atgaggctga tgttaaaact gaaggataaa ctgaaatgtt
2281 actggaatca ctttcttcct gcagtgcacc cagggctgga ttaacataag ggctaggtg
```

B Protein sequence

```
MADVLQLSINSLQVPGEDKSDSTSPSGSPFPSRNECSITPLTPSPSPRTEVRPRLARPFYVVVAIDFGTTSS
GYAFSFIEDPETIHMMRRWEGGDPGVANQKSPTCLLLTPDLRFHSFGFAARDSYHDLDPEEARHWLYFDK
FKMKIHSTSDLTMETELESVSGRRVQAIEVFAHALRFFREHALKEVKDQSSSVLEGNEVRWVITVPAVWRQ
PAKQFMREAAYLAGLVPPDSPEQLLIALEPEAASIYCRKLRLHQVTDLSQRPVTNGFDIDGSRPFDSSFRQ
AREQLRRARHSRTFLVESGTGELWSEMQTGDRYIVADCGGGTVDLTVHQIEQPQGTLKELYKASGGPYG
AVGVDLAFETMLCQIFGTDFIDSFKAKRPAAWVDLTIAFEARKRTAAPGRANTLNISLPFSFIDFYKQHRGQ
SVETALRKSNMNFIKWSSQGMLRLSTEATNELFQPTINNIIKHIENVMQKEEVKGVRFLFLVGGFAESPMLQ
RAIQNTLGRNCRIIIPHDVGLTILKGAVLFGLDPTVVRVRRCPLTYGVGVLNRFVEGRHPHDKLLIKDGREW
CTDILDRFVSVDQSVALGEVVRRSYTPARMGQRKIIINIYCSDTDDITYITDPGVRKCGAITLDLLESGEASAS
TGDNDKGSAFERREIRTTMQFGDTEIKVTAVDVATGRLVRASIDFLSN
```

Suppl. Fig. 3. Sequence of the heat-shock protein gene *hspa12b* in *bum*$^{-/-}$ individuals. (A) Sequencing of the full-length cDNA of the gene encoding the heat-shock protein 12B (*hspa12b*) isolated from *bum*$^{-/-}$ mutant zebrafish revealed no mutations as compared to the wild-type sequence. The start (ATG) and stop codons (TAA) are highlighted in yellow. (B) Predicted protein sequence.

A DNA sequence

```
   1 ATGatgtcca ctccagtyat cctcttgaaa gagggcacag acacctctca gggggtccca
  61 caactggtca gcaacataaa tgcctgccag gttgtggcag aggctgtgcg gaccaccctt
 121 ggcccccgtg gcatggacaa gcttgtggtg gataaccgag gcaaagccac tatttctaat
 181 gatggagcca caattctgaa gcttttggat gttgtgcatc ctgcagccaa gactctggtg
 241 gacattgcta gatctcaaga tgctgaggtc ggagatggta ccacttcagt gactctgctt
 301 gctgctgagt ttctgaagca gttgaaaccg tatgtggaag aagggcttca cccacagacc
 361 atcatcagag cattccgcat cgccacccaa cttgctgtca aaaagatcaa agaaatcgct
 421 gttaccatca aaaaggatga caaacaagaa cagaggaggt tgttggagaa gtgtgctgct
 481 acagctttga actccaagct gatagcaggg cagaaggatt tcttctccaa gatggtggtg
 541 gatgcagtga tgatgctgga tgatctgctg cctctgaaga tgattggagt gaagaaggtg
 601 cagggtggtg ctctggagga gtctcagctt gtggctggtg tggcatttaa gaagactttc
 661 tcttatgctg gttttgagat gcagcccaag cgttacatga acccaaaaat tgccctgctc
 721 aacattgagc tggagttgaa ggcagagaag gacaatgccg aggttcgcgt caactcagtg
 781 gaggactatc aggccattgt tgatgctgaa tggaacatcc tgtatgataa actggagaag
 841 atccacaaat ctggcgctaa agttgtgctg tccaagctgc ccattggaga tgtagccaca
 901 cagtactttg cagacagaga tctgttctgt gcaggccgcg tcgtggagga agatctcaaa
 961 agaactatga tggcttgtgg tggctccatt cagaccagtg ttggttccct gactgatgat
1021 gttcttggcc agtgtgagct atttgaagaa gtgcaggttg gaggagagag atacaatttc
1081 tttaaaggct gcccaaaggc caagacctgc accatcattc tgaggggtgg tgcagagcag
1141 tttatggaag agacggaccg ctcactgcat gatgccatta tgatagtgcg cagggcaatc
1201 aagaatgact ccattgttgc cggtggtggg gcaattgaga tggagttgtc gaagtatctg
1261 agggattatt ctagaacaat tccagggaag cagcaattgc tgatcggagc ctatgccaag
1321 gccctggaga tcattcccag acagctctgt gacaatgcgg gatttgatgc cacaaatatt
1381 ctaaacaaac tgagggccaa gcatgcacag ggtggtatgt ggtatggagt ggatgtgaat
1441 aatgaagaca tagcagataa cttccaggca tgtgtttggg agccctctat agtgcgtatc
1501 aatgccttga ctgctgcatc tgaagctgca tgcctcatac tgtcagtgga tgagaccatc
1561 aagaaccctc gctccagtgt tgatggccca ccggcagctg ctgcagagga aggggtcgtg
1621 gtagaccagc ccatgcccac TAA
```

B Protein sequence

```
MMSTPVILLKEGTDTSQGVPQLVSNINACQVVAEAVRTTLGPRGMDKLVVDNRGKATISNDGATILKLLDV
VHPAAKTLVDIARSQDAEVGDGTTSVTLLAAEFLKQLKPYVEEGLHPQTIIRAFRIATQLAVKKIKEIAVTIKKD
DKQEQRRLLEKCAATALNSKLIAGQKDFFSKMVVDAVMMLDDLLPLKMIGVKKVQGGALEESQLVAGVAF
KKTFSYAGFEMQPKRYMNPKIALLNIELELKAEKDNAEVRVNSVEDYQAIVDAEWNILYDKLEKIHKSGAKV
VLSKLPIGDVATQYFADRDLFCAGRVVEEDLKRTMMACGGSIQTSVGSLTDDVLGQCELFEEVQVGGERY
NFFKGCPKAKTCTIILRGGAEQFMEETDRSLHDAIMIVRRAIKNDSIVAGGGAIEMELSKYLRDYSRTIPGKQ
QLLIGAYAKALEIIPRQLCDNAGFDATNILNKLRAKHAQGGMWYGVDVNNEDIADNFQACVWEPSIVRINAL
TAASEAACLILSVDETIKNPRSSVDGPPAAAAEEGVVVDQPMPT
```

Suppl. Fig. 4. Sequence of *cct7* in *bum*$^{-/-}$ individuals. (A) Sequencing of the full-length cDNA of the gene encoding the chaperonin containing TCP1, subunit 7 (eta) (*cct7*) isolated from *bum*$^{-/-}$ mutant zebrafish revealed no mutations as compared to the wild-type sequence. The start (ATG) and stop codons (TAA) are highlighted in yellow. (B) Predicted protein sequence.

A DNA sequence

```
   1 ATGtatagaa aagaacaagt gctgcaggtc ctgggtctta acattagcca gctggctgtt
  61 aaagtgggac gtggcagtgc aggtggtgta aaaaggagag tggtagacag gatcacagag
 121 ggcagacatg atgaggggaa tgatgaaaaa gtgtttggga gtaaaccaca gtgcctgtgc
 181 ctcatttact ttgctcttgc tgtatctcta agcattaatg atgcagtcac agatgttcaa
 241 gttacctttg ccaagggcac tgacacaacc ccataccttg atgcccaaga tttagaccaa
 301 tctacctcca actgttccca gaacgacgtg tgcacagacg gggtcctgtt accagtgtgg
 361 aatccccaga acccttcagt gggtgacaaa gtggcccgtg ccattgtgta cctggtggca
 421 ctagtttaca tgttcttagg tatgtcaatc atagctgacc gcttcatgac tgccattgaa
 481 gttataactt cacaagagaa ggagatcact acaaaaagac ccaatggtga aacagtcacc
 541 acaacagtcc gcatatggaa tgagactgtc tccaatctaa ccctaatggc tctggggtct
 601 tcagccccag aaatattgct ttcagtcatt gaggtctgcg ggcataattt tgaggctggt
 661 tctctaggtc ccagcaccat tgtgggcagt gctgccttca acatgtttgt aatcattggt
 721 ctctgtgtct atgtggtacc tgaaggtgaa aggcgcaagg tcaaacatct tcgggtgttt
 781 tttgtgactg cagcatggag catgtttgcc tacatttggc tctatcttat ccttgctgta
 841 atctctccag gtgaggtaga agtttgggaa gctgtattga cgttcctctt tttccctctc
 901 tgtgtggtcc aagcctggat cgctgatcgc cgattgcttt tttacaagta tgcacgcaaa
 961 cgctaccgaa ccgataaggg tcgtggaatt atagtgtctg agggtgggga ggaattaggg
1021 aaagaggcgg gattcacaaa gatggacatg ttggaaattg atggaatcac tactcattta
1081 gatggggtct tgggagggga aagtgggctt ggtggacgtg atcaagaaga ggaagccagg
1141 agagaaatgg ccagaactct aaaggaattg aagcagagac atcctgagaa ggacatggag
1201 cagctcatag agatggccaa ctatcaggtt ctgatgcagc agcagaagag cagggctttc
1261 taccgcattc aggcaacaag gatgatgatt ggtgctggga acatcttgaa gaaacatgca
1321 gcggatcagg ctcgtaaagt ggtcagcagt ggggaacccc gagagcagga agatgatcct
1381 catgttacaa gaatagactt tgaaccagcc ctctaccagt gctttgagaa ctgtggatcc
1441 ttaaaactta ccgtacaaag gcatggagga gatgccgggt gtagtgttaa agtggactac
1501 cgcactgaag atggcacagc caatgctggt tctgactatg agtttgcaga gggcacactt
1561 gtcttcaaac ctggcgagaa tgttaaagac atcgcagttg gcattattga tgatgatatc
1621 tttgaggaag atgaatattt ttatgttcgt ttgagcaatc cccgtatagt tgggtgggct
1681 gatggacatc ctattgcttt ggagactgga gctcctgccc ctagtgctgc ccttggtgag
1741 gctcacacgg caacagtgac aatctatgat gatgaccatg ccggaatttt cacatttgag
1801 agtgaatcaa tgcgagtgag tgaaagtatt ggaatcatgc aggtcaaggt ccagagaacg
1861 tctggagccc gtggtctggt ggcggtacca tatcaaacag tggatgggac agcttgtgga
1921 ggggaggact atgaggaagt gtctggaaaa ttggagttcc agaatgatga gacaatgaaa
1981 acaattgagg tgaagattat agacgatgaa gagtatgaaa agaataagac cttcagcatt
2041 gagttaggcg agccagtgct acttgagatt ggacagaagc atggagactc taatgagaat
2101 aagccagaaa tcggggcaga ggaggaggaa gtagcaaaga tgggatgtcc cagtttggga
2161 gaacatactc gattggaggt ggtgattgaa gaatcttatg aatttaagaa tacagtggat
2221 aagctcatta agaagactaa cctagctctg gttgttggca gcagtagctg gagagagcag
2281 tttgtcagtg ctgttactgt cagcgcaggc gacgatgatg aggaggagag tggtgaagaa
2341 cgccttccat cctgctttga ttatatcatg cacttcctga cagtcttctg gaaggttctc
2401 tttgcctttg tcccacctac agagtactgg aatggatggg cttgcttcat tgtttccatc
2461 tttttaatcg gtgcgttgac agcggtcact ggtgatctcg cttcccactt tgggtgcact
2521 gttggcctga aggattcagt caccgctgtg gtctttgttg ccttggggac atcagttcca
2581 gacacttttg ccagcaaagt agctgccatc caagaccaat atgctgacgc ctccattggt
2641 aatgtgacag gcagtaatgc tgtcaatgtt ttcctgggca tcggtgtggc ctggtccatt
2701 gctgccatat actggcggag caagggcaaa tcttttcacg ttgatccggg ctctctggcc
2761 ttctctgtca cactcttcac ggctttggct gtggtgtgtg tcagcgtgct gttgtatcgc
2821 cggcgccccc cagtggctgg aggagaactc ggcggcccac ggacttgcaa gatattgaca
2881 tccttactct tcatttccct ctggctgatc tacatcctgt tggcttcatt ggaaacatac
2941 tgtcacatcc ccggattcTG Aagcagcaat acatggagag gaatatgaca acagccaatg
3001 aaggagcatt ttttttttat ttataattat tagatattta tcttgaagtc tacttactgt
3061 tgtcgatttt tgtatttttt catttcctta tctagaaatt gtgatgatgg catcactcac
3121 tgcttccaag agaacacaaa aagagtgatg ttttatttta gttgagctaa tattaaattg
3181 agatttgttt gttttaatga actgtccctt taagttagct tgaatgcagt atctcaaaca
3241 ccgttccttg ttcccttgcc ttacacttgt ccatctctca gtggtgtctt aaacccatcc
3301 agaccagtaa ccagtaacca atgactcatg tcttttgtac tcctgtttga gccaaaccaa
3361 gcctttggtt actgaatgaa agagtttacc tttttcttgg ggacattttt ctttaataca
3421 aagtgtcagt attactctca tgtacttgta gatatgctgt ttgacaatat attatatatg
3481 aagagaatga ccaaacacaa actttataat gacaaagagc agactgaatg acttactgtt
3541 gctaagatga aaagcatgct ttatcactta ataagaagca gacagttgag aagcatgtca
3601 agtcca
```

B Protein sequence

MYRKEQVLQVLGLNISQLAVKVGRGSAGGVKRRVVDRITEGRHDEGNDEKVFGSKPQCLCLIYFALAVSL
SINDAVTDVQVTFAKGTDTTPYLDAQDLDQSTSNCSQNDVCTDGVLLPVWNPQNPSVGDKVARAIVYLVA
LVYMFLGMSIIADRFMTAIEVITSQEKEITTKRPNGETVTTTVRIWNETVSNLTLMALGSSAPEILLSVIEVCG
HNFEAGSLGPSTIVGSAAFNMFVIIGLCVYVVPEGERRKVKHLRVFFVTAAWSMFAYIWLYLILAVISPGEVE
VWEAVLTFLFFPLCVVQAWIADRRLLFYKYARKRYRTDKGRGIIVSEGGEELGKEAGFTKMDMLEIDGITTH
LDGVLGGESGLGGRDQEEEARREMARTLKELKQRHPEKDMEQLIEMANYQVLMQQQKSRAFYRIQATR
MMIGAGNILKKHAADQARKVVSSGEPREQEDDPHVTRIDFEPALYQCFENCGSLKLTVQRHGGDAGCSVK
VDYRTEDGTANAGSDYEFAEGTLVFKPGENVKDIAVGIIDDDIFEEDEYFYVRLSNPRIVGWADGHPIALET
GAPAPSAALGEAHTATVTIYDDDHAGIFTFESESMRVSESIGIMQVKVQRTSGARGLVAVPYQTVDGTACG
GEDYEEVSGKLEFQNDETMKTIEVKIIDDEEYEKNKTFSIELGEPVLLEIGQKHGDSNENKPEIGAEEEEVAK
MGCPSLGEHTRLEVVIEESYEFKNTVDKLIKKTNLALVVGSSSWREQFVSAVTVSAGDDDEEESGEERLPS
CFDYIMHFLTVFWKVLFAFVPPTEYWNGWACFIVSIFLIGALTAVTGDLASHFGCTVGLKDSVTAVVFVALG
TSVPDTFASKVAAIQDQYADASIGNVTGSNAVNVFLGIGVAWSIAAIYWRSKGKSFHVDPGSLAFSVTLFTA
LAVVCVSVLLYRRRPSVAGGELGGPRTCKILTSLLFISLWLIYILLASLETYCHIPGF

Suppl. Fig. 5. Sequence of the solute carrier family member gene *slc8a4b* in *bum*$^{-/-}$ individuals. (A) Sequencing of the full-length cDNA of the gene encoding the solute carrier family 8 (sodium/calcium exchanger), member 4b (*slc8a4b*) isolated from *bum*$^{-/-}$ mutant zebrafish revealed no mutations as compared to the wild-type sequence. The start (ATG) and stop codons (TGA) are highlighted in yellow. (B) Predicted protein sequence.

5. Computer-Based Analysis of the Optokinetic Response in Zebrafish Larvae

Corinne Hodel[a] and Stephan C. F. Neuhauss[a,1]

[a] Institute of Zoology, Neurobiology, University of Zurich, 8057 Zurich, Switzerland

[1] Corresponding author

Article published in *Cold Spring Harbor Protocols, 2008, prot.4961*

Personal Contribution

Writing of the entire manuscript; designing of all figures

Cite as: Cold Spring Harb. Protoc.; 2008; doi:10.1101/pdb.prot4961

Protocol

Computer-Based Analysis of the Optokinetic Response in Zebrafish Larvae

Corinne Hodel and Stephan C. F. Neuhauss[1]

Institute of Zoology, Neurobiology, University of Zurich, 8057 Zurich, Switzerland

[1]Corresponding author (stephan.neuhauss@zool.uzh.ch)

INTRODUCTION

Large movements in the visual field trigger stereotypic eye movements in vertebrates. This optokinetic response (OKR) is robust in zebrafish (*Danio rerio*) larvae older than 4 days post-fertilization (dpf), and is hence ideally suited for use in the evaluation of visual performance after genetic manipulations. This protocol describes a simple method by which a computer-generated visual stimulus is projected onto a screen and watched by immobilized larvae. The resulting eye movements are recorded and evaluated automatically, using a digital video camera and appropriate computer software. Depending on the sophistication of the software used, the evaluation can be performed in real time during the recording session, or by analyzing the recorded movie files off-line.

MATERIALS

Reagents

E3 medium

Methyl cellulose solution (prewarmed to 28°C)

Zebrafish (adult)

Equipment

Box (wet, wrapped with Parafilm) (optional; see Step 10)

Computer for measurement, including customized software for camera operation, control of the stimulus, and eye recording and analysis

Dedicated commercial software is not available; however, macros can be written easily and used within most image analysis programs, e.g., LabView IMAQ software (National Instruments) or ImageJ (http://rsb.info.nih.gov/ij/).

Computer for stimulation, including software for generation of stimulus pattern (e.g., Simple DirectMedia Layer [SDL], http://www.libsdl.org)

Diffusion screen (cylindrical) consisting of translucent wax paper (110 g/m^2) (Rustik; Artoz Papier AG)

Equipment for breeding and raising zebrafish

Frame grabber card (programmable), for digitization of the video signal (e.g., PCI-1409; National Instruments)

Incubator preset to 28°C

Infrared light source (e.g., KL 1500; Zeiss)

Light projector (digital) (e.g., Proxima 4200; Proxima)

Digital light processing (DLP) technology is highly recommended; see Step 3.

Microscope (binocular, with a phototube) (e.g., SV8; Zeiss)

Needle (in pin holder)

Optical bench, including 50-mm and 100-mm convex lenses, iris, and optional optical density (OD) filters

Petri dishes (35 mm, 90 mm)

Photometer (e.g., J18; Tektronics)

Pipettes (plastic)

SVGA graphics board (e.g., GeForce 4; NVIDIA), with a frame rate of 60 Hz and an 8-bit intensity resolution, for generation of the stimulation pattern

Trigger for video camera, customized with an electronic circuit for on-chip frame integration recording up to 12.5 frames/sec

Five frames/sec is sufficient for detection of differences between wild type and mutant zebrafish larvae. For a more detailed description of visual performance, a higher frame rate is recommended.

Video camera (charge-coupled device [CCD]) (custom modified, infrared black/white) (e.g., XT-SC50; Sony)

METHOD

Assembling a Computer-Based Setup for OKR

Steps 1 to 7 are performed only once to configure the system. The system must be assembled in a darkroom to allow measurement of OKR. A schematic drawing of the OKR setup is depicted in Figure 1*. See* Figure 2 *for a photo of the assembly.*

1. Connect the DLP projector to the graphics board of the stimulus computer (equipped with software for generation and control of the stimulus pattern) and set up an image-mapping function.
Because a flat image is projected onto the curved surface of the screen, the program must use a mapping function. We use x' = R *x tan (*x / R*), where* x' *is the horizontal coordinate on the screen,* x *is the position where the ray would hit a flat screen, and* R *is the radius of the screen.*

2. Project the light beam via an optical bench consisting of two convex lenses, an iris, and optional OD filters to a cylindrical translucent diffusion screen. Attach the diffusion screen to a 90-mm Petri dish.
The size of the projection on the screen should cover the entire visual field of the eye as it is exposed to the screen. For 5-d-old zebrafish larvae, we use 99° horizontally and 52° vertically.
3. Linearize the DLP projector manually, by measuring the light intensity of different projector settings on the screen using a photometer.

4. Illuminate the binocular microscope with infrared light from below.

5. Connect the video camera to the binocular microscope and to its trigger.

6. Connect the video camera and camera trigger to the grabber card of the measurement computer (equipped with customized software for recording and analyzing images from the video camera).

7. Connect the measurement and stimulus computers to each other.

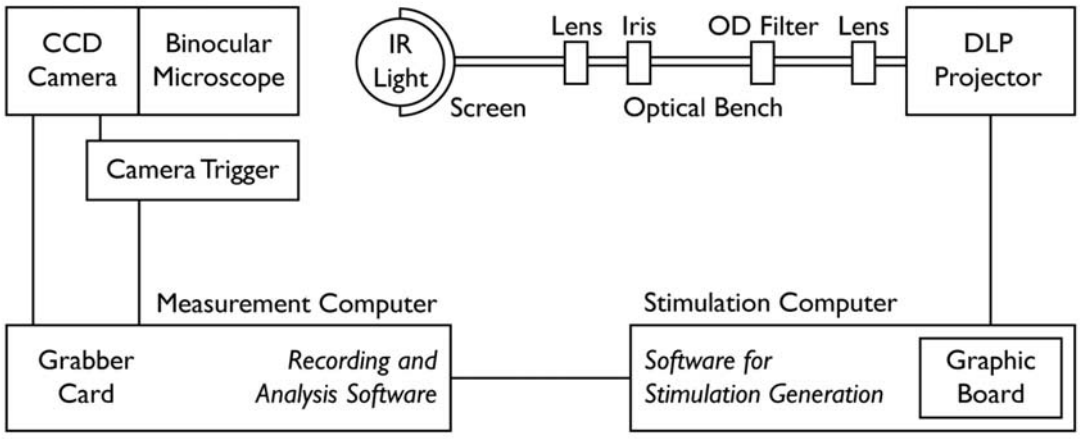

Figure 1. Schematic drawing of all components and connections of the computer-based OKR setup. Elements indicated in italics are custom-modified software. IR: infrared.

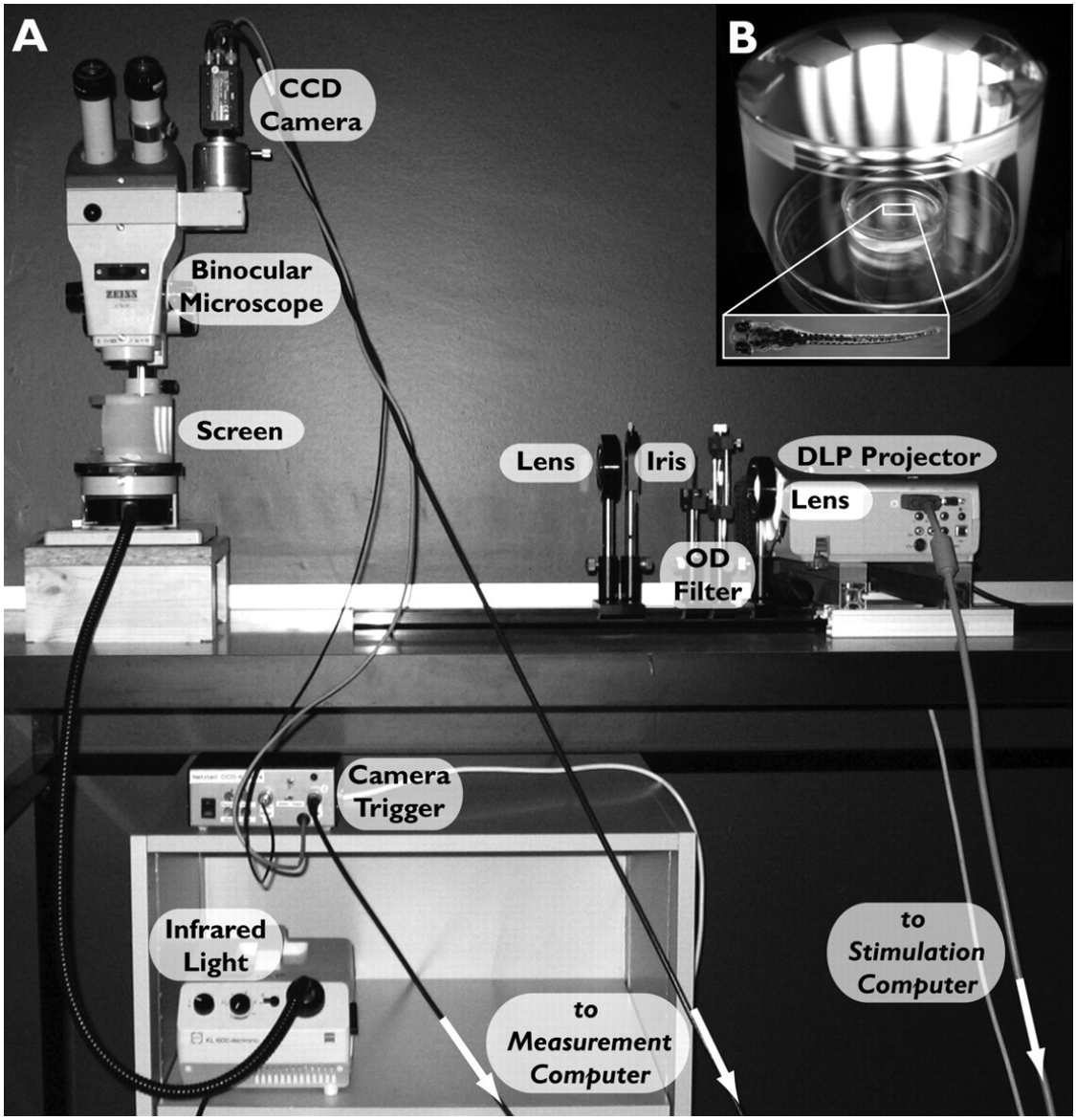

Figure 2. (*A*) Photo of all components of the OKR setup except the two computers. (*B*) Blow-up of the screen (rotated 90° counterclockwise horizontally). The larva inside the Petri dish is placed orthogonally to the light beam. Thus, only one eye is exposed to the stimulation pattern.

Preparation of Larvae

Larvae survive this procedure without difficulty, and thus, can be used for further analyses.

8. Mate adult zebrafish and collect eggs the following day.

9. Raise embryos in E3 medium at 28°C in a constant light/dark cycle.

Measurement of OKR

Measurements can be performed using embryos between 4 and 10 dpf.

10. Embed a zebrafish larva in the center of a 35-mm Petri dish filled with prewarmed (28°C) methyl cellulose solution, using a needle (in a pin holder). Embed one larva per dish, dorsal side up.
To reuse methyl cellulose solution, store at 28°C in a wet box wrapped with Parafilm.
See Troubleshooting.

11. Switch on the video camera and its trigger, the projector, the infrared lamp, and both computers.

12. Place a larva under the binocular microscope orthogonally to the light beam (so that only one eye is exposed to the screen), and center the larva in the visual field of the camera.
See Figure 2.
See Troubleshooting.

13. Start the stimulus pattern on the stimulation computer.
We set standard stimulus velocity to 60 pixels/sec with a screen resolution of 800 x 600 pixels, one-way stimulus duration to 3 sec, and spatial frequency to 0.6 cycles/degree. Depending on the paradigm, parameters are changed (stepwise) within a range of 1%-100% for contrast, 0.2-5.0 cycles/degree for spatial frequency, and 20-180 pixels/sec for temporal frequency.

14. Record the eye movement with the customized recording software on the measurement computer, and evaluate the angular position of the eye. Calculate eye velocity (deg/sec) from this.
An example of a typical measurement using real-time tracking is shown in Figure 3 *. The stored movie files also can be evaluated after the recording session is over (e.g., using ImageJ software, available at http://rsb.info.nih.gov/ij/), instead of taking real-time measurements.*
See Troubleshooting.

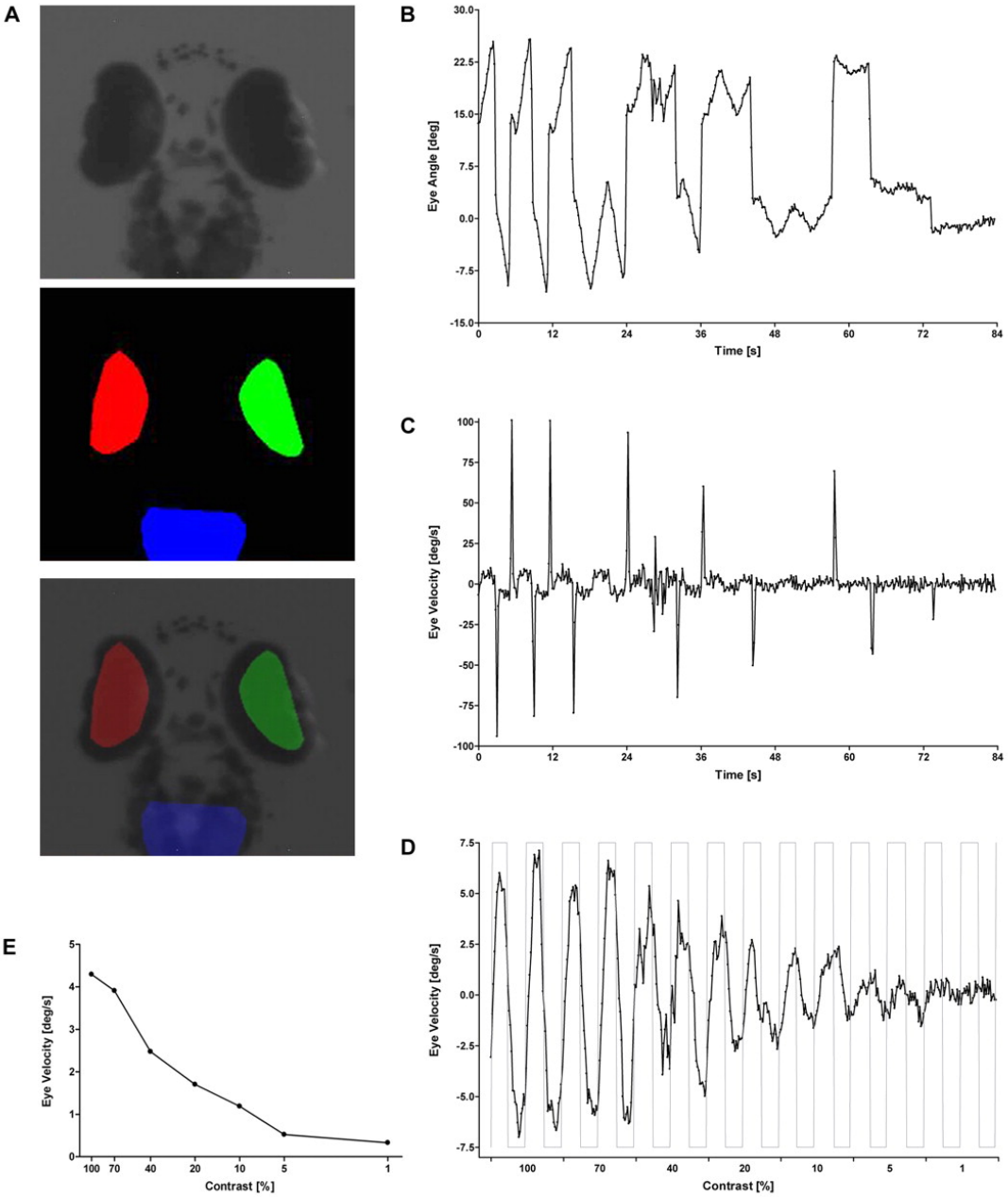

Figure 3. Example of an OKR measurement in which contrast was decreased, stepwise, from 100% to 1%. (*A*) Camera image of the 5-d-old larva showing the computer-based extraction of the eyes (identified because of their strong pigmentation). The *lowest* panel shows the overlay. Real-time tracking of the eye extraction image revealed the eye movement in terms of eye angle (*B*) and eye velocity (*C*). After the measurements were taken, the raw, real-time data shown in *B* and *C* were filtered for saccadic eye movements (*D*) and averaged for each contrast condition (*E*).

TROUBLESHOOTING

Problem: Methyl cellulose solution is too fluid when reused.

[Step 10]

Solution: During the transfer of the larva from the E3 medium to the methyl cellulose solution, try to avoid dilution of the methyl cellulose solution with medium.

Problem: Methyl cellulose solution is too sticky when reused.

[Step 10]

Solution: Make sure that the storage box is thoroughly wet and completely closed. It may also help to wrap each Petri dish with Parafilm.

Problem: Larva is not immobile for measurement.

[Step 12]

Solutions: Consider the following:

- Wait a couple of minutes after embedding the larva in methyl cellulose solution before measurement; the larva should eventually become calm.
- Make sure that the larva is positioned dorsal side up instead of ventral side up.
- Use light-adapted animals when compatible with the experiment; they tend to be less mobile during the measurement.
- Use new methyl cellulose solution (it could be too diluted), or try a higher concentration of methyl cellulose.

Problem: No eye movement is observed.

[Step 14]

Solution: Consider the following:

- Make sure that the larva is still alive by checking blood flow under the binocular microscope.
- The larva could be blind; measure a healthy wild-type larva as a control.
- There may not be stimulation on the screen or it may be too weak; check the stimulation computer, projector, and optical bench.

Problem: The velocity of eye movements is low.

[Step 14]

Solution: Consider the following:

- Make sure that the stimulation computer runs stably; program and use an acoustic signal to indicate any irregularities in stimulus pattern velocity.
- Look for light sources in the behavior room which could influence the stimulation itself or the recording of the CCD camera. Optionally, turn off the screens of both computers during the measurement.
- Make sure that the larva is positioned dorsal side up instead of ventral side up.
- Check the quality of the methyl cellulose solution, noting bubbles, specks, or blurry color, and replace if necessary.
- Readjust the optical bench.
- Measure the light intensity of the projector lamp with a photometer.
- Check the communication between the camera trigger and the camera.
- Check the communication between the measurement computer and the camera and camera trigger.

DISCUSSION

The computer-based OKR setup described here can also be used for other fish or amphibian larvae, provided the eyes are clearly silhouetted against the rest of the body and there is enough oxygen supply through the skin.

OKR in zebrafish larvae can be reliably recorded from 4 dpf until ~10 dpf. At later stages, oxygen supply through the skin is no longer sufficient, presumably due to scale formation (reviewed in Huang and Neuhauss 2008).

The advantage of computer-driven stimulation, in contrast to rotating drums fitted with stripe patterns, is that the stimulus can be precisely controlled during the experiment (Rinner et al. 2005). The described setup uses monocular stimulation, which is advantageous for a number of applications. With slight modification of the recording setup, the movements of the unstimulated eye can also be evaluated, e.g., to study the degree of conjunction.

ACKNOWLEDGMENTS

The work in our lab is supported by grants from the EU (ZF-MODELS), the Swiss National Science Foundation, and the Neuroscience Center Zürich. We thank Dr. Oliver Rinner for perfection of the setup.

REFERENCES

Huang, Y.Y. and Neuhauss, S.C. 2008. The optokinetic response in zebrafish and its applications. *Front. Biosci.* **13:** 1899–1916.[Medline]

Rinner, O., Rick, J.M., and Neuhauss, S.C. 2005. Contrast sensitivity, spatial and temporal tuning of the larval zebrafish optokinetic response. *Invest. Ophthalmol. Vis. Sci.* **46:** 137–142.[Abstract/Free Full Text]

Recipe

E3 medium

- 5 mM NaCl
- 0.17 mM KCl
- 0.33 mM $CaCl_2$
- 0.33 mM $MgSO_4$
- 0.1% methylene blue (Sigma)

Recipe

Methyl cellulose solution

Heat H_2O to 60°C, add methyl cellulose (Sigma) (3% by weight; adjust viscosity if needed), and mix with a glass rod. Place the solution (including any undissolved particles) in a –20°C freezer and stir every 30 min until frozen. Store overnight in a refrigerator. The solution should be clear without visible specks of methyl cellulose. Store in 50-mL tubes in a larval incubator (28°C).

6. THE ELECTRIC RETINA: AN INTERPLAY OF MEDIA ART AND NEUROSCIENCE

Corinne Hodel [a], Stephan C.F. Neuhauss [a] and Jill Scott [b]

[a] Institute of Zoology, Neurobiology, University of Zurich, 8057 Zurich, Switzerland

[b] Institute of Cultural Studies, Zurich University of the Arts, Austellungsstrasse 60, 8031 Zurich, Switzerland

Article published in *Leonardo, 2010, 43:3, in press*

Personal Contribution

Writing of the manuscript, designing of both figures [photographs were provided by Jill Scott (Figure 1) and Colette Maurer (Figure 2)]

The Electric Retina: An Interplay of Media Art and Neuroscience

Corinne Hodel and Stephan C.F. Neuhauss with Artist's Statement by Jill Scott

Corinne Hodel (biologist), Institute of Zoology, University of Zurich, Winterthurerstrasse 190, 8057 Zurich, Switzerland. E-mail: corinne.hodel@imls.uzh.ch.

Stephan C.F. Neuhauss (biologist), Institute of Zoology, University of Zurich, Winterthurerstrasse 190, 8057 Zurich, Switzerland. E-mail: stephan.neuhauss@imls.uzh.ch.

Jill Scott (artist), Institute of Cultural Studies, Zurich University of the Arts, Austellungsstrasse 60, 8031 Zurich, Switzerland. E-mail: jillian.scott@zhdk.ch. Web site: www.jillscott.org.

ABSTRACT

The Electric Retina is an interactive sculpture built by the artist Jill Scott. This project is the result of her residency in her coauthors' neurobiological laboratory and is an artistic interpretation of their research on zebrafish vision. This trans-disciplinary collaboration has served to communicate scientific findings to the general public. Moreover, the different styles and modes of communication required with the general public and with the artist have been a worthwhile experience for the scientists involved.

BACKGROUND

Jill Scott's background is in media art; she constructs video artworks and interactive performances. She is also co-director of the Artists in Labs program, located in the Institute of Cultural Studies at the Zurich University of the Arts. This program enables Swiss artists to work as residents in specific Swiss scientific laboratories for several months, and as Scott wanted the experience herself, she applied to our lab as an extra resident, not funded by her organization. The intensity of her involvement required her to be part of our research group rather than a momentary visitor. This approach reflects the conception of the program itself and allows for a much more intensive knowledge transfer between artists and scientists, leading to new encounters at multiple levels. Here we describe Scott's

residency in our neurobiology lab at the Zoological Institute of the University of Zurich from our point of view as participating scientists.

Scott's Residency

In our laboratory, the focus of our research is the zebrafish retina. Zebrafish are small tropical fish and are used as model organisms in vertebrate biology around the world. This fish offers multiple advantages for visual research [1]. Their larvae have to catch prey by the tender age of five days (post-fertilization), and acute vision at this early stage is indispensable for their survival. Therefore, the retina has to develop very quickly and is particularly accessible in five-day-old larvae. In the laboratory, blind larvae survive only if raised in a medium containing high concentrations of living food such as paramecia. Under this paradisiacal condition, nutrition can be passively obtained simply by opening the mouth.

We are able to evoke an optokinetic response (OKR), that is stereotyped eye movements, in a "movie theater" for fish by projecting moving stripes onto a screen watched by the larvae. Presentation of movement in the surround triggers eye movements that can be analyzed in real time using custom-designed software. In this way, we are able to test quantifiably the visual performance of larvae, even though they are only about 7mm in length. The velocity of eye movement gives us information about levels of visual impairment. For instance, the absence of eye movement (apart from spontaneous movements) after visual stimulation is a reliable indication of complete blindness. Zebrafish strains with impaired visual performance in the OKR movie theater can be further analyzed by electrophysiological analysis. The electric response of the retina to flashing light is measured with a tiny electrode, which sits on the cornea of the eye surface. Depending on the site of the defect in the visual pathway, the response will show typical characteristics indicative of the cellular localization of the defect. Histological sections of the zebrafish eye can be also viewed with a microscope, and this process reveals further details of abnormalities in the retina. As in the human eye, the retina harbors light-sensitive photoreceptors and other neuronal cells that process the signal from the photoreceptor and send it to the optic nerve. In zebrafish, photoreceptors are arranged in a rigid pattern array over the retina.

When Jill Scott started her residency, she accompanied us during all stages of our research process. These hands-on demonstrations were supplemented by tutorials conveying basic concepts of neurobiology, ophthalmology and genetics. As an honorary member of our research group, she also took part in our weekly seminars and meetings. Finally,

she worked alongside the scientists and performed her own experiments. This deep insight into our day-to-day activities was essential for creating a piece of art that could reflect and interpret our research in a robust manner. However, this exchange turned out to be bidirectional, as lab members soon became involved in the artist's process. The ideas for the final artwork evolved through mutual interaction over several brainstorming sessions and other discussions. After a year, *The Electric Retina* was ready for its first public exhibition, at the BrainFair 2008 on the occasion of the 175th birthday of the University of Zurich.

THE PRODUCT

The Electric Retina

The artwork resulting from Scott's residency in our laboratory is a sculpture symbolizing a part of the retina, with which the audience can interact (Fig. 1). The base of the sculpture is composed of a metal socket, which harbors technical components such as a media player, sound devices and touch sensors. The socket supports an appealing giant sphere with a diameter of 120 cm, which aroused the curiosity of the spectators (Fig. 1A). Here two white hemispheres coalesce into a round eyeball. At the front, the iris of the eye serves as a window guiding the light beam from the internal video projector onto a screen about 3 meters away from the sculpture. The audience can choose between five thematically different sets of movies by turning a lens on the front of the "iris" (Fig. 1B). Once the lens-carrying wheel is latched in a new position, the movie linked with this setting starts. The projected movies are the result of a post-edited underwater shoot off the coast of Australia. Subsequent image processing of the pictures by Jill Scott resulted in an

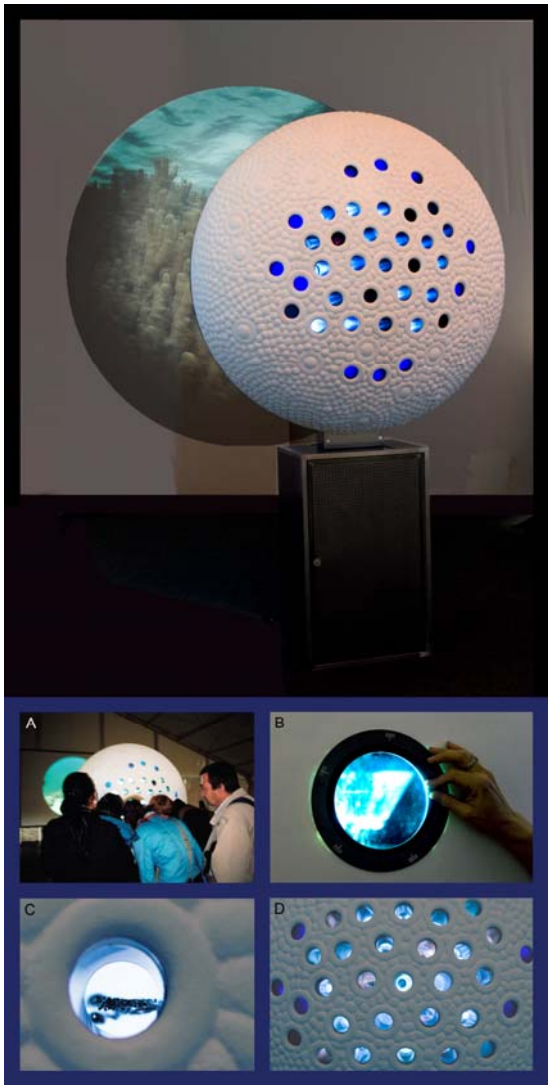

Figure 1
The Electric Retina exhibited in a public space. For a short documentary about *The Electric Retina* see www.vimeo.com/1387705

artistic representation of this ocean environment seen from the perspectives of zebrafish afflicted with particular eye diseases. These diseases were chosen from animal models used in our research, as well as from common human visual afflictions. In the case of progressive diseases such as retinitis pigmentosa, the movie starts with an original scene which is gradually modified according to the course of disease. Apart from these public movies seen by all spectators, there are private viewing holes or oculars that display representative macro images and animated sequences from studies actually made in our laboratory (Fig. 1C). These oculars represent the photoreceptors' pattern array spread irregularly over the back hemisphere (Fig. 1D). The images are displayed on a huge LCD screen inside the sculpture. The content of the oculars changes simultaneously with the projected movies as the large lens is rotated. In addition to the regular selection of movie sets, there is another, more subtle interface between sculpture and spectator. If no one interacts with the sculpture for several minutes, a sixth set of movies starts automatically. This attract loop is immediately interrupted when a spectator approaches the sculpture and touches the border of an ocular, starting one of the five other movie sets. A touch sensor underneath the surface connected to the media player mediates this elaborate human-machine interaction.

Exemplary Movie Set: Healing Disease with a Special Diet

Here, we describe the science underlying one movie set, based on research on the zebrafish strain *noir*, which suffers from a hereditary disease. As its name implies, sick offspring of this fish line have a darker appearance than healthy siblings. Black body pigmentation is often associated with blindness (Fig. 2). As pigment cells develop, zebrafish larvae start to adjust the degree of their body pigmentation to the background illumination by spreading or concentrating pigment granules within the cell. Thus, a light-adapted larva is brighter than a dark-adapted individual - unless it is unable to sense light and lives in perpetual internal darkness. The defective protein underlying the disease in *noir* plays an important role in most cells, not only those involved in vision. It is part of a complex (pyruvate dehydrogenase) that boosts the synthesis of a key molecule (acetyl coenzyme A) involved in carbohydrate metabolism. As a result, in *noir* mutants a central metabolic pathway is blocked. Considering the biochemical pathway supplying a fatty acid diet to the affected fish can circumvent this block. Indeed, *noir* can be almost completely cured of these symptoms simply by feeding with a mixture of fatty acids. The diet and its consequence are comparable to the nutrition of essential provitamins for humans. By nature, the human body is unable to synthesize certain

vitamins; food containing those vitamins is thus indispensable for our health. *The Electric Retina* highlighted our research on the *noir* fish. Looking more closely at the oculars, viewers can see photographs and animated pictures from the experiments made with *noir*. Simultaneously, the screen shows a blurry underwater landscape – modeled by computer - from the conjectured perspective of the visually impaired *noir* fish. As soon as the conjectured fish starts to feed on floating morsels of food (symbolizing the supplied fatty acids), the blurry scenery is replaced by a clear image of the ocean.

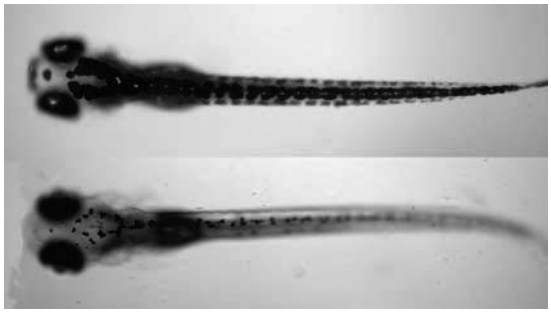

Figure 2
Five-day-old zebrafish larvae. In contrast to the blind *noir* mutant (top panel) having a darker outer appearance, genetically unmodified wild-type larvae (bottom panel) are able to adapt body pigmentation to a bright background.

DISCUSSION

The *Electric Retina* in a Public Space

Beyond a doubt, an artwork is an unconventional form for transmitting scientific findings from the lab. A research project would normally culminate in an article published in a scientific journal. Along the way, scientists may present their results orally at talks or in front of posters at research conferences, but, obviously, such exchanges are restricted to a limited circle of experts. In contrast to these closed channels of communication, the exhibition of art is an experience open to the general public. Artists aspire to reach as many people as possible, and it may be argued that previous knowledge is not required for the audience to experience (and, one hopes, enjoy) a piece of art. Presenting scientific knowledge in the public domain as "art" opens an additional channel for interested outsiders to gain insight into scientific research. This kind of interaction is similar to an exhibition in a science museum; however, an artwork often aims not only to present the underlying research but also to provide an artistic interpretation. It is this "interpretation" that can foster increased dialogue between the scientific researcher and the general public. Discussions at the site of the exhibition of *The Electric Retina* at BrainFair Zurich 2008 and the festivities for the 175th anniversary of the University of Zurich constituted a two-sided experience for the audience. On the one hand, they encountered cutting-edge research on visual impairment by looking into the oculars. On the other hand, by watching the projected movies, they received a reflected perspective on the perceived effects of visual impairment. Such a confrontation spurred many interesting

questions concerning experimental setup, animal testing or underlying mechanisms of eye diseases from the audience. Their questions were directly debated with the scientists involved in this research, who were also often present at the sculpture. The audience not only had the opportunity to get first-hand information from people directly involved in scientific research but, from our point of view, it was a novel experience to discuss our data thoroughly in this format. It helped to increase the awareness and interest of people without biological or medical backgrounds. In answering the audience's questions, we had to adapt our vocabulary and simplify complex occurrences so that the issues behind our research remained coherent. As Albert Einstein once suggested, things should be made as simple as possible but not simpler. This is still a proverbial task for scientists. We also gained insight into the main interest of the general public: how to recognize and treat medical problems and their eyesight. Some people even needed to be redirected to eye doctors.

The Trans-Disciplinary Collaboration

The creation of such an artwork as *The Electric Retina* can be an intense trans-disciplinary collaboration. During the process of development and construction of the artwork, all participants can learn and profit from one another. When Jill Scott came to our lab, she knew only that we study the zebrafish eye by modifying the fish's genetics and testing its resultant behavior. She knew that this information was not sufficient to build a trans-disciplinary artwork. Consequently, she learned the basic principles of our research field in order to gain a deeper insight into our scientific subject. This process was also important for the adjustment of our combined vocabularies and to speak with us in our language. The artist has to understand the scientific terminology and the underlying concepts. For example, a biologist may use the term evolution exclusively in a Darwinian context, whereas an artist may use it instead as a synonym for development or maturation in general. Hence, for the artist evolution may have a goal-directed component aiming at improvement. In a biological sense, evolution is a random process, and the directing force is selection by adaptation to a constantly changing environment. Thus, a long process of discussions and considerations should not be confused with a trivial simplification of a complex topic. As a temporary member of the research group, Scott gained increasing familiarity with the conceptual background of our research and became engaged in our discussions. Such in-depth insight is an indispensable requirement for building a meaningful artwork that includes scientific research.

From Inspiration to the Final Sculpture

When we showed Scott an image of the photoreceptor pattern array taken with a scanning electron microscope, she was immediately drawn to the regular tiling of these cells. This image became the start of her artistic inspiration; she was simply fascinated by its aesthetics, and we described its biological aspects, such as the ultra-structure of the cells and the implied structure-function relationships. Thus, this picture was the starting point for the external appearance of the sculpture, and we began to discuss how to associate our research with the artwork. Jill Scott wondered how a zebrafish suffering from a certain eye disease would experience its immediate environment. While we often address the same question when we measure visual behavior in our OKR movie theater, we use a different angle. Our main interest is to define the exact limits of sensory processing, derived from correlation of the response of the larva to stimulus properties. Scott was interested in how the appearance of the natural environment, be it that of a human or of a fish, shifts because of the relevant eye disease. She asked herself to what degree a sick fish has to forgo the orientation and beauty of its own underwater world. While we are focused on computational analysis of the response to an unnatural stimulus, shifts in the aesthesis of our planet stood as the central problem for the artist. These different points of view are inherited from being situated inside either an artistic or a scientific culture; therefore the exchange has a cross-pollinating effect. This awareness has helped us to reflect on aspects of our science that we have neglected, and artistic interaction may help to establish more fruitful communication with the general public in the future. Although both fields are human-specific enterprises, to see them merging at least at the edges is a truly satisfying experience.

Acknowledgments

We would like to thank all participating lab members (Oliver Biehlmaier, Ursina Gurzeler, Marion Haug, Miriam Henze, Ying-Yu Huang, Tiziana Jametti, Thomas Labhart, Colette Maurer, Kaspar Müller, Sabine Renninger and Markus Tschopp), who not only were an integral part of the whole project but also participated with great enthusiasm at the public events. We further acknowledge financial support for Corinne Hodel from the Neuroscience Center Zurich (ZNZ).

COMMENT from the Artist Jill Scott

Since 1975, I have been a media artist, working on our ideological and historical perception of the human body or on its sensory perception of its immediate environment. In the last five years, I have concentrated on neurobiology and cognition because I wanted to follow this particular scientific research in order to gain a deeper understanding of cross-modal perception. This quest has resulted in a set of "Neuromedia" artworks that attempt to augment interactive potentials of the viewer. At first I was resident in the Artificial Intelligence Laboratory at the University of Zurich (2002 - 2006), where I worked on a wearable computing project based on combined tactile and sound perception for the visually impaired (e-skin). From related workshops with visually impaired users, I became interested in the neurobiology research at the Stephan Neuhauss Group in Neurobiology in the Institute of Zoology University of Zurich. I joined the lab in 2007 as a resident to learn about the retinal and optical functions of the brain in relation to genetic behavior. Through this "learning curve" experience, I have become interested in art's potential as an interpretative catalyst for neuroscientific research, not only because the public needs to understand more about the complexities of human perception but because artists need to design more informed human computer interfaces (HCI). Many artists are interested in this research [2 - 5], but access to a deeper level of analysis can only warrant more scientifically robust inspiration. Furthermore, the residency in neurobiology was particularly exciting because the scientists actually wanted to work alongside me on the content of the proposed project: *The Electric Retina*. Our shared aspiration became to blend retinal research with interactive media art in order to realize some more artistic metaphorical associations that might help to demystify the complexity of visual perception research for the general public. The object has a responsive tactile surface, evoking connections between tactile and visual perception for the viewer. This interaction with the sculpture was achieved in two ways: firstly, through proximity sensors embedded into the rims of the ocular cones, which allowed the viewer to shift the animations through the act of "looking closely." The second interaction occurred on the opposite side of the sculpture, where the viewer could shift an enlarged microscopic lens to trigger new movies. This lens matched the size and scale of the photoreceptors' surface, which stands 210 cm high and gives the viewers the impression that they are standing in behind in the optic nerve looking back out through the photoreceptors to the surrounding environment.

The resultant project not only reflected the researchers' work at the lab but represented my own personal

experience of learning about visual perception and the relation between the lab's research and clinical analysis. It was during my research at this lab that I discovered that I suffer from Low Pressure Glaucoma (in my case, a genetic disease of the optic nerve), which is difficult to diagnose because of the dominant behavioral tendency to visually compensate for the deficiency with the healthier eye. Therefore, the project finally included my own visual disease alongside the research in the lab, where the focus is to search for cures for many other human diseases by gaining genetic control of visual system development and function by analysis of zebrafish mutants. My artistic development came directly from the process of the residency as, on the one hand, I was engaged with practical scientific research, and on the other hand, I discussed the affect of these impairments on vision with a research ophthalmologist.

After Stephan Neuhauss invited me to talk at the Swiss Eye Week Conference (2008), I realized that an artist's mediation between researchers and eye doctors was proof that media art could have a very important communicative role. Only by being immersed in the lab did I realize that visual behavior of mutants represents the mutant perspective. I was fascinated by this and tried to translate this to a human perspective. Furthermore, the researchers were friendlier and more open to debate about the public appreciation of science than I thought they would be - particularly Stephan Neuhauss and his Ph.D. researcher Corinne Hodel, who both thought about the impact of the group's research on society and viewed new creative approaches as a gift.

Of course, sometimes I still felt like an outsider. Still, I really enjoyed brainstorming with the researchers about the relevance of research to problems in the developing world or about the ethical analysis of experimentation. Also, as all our other Artists in Labs residents agree, it is indeed impressive to witness the high level of team effort and mutual credit in any science lab. I particularly liked to learning how to use their machines and imaging techniques, which I now regard as a set of new media for the media artist in the future. However, by far the most rewarding experience for me was to be included in the scientists' brainstorming sessions, particularly those about how to design experiments for new measurement potentials in their own scientific research. I can imagine that more artists and designers could become serious participants in teams performing scientific experiments at earlier stages of their development. From our experience in the Artist in Labs program, having placed 28 artist residencies in 21 science research centers, there is no doubt that scientists can also learn a great deal about communication from us. In addition to the sharing of ideas in the development of public projects like *The Electric Retina*,

this exchange**,** in my view, is the point where the creative potentials of media art and science may actually meet on a more practical level in the future.

Acknowledgments

I thank the Neuhauss Lab, especially Corinne Hodel, Stephan Neuhauss, Colette Maurer, Oliver Biehlmaier, Melody Huang, Markus Tschopp, Marion Haug. Special thanks to Marille Hahne (editing support), Andreas Schiffler and Marcus Dusseiller (programming and sensors), Simone Lüling and Beat Schlaepfer (steel and surface construction help).

REFERENCES AND NOTES

1. Stephan Neuhauss, 2003, Behavioral Genetic Approaches to Visual System Development in Zebrafish, *Journal of Neurobiology* 54, 148—160.

2. Ellen K. Levy, 2009, Stealing Attention, Michael Steinberg Fine Art, New York City www.complexityart.com/Flash/flash_page.htm

3. Andrew Carnie, 2004, Slices and Snapshots, Stanley Picker Gallery, London www.tram.ndo.co.uk/eye.ttmd.htm

4. Suzanne Anker, 2002, Butterfly in the Brain, Universal Concepts Unlimited, New York City www.artbrain.org/gallery2/anker.html

5. Mark Rollins, 2005, Cross-Modal Effects in Motion Picture Perception: Toward an Interactive Theory of Film, Art and Cognition Workshops www.interdisciplines.org/artcognition/papers/11

BIOGRAPHY

Corinne Hodel is a Ph.D. student in the laboratory of Stephan Neuhauss, Ph.D., at the Institute of Zoology of the University of Zurich. Both are neurobiologists interested in the genetic control of vision.

Jill Scott is Professor for Research in the Institute Cultural Studies in Art, Media and Design at the Zurich University of the Arts (ZhdK) in Zürich and Co-Director of the Artists in Labs Program.

7. GENERAL DISCUSSION

7.1. Zebrafish's swim to fame or the rocky road from fish tank to bedside

Zebrafish *Danio rerio* is a shoaling freshwater fish native to slow-moving or stagnant waters in south-east Asia. It is an omnivorous cyprinid also popular as an aquarium fish. In the early 1980s the zebrafish's career as a model organism began (Streisinger et al., 1981). Today, a PubMed search of 'zebrafish' results in hits of more than 10'000 publications (http://www.ncbi.nlm.nih.gov/pubmed/). For reasons listed in the 'General Introduction' (→ see Chapter 1 of this thesis) the majority of these articles deal with the genetic analysis of development. In order to unveil gene functions researchers make use of both morphant and mutant phenotype analyses at embryonic or larval stages. While the effect of injected Morpholino antisense oligomers is only transient and the morphant starts to recover after a few days (Nasevicius and Ekker, 2000), mutants usually die within 10 days due to unspecific lethal effects. Therefore, both forward and reverse genetics approaches are almost completely restricted to zebrafish embryos and larvae even though it would be of great interest to be able to examine the progression of a disease over months or even years. The lens mutant *bumper* is a rare example of a mutant surviving until adulthood even able to reproduce (Schonthaler et al., 2010 → 'Chapter 5'). Together with the introduction of new techniques such as TILLING (Wienholds et al., 2003), zinc finger nucleases (Doyon et al., 2008; Meng et al., 2008) and transgenesis adult zebrafish appears more and more in the spotlight of research. However, it has to be considered that not every technique established for larval zebrafish can simply be applied to adult fish. Especially in the field of behavioural research it is indispensable to adjust assays which have been developed for larvae to adult fish. For instance when the optokinetic response is measured a larva is immobilised in viscous methylcellulose (Hodel and Neuhauss, 2008 → Chapter 4). This approach cannot be applied to adult fish as the gills have to be exposed to a constant water flow (Mueller and Neuhauss, 2010).

In addition to the prominent role in development biology, zebrafish also became a popular model organism in vertebrate vision research. Zebrafish eyes feature a typical vertebrate retina comprised of ciliary cone and rod photoreceptors and, being diurnal animals their retina is functionally cone dominant. Hence the zebrafish retina's structure and function can be compared to the human one to a great extent. Nevertheless, it is not surprising that there are major differences between eyes of different vertebrate classes -

such as bony fish and mammals - in terms of morphology, function and development. The fovea of the human retina contains a high density of red and green cones. The zebrafish retina in contrast lacks a fovea at all but instead the four cone types are arranged in a very regular pattern array. The number of cone types brings us to the next difference between zebrafish and man. Zebrafish as many other teleosts possess an additional cone type having its absorption maximum in the ultraviolet range of the light spectrum. Moreover, the inner segments of zebrafish red and green cones are in close contact forming so called double cones. The retina of humans and all other eutheria is exceptional in terms of having lost any kind of multiple cones which are found in all other vertebrates having a calcified skeleton. Not only the cone arrangement and number of cone types are different but also some features of cone anatomy. One difference can be found in the cone outer segment. Whereas human cone outer segments embed an axonemal cytoplasmic part, zebrafish have their accessory outer segment only connected to the outer segment via a thin plasma bridge (→ Chapter 3). The vertebrate cone inner segment in general comprises ellipsoid and myoid. In contrast to the human myoid, the zebrafish myoid is a very dynamic structure able to retract and elongate during light and dark adaptation processes (Hodel et al., 2006). This adaptive behaviour of photoreceptors is called retinomotor movement and not found in mammals. Regarding lens development the fate of the lens placode takes a different route in zebrafish and mammalian development. Whereas the mammalian lens placode delaminates from the surface ectoderm as a hollow lens vesicle, the zebrafish lens placode becomes a solid cell mass of primary lens fibres (Dahm et al., 2007). Therefore, the *bumper* mutant (Schonthaler et al., 2010 → 'Chapter 5') is rather applicable to study progression and regression of tumour-like hyperproliferation than lens developmental mechanisms. Likewise, the zebrafish mutant *mariner* defective in *myosinVIIa* (→ Chapter 3) was praised as a new animal model for human Usher Syndrome 1B (Ernest et al., 2000) – especially for studying the development of retinal degeneration, a cardinal symptom of the human disease not present in the mouse model *shaker-1* (Gibson et al., 1995). Unfortunately, also *mariner* fish do not show typical signs of degeneration and in wild-type fish MyosinVIIa is specifically expressed in a teleost specific structure not found in humans. Maybe retinomotor movement – an adaptation mechanism also not found in mammals - is impaired (Hodel, 2005). This result is arguable as the genotype of *mariner* founder fish could not be confirmed.

Without doubt, in developmental biology zebrafish has long been accepted and established as a model organism. The zebrafish as a model organism for human diseases has lots of potential. How much of this potential is realized? Of course, zebrafish research is basic research and the way from aquarium to clinical application is long and not

necessarily straightforward. Any animal model may not always cover all features and symptoms of the respective pathology so that insight may be limited to one or few aspects only. It is pivotal to take species-specific differences into account when translating findings from a zebrafish model to human health and disease.

7.2. We need artists who care about the *thing in itself*

During my thesis I had the unique chance to be part of an art project. In the context of the Swiss Artists-in-Labs program the artist Jill Scott came to our lab in order to get insight into zebrafish vision research. I taught her some theoretical background and also provided her with hands-on experiences. This mutually exciting and fruitful collaboration culminated in a joint creation *The Electric Retina*, an interactive sculpture (Hodel et al., 2010 → Chapter 6).

During this project I started to realise that a meaningful collaboration between art and science needs artists who interpret, deduce and conclude. It needs artists who care. Or to state in Immanuel Kant's terminology, the artist has not to simply illustrate the *object* but to be aware of the *thing in itself*. To quote an example related to zebrafish vision research: I do not see the role of the artist in drawing how the eye of a blind fish looks like compared to the eye of a healthy fish. This would be an artistically modified Facsimile of what researches have found by means of histology or any other imaging technique. Rather, an artist intrigued in zebrafish vision research should get to the bottom of the matter and give an idea about how a visually impaired fish perceive the underwater landscape and how its perception changes after genetic manipulations. Indeed, Jill dove into the Australian ocean and took pictures of the beautiful coral reef. In the studio she modified film excerpts in order to illustrate the perception of a visually impaired zebrafish mutant investigated in our lab. Of course, zebrafish are not native to Australian marine water at all and the post-editing does not accurately depict consequences of visual defects. However, the freedom of artistic expression allows being scientifically incorrect. Instead, the destruction of the ocean's beautiful images emotionally demonstrates the world of blind or visually impaired patients and at the same time links human eye disease to zebrafish vision research.

"L'art pour l'art" is not in the centre of attention when art meets science in my opinion. The output of an art-science collaboration should be more than a pure piece of art. "Art, science and society" is the phrase I go for. Art is an outstanding tool to communicate science. Even though scientists giving public talks try to avoid technical expression and to use comprehensible metaphors when explaining the own research, they still communicate within a closed channel mostly not truly accessible for laypersons. Scientist having a didactic education or at least a flair for access the general public are rare. Art can help to bridge the cap between the scientific community and the general public.

Moreover, I see great potential to bring art into play in the context of development aid. Promising examples are art panels showing administration of malaria medication explicitly made for illiterates (Ajayi et al., 2009; Ngoh and Shepherd, 1997). Art could also provoke a discourse about research concerning tropical diseases most problematical in countries not having the financial means to substantially enforce research such as vaccine development. Maybe a vaccination against malaria would have been developed long ago if infected anopheles would be still native to the northern hemisphere and not only to South America, Asia or Africa.

7.3. Reference

Ajayi, I. O., Oladepo, O., Falade, C. O., Bamgboye, E. A., and Kale, O. (2009). The development of a treatment guideline for childhood malaria in rural Southwest Nigeria using participatory approach. Patient Educ Couns *75*, 227-237.

Dahm, R., Schonthaler, H. B., Soehn, A. S., van Marle, J., and Vrensen, G. F. (2007). Development and adult morphology of the eye lens in the zebrafish. Exp Eye Res *85*, 74-89.

Doyon, Y., McCammon, J. M., Miller, J. C., Faraji, F., Ngo, C., Katibah, G. E., Amora, R., Hocking, T. D., Zhang, L., Rebar, E. J.*, et al.* (2008). Heritable targeted gene disruption in zebrafish using designed zinc-finger nucleases. Nat Biotechnol *26*, 702-708.

Ernest, S., Rauch, G. J., Haffter, P., Geisler, R., Petit, C., and Nicolson, T. (2000). Mariner is defective in myosin VIIA: a zebrafish model for human hereditary deafness. Hum Mol Genet *9*, 2189-2196.

Gibson, F., Walsh, J., Mburu, P., Varela, A., Brown, K. A., Antonio, M., Beisel, K. W., Steel, K. P., and Brown, S. D. (1995). A type VII myosin encoded by the mouse deafness gene shaker-1. Nature *374*, 62-64.

Hodel, C. (2005). Analysis of dark and light adaptation in wild-type and mutant zebrafish. Diploma Thesis.

Hodel, C., and Neuhauss, S. C. (2008). Computer-based analysis of the optokinetic response in zebrafish larvae. CSH Protocols *2008*, prot4961.

Hodel, C., Neuhauss, S. C., and Biehlmaier, O. (2006). Time course and development of light adaptation processes in the outer zebrafish retina. Anat Rec A Discov Mol Cell Evol Biol *288*, 653-662.

Hodel, C., Neuhauss, S. C. F., and Scott, J. (2010). The electric retina: An interplay of media art and neuroscience. Leonardo *43*, in press.

Meng, X., Noyes, M. B., Zhu, L. J., Lawson, N. D., and Wolfe, S. A. (2008). Targeted gene inactivation in zebrafish using engineered zinc-finger nucleases. Nat Biotechnol *26*, 695-701.

Mueller, K. P., and Neuhauss, S. C. (2010). Quantitative measurements of the optokinetic response in adult fish. J Neurosci Methods *186*, 29-34.

Nasevicius, A., and Ekker, S. C. (2000). Effective targeted gene 'knockdown' in zebrafish. Nat Genet *26*, 216-220.

Ngoh, L. N., and Shepherd, M. D. (1997). Design, development, and evaluation of visual aids for communicating prescription drug instructions to nonliterate patients in rural Cameroon. Patient Educ Couns *31*, 245-261.

Schonthaler, H. B., Franz-Odendaal, T. A., Hodel, C., Gehring, I., Geisler, R., Schwarz, H., Neuhauss, S. C., and Dahm, R. (2010). The zebrafish mutant bumper shows a hyperproliferation of lens epithelial cells and fibre cell degeneration leading to functional blindness. Mech Dev *127*, 203-2019.

Streisinger, G., Walker, C., Dower, N., Knauber, D., and Singer, F. (1981). Production of clones of homozygous diploid zebra fish (Brachydanio rerio). Nature *291*, 293-296.

Wienholds, E., van Eeden, F., Kosters, M., Mudde, J., Plasterk, R. H., and Cuppen, E. (2003). Efficient target-selected mutagenesis in zebrafish. Genome Res *13*, 2700-2707.

ACKNOWLEDGMENTS

I am grateful to Prof. Stephan Neuhauss for supervising my thesis, for fruitful discussions beyond neuroscience and for giving me the freedom to try own ideas.

To Prof. Christian Grimm and Prof. Esther Stoeckli for the supervision of my PhD thesis.

To all present and past lab members, especially to Colette for talking about PCR problems and the human nature, to Edda for her contagious smile and for her skilled advice, to Kara for her enthusiastic ways in keeping lab and fishroom organized and running, to Kaspar for being a first-class office and meeting mate, Marion for her impressive demonstration of work-life-balance, Martina for being my hard-working master student, Matthias for sharing his large treasure of knowledge and experience and to Peter for empathically taking care of our fish.

To Jill Scott for being friend and mentor.

To my friends, especially to Claudia, Sarah and Daniele.

To the 'NJUBA – Children Relief Uganda' for showing me that things can be worse than having the wrong fish in the tank.

To my parents for giving me roots and wings. To my sister Rebecca and my brother Manuel and their partners for breaking the work routine.

To my partner Helge for being my anchor windward.

Part of my thesis was founded by a PhD fellowship of the Neuroscience Center Zurich (ZNZ) and by a research grant of the Swiss National Science Foundation (SNF).

CURRICULUM VITAE

Personal Information

Name	**Corinne Hodel**
Contact	Kirchenackerweg 11 8050 Zürich +41 77 417 65 73 corinne.hodel@imls.uzh.ch
Date of birth	August 10th 1981
Citizenship	Switzerland

Education

1994 – 2001	**Secondary school**, Kantonsschule Reussbühl, Switzerland
06/2001	Matura Typus B (A-Levels in arts; focus on Latin and Philosophy)
2001-2003	**Undergraduate studies of Biology,** Swiss Federal Institute of Technology (ETH) Zurich
2003-2006	**Graduate studies of Neuroscience**, ETH Zurich
05/2006	Diploma in Natural Science (equivalent to Master Degree ETH) Diploma thesis at the Brain Research Institute, ETH Zurich in the laboratory of Prof. Stephan Neuhauss: *Analysis of dark and light adaptation in wild-type and mutant zebrafish*
2003-2010	**Teacher education**, ETH Zurich
01/2010	Certificate of Teaching Ability Biology (teaching degree for secondary schools)
since 07/2006	**PhD thesis** at the Institute of Molecular Life Science (formerly Institute of Zoology), University of Zurich in the laboratory of Prof. Stephan Neuhauss: *Visual Behaviour and Ocular Morphology of Larval and Adult Zebrafish with an Eye towards Art*

Scholarship

2007-2009 **PhD grant**, Neuroscience Centre Zurich (ZNZ)

Professional Experience

04-07/2006 **School teaching** (secondary school and college of education)
Kantonsschule Musegg and Pädagogische Hochschule Zentralschweiz; Luzern, Switzerland

since 07/2006 **International Ph.D. program** in neuroscience
Neuroscience Centre Zurich (ZNZ); Zurich, Switzerland

since 07/2006 **Teaching assistant** in undergraduate and graduate practical neurobiology courses, scientific communication course, internships and BrainFair Zurich
University of Zurich; Zurich, Switzerland

since 05/2008 **IT- delegate** Neuhauss Laboratory
University of Zurich; Zurich, Switzerland

07/2008 – 10/2009 **Supervision master thesis** Martina Heidemann
University of Zurich; Zurich, Switzerland

09/2008 **Expert "Schweizer Jugend forscht"**
43. National contest for young scientist 2009; Bern, Switzerland

06/2010 **Session chair** *Through the Public Lens of Neuroscience and Art*
ESCITE Conference; Dortmund, Germany

Presentations at Scientific Meetings (first authorships only)

01/2005 **Swiss Retina Meeting**; Brunnen, Switzerland
Talk: *Characterization of the visual mutant mariner: a zebrafish model for human usher syndrome 1B*

02/2005 **USGEB-SSN-SSBP Meeting**; Zurich, Switzerland
Poster: *Characterization of the visual mutant mariner: a zebrafish model for human usher syndrome 1B*

2006-09 **Annual ZNZ Symposia**; Zurich, Switzerland
Posters of different topics

03/2007 **7th Göttingen Meeting of the German Neuroscience Society**; Gottingen, Germany
Poster: *Zebrafish Model for Human Usher Syndrome Shows Light Adaptation Defects and Retinal Degeneration*

05/2007 **ZNZ PhD Retreat**; Valens, Switzerland
Talk: *mariner: Zebrafish Model for Human Usher Syndrome 1B*

07/2007 **Digital Art Weeks**; Zurich, Switzerland
Talk: *The Electric Retina*

10/2007 **European Retina Meeting**; Frankfurt, Germany
Poster: *Retinal MyosinVIIa Expression in Zebrafish*

02/2008 **Swiss Eye Research Meeting**; Brunnen, Switzerland
Talk: *The Electric Retina*

03/2008 **Parcours des Wissens**; Zurich, Switzerland
Exhibition: *The Electric Retina*

04/2008 **Art and Science**; Zurich, Switzerland
Exhibition: *The Electric Retina*

03/2009 **8th Göttingen Meeting of the German Neuroscience Society**; Gottingen, Germany
Poster: *Usher Protein MyosinVIIa Expression in the Zebrafish Retina*

05/2009 **ARVO Annual Meeting**; Fort Lauderdale, Florida
Poster: *Expression of MyosinVII Paralogs in Zebrafish*

Published Articles

Hodel et al. 2010 — **Hodel, C.**, Neuhauss, S.C.F., and Scott, J.M. (2010) The Electric Retina: An interplay of media art and neuroscience. Leonardo *43:3 in press*

Schönthaler et al. 2010 — Schönthaler, H.B.*, Franz-Odendaal, T.A.*, **Hodel, C.***, Gehring, I., Geisler, R., Schwarz, H., Neuhauss, S.C.F., and Dahm, R. (2010) The zebrafish mutant bumper shows a hyper-proliferation of lens epithelial cells and fibre cell degeneration leading to functional blindness. Mech Dev *127:3-4*, 203-219 **These authors contributed equally*

Hodel & Neuhauss 2008 — **Hodel, C.**, and Neuhauss, S.C.F. (2008). Computer-based analysis of the optokinetic response in zebrafish larvae, CSH Protocols *2008*, prot4961

Hodel et al. 2006 — **Hodel, C.**, Neuhauss, S.C.F., and Biehlmaier O. (2006). Time course and development of light adaptation processes in the outer zebrafish retina. Anat Rec A Discov Mol Cell Evol Biol *288:6*, 653-62

Article in Preparation

Hodel et al. *in preparation* — **Hodel, C.**, Biehlmaier O., Heidemann, M., Klooster J., Gesemann M., Kamermans M. and Neuhauss S.C.F. MyosinVIIa as a Marker for the Cone Accessory Outer Segment